UNIVERSITY OF BIRMINGHAM

MIBTP
Midlands Integrative Biosciences Training Partnership

Insights into the Bacterial Mechanotransduction Mechanisms Induced by Vibrational Stimuli

University of Birmingham - School of Chemical Engineering

Student: Dario G. BAZZOLI

Supervisors: Prof. P. MENDES & Dr. T. W. OVERTON

Abstract: *Mechanical forces shapes living matter from the macro to the micro. No organism has escaped their influence or failed on taking advantage of them as both eukaryotic and prokaryotic cells are subjects and wielders of the force. However, while we know much of how this happens in mammalian cells, our appreciation of how rich this same process is in bacteria have been late to come. Consequently, while mechanical forces and their vast mechanobiology have been used to alter and control mammalian cells behaviour, we are lacking this same level of novelty in bacteria. With my work I would like to amend this and explore how bacteria can also be controlled through mechanical signals. To do this, I aimed influencing one of bacteria most mechanically rich and technologically appealing processes: surface colonisation. I found that nanometric surface vibrations of pN intensities and kHz frequencies, reduce surface colonisation. I found this response mediated by both cells' membrane potential and flagella's motors as, when these were suppressed, vibrations effect on cells surface behaviour was limited. I suggest that by crippling cells hyperpolarisation, vibrational stimulation hinder flagella's mechanotransduction so hampering surface colonisation. While these findings prove that cells' adhesion can be influence by mechanical forces, they also show that through a similar tickling sensation, mechanical cues can effectively be used as a novel tool to communicate and control bacteria.*

À vous tous et à toi, merci.

Table of Contents

LIST OF FIGURES:

LIST OF TABLES:

LIST ACHRONIMS & ABREVIATIONS:

BMF: Bacteria flagella's motor

CCCP: Carbonyl cyanide m-chlorophenyl hydrazine

CSK: Cytoskeleton

$DiOC_2(3)$: 3,3'-Diethyloxacarbocyanine iodide

DNA: Deoxyribonucleic acid

ECM: Extracellular matrix

EPS: Extracellular polymeric substances

PDMS: Polydimethylsiloxane

PI: Propidium iodide

UV: Ultraviolet

1. INTRODUCTION

Forces shapes everything around us, living and non-living objects alike. While their relevance in the macroscopic world is manifest, it may be surprising how in the microscopic playground they can also influence cells and their biology. In fact, the ability to sense and respond to mechanical forces appear to be a common feature throughout all the living organism from eukarya to bacteria. Between the two however a staggering contrast persist. In fact, despite the vast canopy of cells functions which are shaped by mechanical forces, while this have been used to control eukaryotic behaviour the same has not yet happened with bacteria. Here is therefore where our work is located. By being carefully guided from the recent developments in the field of bacteria mechanobiology and sensing, I would like to assess how these can serve human needs as they eukaryotic counterpart already did. In the coming pages, I will discuss mechanical forces, their effect on cells and the use we can make of them to control one of bacteria's most relevant process: surface colonisation. Before going there however, we need to see the broader context of my work, how it relates with the current scientific knowledge, what is known and, most importantly, what is still missing. So, let's begin by going back to where I started: forces.

1.1 Shaping forces and Mechanobiology

Of the roughly 10.000 years of human culture, the concept of natural forces shaping the world is recent as one of its first records dates the fifth century B.C. by the time of the presocratic philosopher Empedocles. For him, the world was in fact brought about but the perpetual contraposition of two opposing natural forces, love and strife [1].

Despite the yet vague and quite anthropomorphic terminology, these represents one of the earliest attempts in our species at formalising the idea that natural forces are responsible for the world we see. In fact, the eternal struggle or "tension" he describes existing between the two was for him what brought objects together and apart, giving the world its rhythm and explaining its changing with time. Realising the role of natural forces in modelling our world made for one of the greatest intellectual achievements of all times as it meant abandoning an animistic view in favour of a materialistic one This one, eventually, kept growing until it was finally formalised by the work of Newton and our modern interpretation of natural forces. However, if their involvement in shaping the world was appreciated since classical antiquity, it took millennia for this to be extended to living organisms.

This conception of force affecting animal shapes and behaviour was in fact spring boarded at the beginning of the twentieth century by the work of the Scottish biologist d'Arcy Thompson and its influential book *On Growth and Form* [2]. Today we know this to be true and we understand the relevant role that forces plays and had played in the past to shape both organism's evolution and development. On a macroscopic level, coping with mechanical forces for an organism mostly means to be able to deal with gravity. Its omnipresence in time and space makes so that the most fundamental feature of any organism took form: structure. Most of the time an organism body is a necessary scaffolding that prevents them from crushing under their own weight and that over evolutionary times had been adjusted to meet some purpose. Bark, bones, carapaces and shells, when these have not been weaponised by evolution, are there to provide structural support to the organism.

However, response to gravity and weight is not the only place where we see the

wide effect of mechanical forces on organism as, despite being more subtle, the sense of touch and hearing also are. While their presence is widespread among multicellular organism, this beg the question of how these are brought about? Here is where things get more interesting. In fact, apposite sensory tissues and cells exist which are capable to sense a mechanical stimulus and transform it into a chemical or electrical signals organism can sense [3]. This simple and common experience with forces brings us down to a smaller realm as we leave the macro for the micro. Here, despite the loosen grip of gravity, cells do still have to retain structure as mechanical forces keep shaping them in even more unexpected and drastic ways.

1.2 As above so below, mechanobiology and the cell

When entering the microscopic realm, the interplay between forces and organisms is pushed even further as these take on even richer roles. In fact, not only forces influence cells need for structural support and sensing, but they can go as far as changings their shape, kind, functioning and even behaviour. Mechanobiology is the expanding science which is tasked to understand all these effects forces have on cells physiology [4]. These can be classified as belonging to two main branches: mechanosensing and mechanotransduction. Mechanosensitivity investigate the effect that mechanical forces have on the structure and function of different cellular components, such as organelles or proteins. Mechanotransduction follow instead the internalisation of mechanical cues and how their transduction into chemical or electric signal allows cells to understand the environment and alter their behaviour.

Through the lenses of mechanobiology we now see how force involvement in the life of cells is universal as it is shared by both eukaryotic and prokaryotic cells [5,6]. Despite

this, our knowledge is skewed toward the former both in amount and depth. The reasons behind this are split but they might lie both on technological and scientific biases. From a technological perspective, while eukaryotes are harder to culture and keep viable, they have been simpler to study in the past because of their bigger sizes which did not require the same level of micro or nano control. Scientific biases could also have contributed as the view of bacteria being much simpler organism lasted until the end of the 20th century. Until then bacteria were known to be pathogenic organism swimming in their environment without too much of an agency. Chemotaxis and behavioural adjustment based on chemical inputs was considered top notch technology for them, but it was a far cry from viewing them capable to also sense mechanical cues. Or, maybe, sometimes things are simply out of fashion in science and only a brave bunch considered the subject worth being explored.

No matter what the cause of this knowledge anisotropy was, the end results is that we now have a superior knowledge of the influence that mechanical forces have on eukaryotic and more specifically mammalian cells. This superiority involves a wider appreciation of both the mechanism and physiological impact of mammalian mechanobiology. Many mechanotransductive pathways have been discovered which turns mechanical forces into many different cells' behaviours and functions [7]. These effects reverberate across several order of magnitudes as forces are sensed and transferred from the level of the cell to that of the tissue. Specifically, on a sub-cellular level, through dynamic molecular processes [8], forces direct organelles organisation [9], nucleus structure [10,11] and genetic expression [12,13] that can then influence cells motility [14], development [15,16] and their differentiation [17,18] with drastic effects at the level of tissues and organs such as cartilage [19,20] and bone [21] formation or muscles [22] and brain functioning [23,24]. Moreover,

forces do not only have a hierarchical effect on cells and tissues but can even influence less centralised networks as the immune system [25,26].

In mammalian cells, the above vast stretch of physiological outcomes from mechanical inputs is mostly brought about by the interaction between forces and cells extracellular structure. Like spiders sitting at the centre of their webs and sensing forces through them, cells are embedded and sense forces through a web of their own, the extracellular matrix (ECM) [27]. This bi- or tri-dimensional scaffolding is mostly made of collagen proteins the thickness of which dictates the mechanical properties of the final tissue. Thick and aligned fibres are found in tensile and robust tissues such as tendons while thin and meshed ones are usually a feature of brittle and transparent ones like the cornea. Thanks to its adaptable nature, the ECM made many things for cells viability but from a mechanobiological perspective it provides structural support and allow the transfer of mechanical information. This can then be internalised by the cells through a similar fibrous network: the cytoskeleton (CSK) [28]. Similarly to the ECM, cytoskeleton provides structural support while it also allows the transfer of mechanical signals through its reticular network. Three proteins make most of the CSK and dictate its behaviour: actin, microtubules and intermediate filaments. The former act as a push and pull system that via polymerisation and depolymerisation cycles allow cells to expand and contract depending on their needs. Intermediate filaments provide instead a more passive support to cells through their more thermodynamically stable structure. Through the connection of these external (ECM) and internal (CSK) protein webs, cells can sense many different mechanical forces. Shear, pressure and stress can all be transferred from the tissues to the cell where they are finally internalised, influencing genetic expression and ultimately their behaviour.

Many more players belong to the established science of mechanobiology but we now have a feel of the profound interconnectedness that in mammalian cells allow forces to be put to use in many different ways. However, all I have discussed so far regarded mammalian cells but our argument started by introducing the fact that they are not alone in this as we have to meet the other bunch of force wielders: bacteria.

1.3 A peek on bacteria mechanobiology

It was 1982 when Koch first suggested the idea that bacteria could also be sensitive to their mechanical environment [29], a hypothesis that within the same decade was confirmed by the discovery that mechanosensitive elements like those of mammalian cells also existed in bacteria [30]. Despite its younger history, bacteria mechanobiology have grown widely since these preliminary work and today mechanical forces are known to influence many aspects of their biology. While the body of knowledge covering mammalian mechanobiology is broader, older and deeper, the last decade had greatly compensated for the tardive appreciation of this phenomenon in bacteria.

Bacteria mechanobiology is somewhat different and yet akin to its mammalian counterpart as this is partially explained by the difference and similarities which exist in their biomechanics. First, bacteria are smaller, about 40 times smaller [31]. Their membrane is also different. Mammalian cells have smooth more malleable lipid membranes while bacteria have both multiple and stiffer ones due to the presence of both a lipid but also a peptidoglycan layer [32,33]. This act as a safety net which evolved in response to the variable osmotic environments bacteria use to experience and which make them susceptible to sudden changes in internal pressure. Contrary to this, mammalian cells live in more stable environments while embedded in their self-produced extracellular matrix which bacteria

are also lacking. Except for their communal behaviour in biofilms, which I would touch upon very soon, single bacteria do not possess neither ECM nor an internal cytoskeleton. What is most reminiscent of this last feature are instead proteins that give bacteria their shapes and prepare them for duplication: MreB and FtsZ. The former is an homologue of the actin protein we encountered before in mammalian CSK. In bacteria, this performs a similar role as by polymerising within their membrane along the major axis it allows rod shaped bacteria to retain their form [34]. FtsZ is instead a tubulin homologue that help bacteria during their duplication [35]. The way this work is similar to a noose. In fact, while the cell elongates along its major axis, FtsZ, together with other proteins, polymerise around the inner membrane of the mother cells to form a ring structure known as Z-ring. Toward the end of duplication, this one would then start contracting and reduce in diameter, a process that eventually leads to septum formation and cells separation.

However, both MreB and FtsZ capture CSK structural function but their connection to mechanobiology have yet to be established making them a far cry from CSK central role in mammalian mechanobiology.

So, to recap, bacteria are smaller, stiffer, do not have neither an extracellular matrix nor a cytoskeleton and yet they can respond to forces. How they do this is still a matter of debate as, while we have many accounts of this process and its effect on cells, we still miss its grand picture. Nonetheless, several unifying themes are beginning to appear. Similarly to mammalian cells and higher organism, bacteria mechanobiology influence their physiology and behaviour through either mechanosensitive elements and mechanostranductive pathways [36,37]. While mechanosensation is more of a self-reliant process where forces alter protein structure and their functioning, mechanotransduction is a causal chain of events that transform a mechanical input into either chemical or

electrical outputs. Following this transduction, mechanical cues are now in a format that cells can understand and react to by altering their behaviour. Within their pathway structure, mechanotransduction usually rely on some mechanosensitive element to sit at the top of its signalling cascade as this allows force to be converted into structural changes that generate electrochemical signals. These so crafted pathways are what allow force inputs to reverberate onto cells physiology (Figure 1). Different mechansensitive and mechanotransductive processes have been identified in bacteria of which discussing a few would provide the reader with the perspective necessary to better locate our work within its scientific landscape.

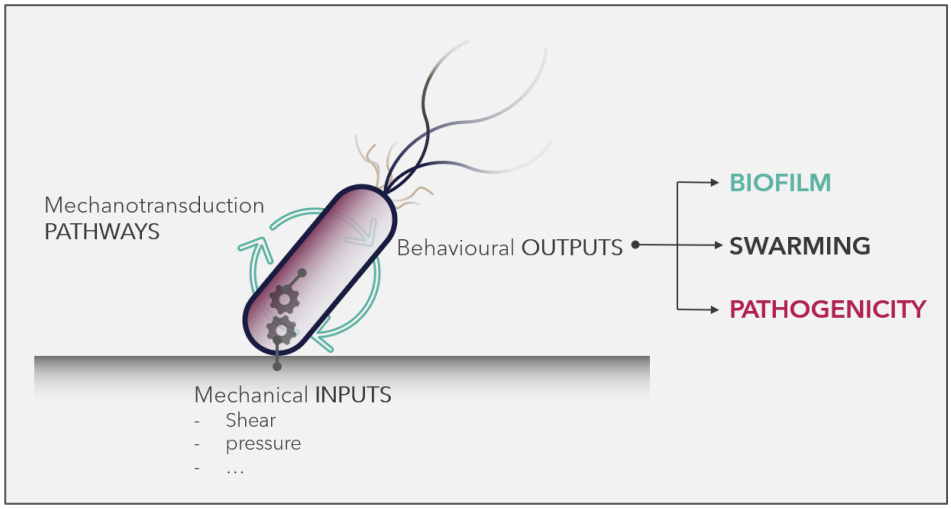

Figure 1: Bacteria mechanobiology. Mechanical inputs from solid surfaces and the environment are sensed and, through several mechanotransduction pathways, are then converted into different behavioural outcomes. These mostly affect biofilm formation, swarming motility and cells pathogenicity.

1-3.1 Mechanosensation in bacteria

Mechanosensitive elements in bacteria have been identified in both their membrane and motorised appendages. Forces acting on them induce some

conformational change that alter their function which, because of mechanosensors location within the cells, most of the time results in their altered adhesion and motility.

The older and better understood examples of mechanosensation in bacteria are mechanosensitive channels (MSC) [38]. These have been first identified in eukaryotic cells but they are also common to bacteria where they assume the same role of their mammalian counterpart: safety pressure valves. In fact, pressure, specifically osmotic pressure is something cells must deal with constantly [39]. Sudden drops or increases of ions in the medium can cause hypo and hyper-osmotic shocks as water rapidly enter or leave the cells

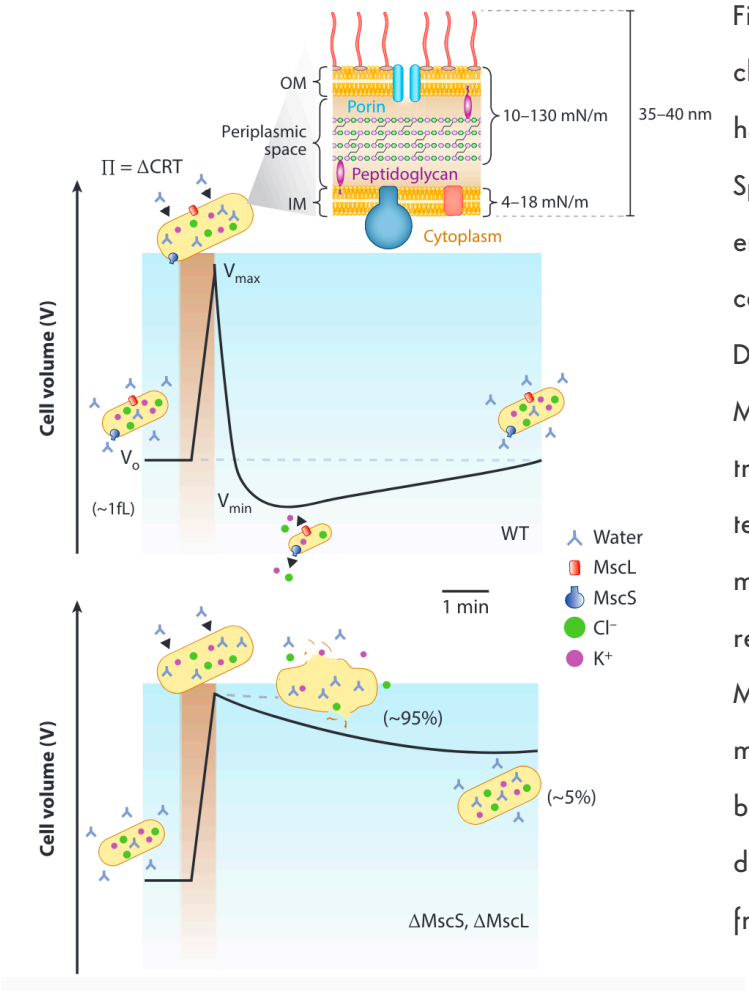

Figure 2: Bacteria mechanosensitive channels provide protection toward harmful hypo-osmotic shocks. Specifically, when osmolarity in the environment drop, water influxes cause cells volume to inflate within milliseconds. Depending on the strength of the shock, MscS and MscL opening is sequentially triggered by the increase membrane tension. Their opening cause the millisecond release of ions and the recovery of normal osmotic pressures. Mutants lacking these channels are found much more susceptible to shock induced bursting that the wild type proving their direct effect on cells viability. Adapted from [41].

causing their bloating or withering [40]. Of these, hypo-osmotic shocks are by far the greater threat to cells integrity as sudden water influxes can lead to pressure spikes which, if not released, can burst cells open [41] (Figure 2). This is where mechanosensitive channels come into play. Their ability to open in response to increasing membrane tension allow cells to quickly adjusting their ion content, releasing osmotic pressure and enabling cells to survive otherwise fatal shocks [42].

How this is brought about and how MSCs can be activated by mechanical forces it depends entirely on their structure. Less than a dozen channels have been identified in bacteria and these belongs to either the small (MscS) or large (MscL) families [43-45]. These barrel like intermembrane proteins are expressed in lower number within a cell and tightly bind to their membrane. Upon pressure, the tension acting on them cause their opening following a mechanism similar to that of a camera objective [46] (Figure 3). It takes few

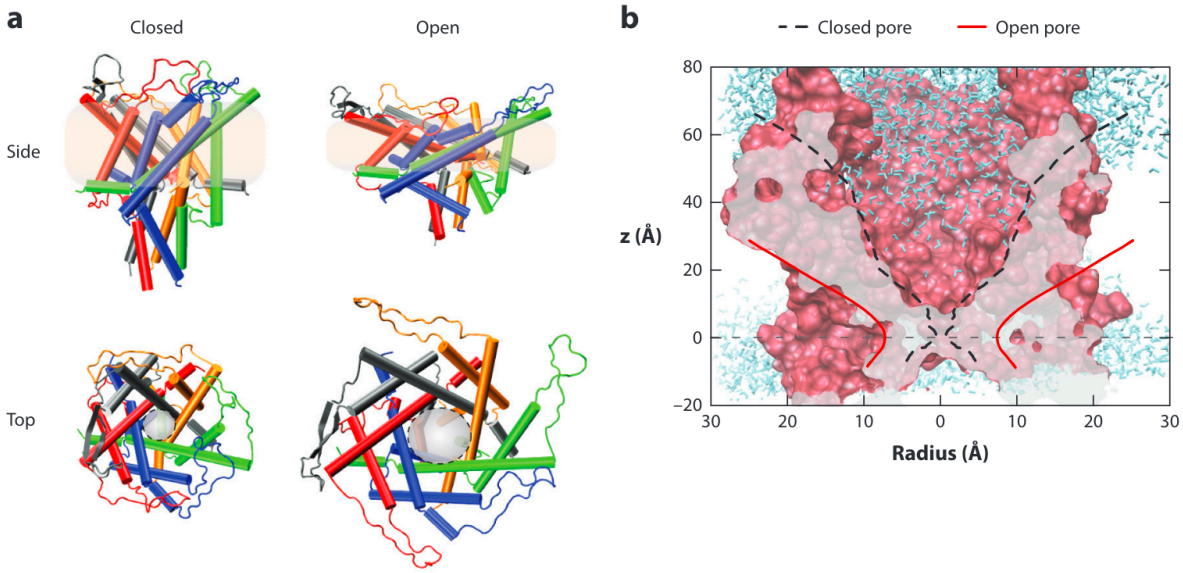

Figure 3 a) Top and side view of *E.coli* MscL channel and its open and closed states. Following increasing tension from the membrane, its barrel structure stretches and open following an iris-like mechanism. b) Molecular dynamics of the open and closed states. Dashed-black and solid-red lines are the edges of the channels cavity as closed and open respectively. Adapted from [41].

milliseconds to open a channel and, depending on its conductance, it can release between thousands and millions of ions per second. While most of the channels are nonspecific, some can selectively release only one ion such as some potassium specific mechanosensitive channels [47]. To widen the protection and response based on the intensity of the shock, channels have different gating pressures and conductances. Specifically, MscS channels are tiggered by lower membrane strain and have smaller conductance than MscL. This ensure that faster voiding of precious internal ions is achieved only under threatening osmotic pressures. Their effect on cells have been proved fundamental for their viability under shock but their triggering also correlates with reduced cells growth and intracellular signalling [48]. While at present no mechanoensitive channels have been associated to any mechanotrasductive pathway, it is tempting to suggest that the sudden drop in ionic content and its effect on both membrane potential and pH could serve as part of a mechanical signal transduction although this remains to

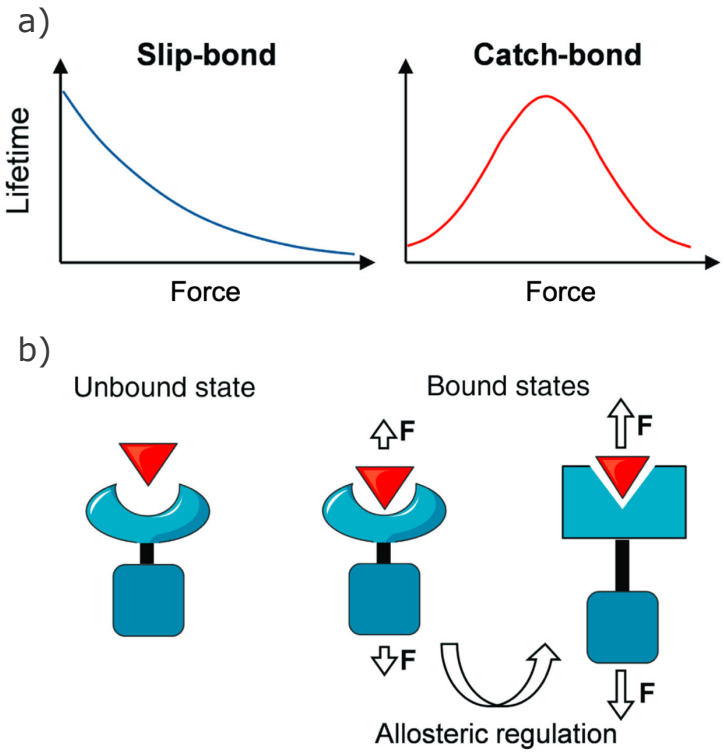

Figure 4: Contrary to normal (slip) bonds which decrease in strength with applied load, catch bond resilience to rupture increase with tensile force (a). This is brought about by force dependent allosteric changings in the bond conformation (b). Specifically, as is the case for FimH (blue) and mannose (red), substrate specificity increases when these are subjected to forces. Adapted from [49].

be elucidated.

Aside from mechanosensitive channels, mechanosensitivity have also been observed in membrane bound adhesins. One of the most striking example of this are *E. coli* fimbriae catch bonds [49]. Fimbriae are surface adhesins abundant in pathogenic *E. coli* and they are structurally akin to non-motorised pili. Particularly, one of its tip proteins (FimH) has catch bonding properties that, contrary to normal ones, strengthen with increasing load [50] (**Error! Reference source not found.**). This makes fimbriae act as safe belts, allowing cells to steadily attach onto surfaces and withstand drag forces which could otherwise lift them off. From a mechanistic point of view, the way *E. coli* FimH do this is through yet another force induced conformational change. Specifically, FimH attach to the mannose residues which decorate many mammalian cells membranes. When extra load is applied to the bond, rather than breaking or weakening, FimH change conformation, exposing aminoacidic residues that further boost their compatibility to mannose

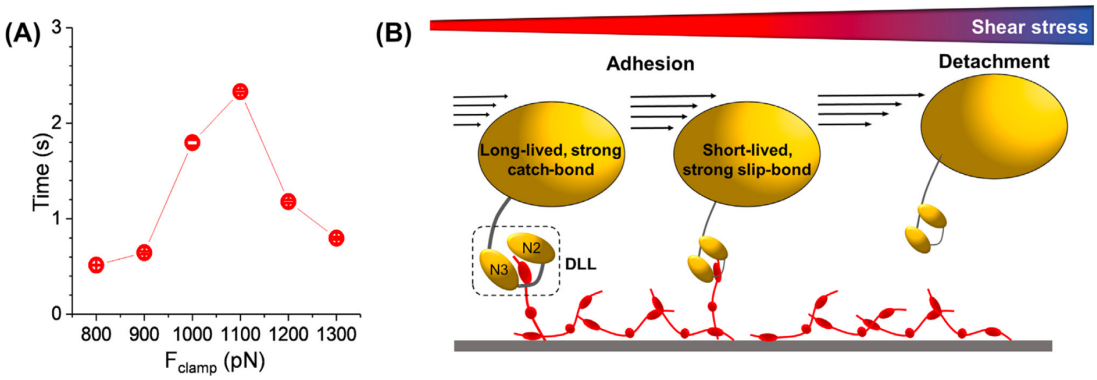

Figure 5: A) FimH rupture time increase with applied tensile force. B) This mechanism gives pathogenic strains of *E.coli* an edge when colonising hosts under variable shear stress such as in the urinary tract. In fact, following increasing hydrodynamic flow cells won't lose grip on target cells and tissues. This is achieved via a changing in conformation of tip subdomains which increase substrate's affinity and adhesin bonding to it. Adapted from [50].

ultimately strengthening FimH adhesion to it. This way, uropathogenic E.coli can withstand stronger rheological load allowing them to better infect cells and the organism [51-53] (Figure 5).

The examples above shows how membrane bound mechanosensitive elements exists in cells and support their adhesion and membrane integrity. A second class of these sensors exists in their motorised apparatuses, flagella and pili, which use forces to adjust another aspect of cell's physiology: surface motility [54]. Starting with flagella, their motors represent the second most widely understood and reported mechanosensitive elements in bacteria. Flagella are whip like structures that enable motility in liquid environments and surfaces. Their machinery spans the entire cells membrane and are roughly made of three main components: the whip which protrude at the exterior of the cell, the rotor, a sort of wheel-like structure connected to the whip and embedded in cells membrane and lastly the motors, membrane anchored proteins that surround the rotor and power its motion [55]

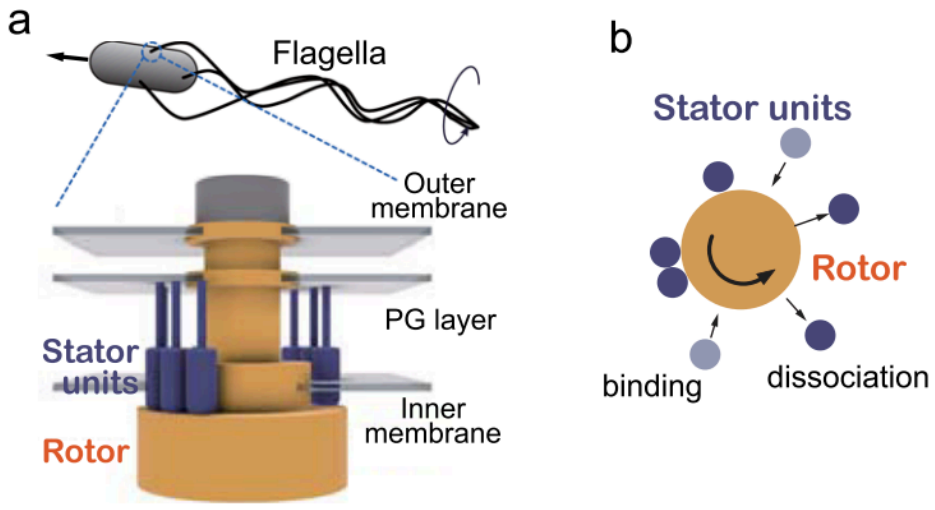

Figure 6: a) Schematic flagella structure. In grey, orange and blue are the filament, rotor and motors respectively. b) Top view of the dynamic assembly of motor (stator) units surrounding the rotor and fuelling its rotation. Adapted from [61].

(Figure 6). The whole apparatus can be imagined as a spinning wheel where the wheel is the flagella's rotor and the propelling motors are the pulleys that rotate the wheel. As mechanosensitive channels were an evolutionary response to variable osmotic environments, flagella mechanosensitivity is a response to their variable viscosity.

In fact, as this increase so does the load applied to the flagella which ultimately decrease their rotation frequency [56]. To compensate for this and restore optimal swimming speed, *E.coli* rise their rotational power by increasing the number of motors that binds to them [57-59]. As for the preceding examples this is achieved by a force induced conformational change in the motors' structure [60]. More precisely, as rotational torque increases, the extra force applied to the motors change their conformation which tighten their membrane bonds and makes them prone to cooperatively bind more sub-units

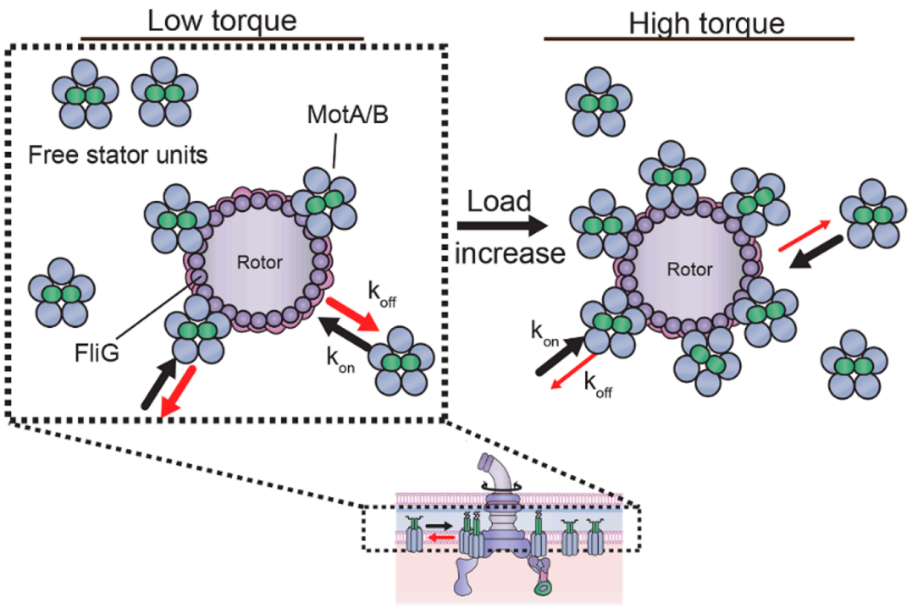

Figure 7: In *E.coli* increased torque on flagella promote the cooperative binding of motor units surrounding the rotor. This way cells can recover optimal rotation frequency upon entering mechanically challenging environments such as surfaces of viscous media. Adapted from [223].

around the rotor [61] (Figure 7).

A second example of how flagella mechanosensitivity feedback on their motility comes from *P. aeruginosa*. Within this species, viscosity dependent reduction of rotational frequency is compensated by a true change of gears. In fact, *P. aeruginosa* has two kind of flagella motors, the low and high torque generators MotAB and MotCD. Upon increasing medium viscosity *P. aeuruginosa* has been proved to shift from the more energy efficient MotAB to the power intensive MotCD, which allows it to resume optimal motility speed [62,63]. Contrary to *E. coli*, work remains to be done to elucidate the mechanism of this shift.

Together with flagella, bacteria second motorised appendages have proved capable of mechanosensitivity: pili. Specifically, type-IV pili (T4P) possess a similar structure to flagella in which they have a polymeric filament that protrude from the cell body and membrane embedded motors [64]. This time, rather than rotating, two sets of motors takes turn to either poliserised and depolimerised the filament sub-units respectively allowing its extension and retraction. When this mechanism is applied on surfaces it originates a kind of motility known as twitching where bacteria use pili to crawl on surfaces [65]. During this motion, *P. aeruginosa* T4P have been proved to adjust their retraction force on a load dependent manner. Similarly to what we have just seen happening for its flagella, *P. aeruginosa* also change pili's gears. In fact, this one has two pairs of retractive motors: PilT and PilU. When under low tensile retraction, cells mostly use PilT to retract their filaments. However, when this increase, a joint combination of PilT and PilU have been observed to exert higher retraction forces than PilT alone [66] (Figure 8). The reminiscence of this mechanism to what we have seen happening to flagella's motors suggests that, for motorised apparatuses, this gear shifting strategy could be a widespread feature in the

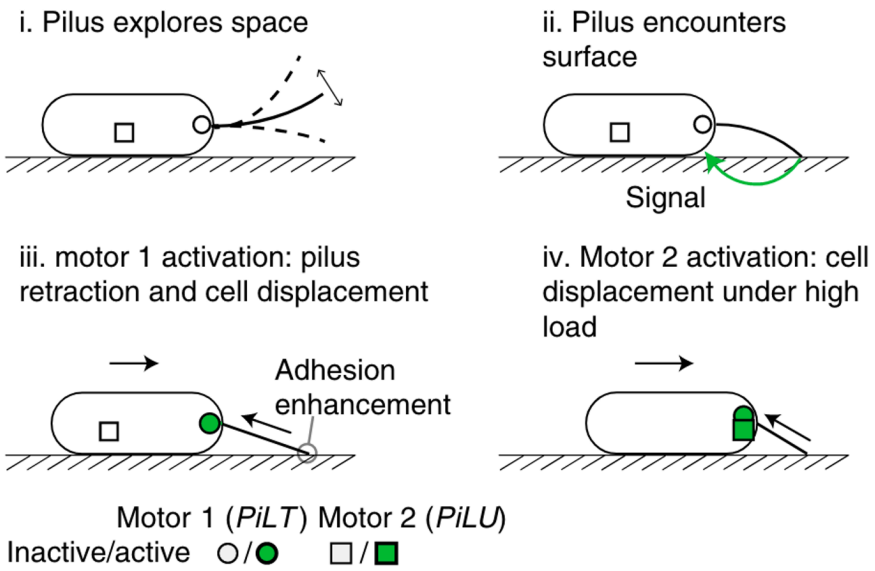

Figure 8: T4P retraction strength is load dependent in *P.aeruginosa*. Specifically, pili are in their extended conformation until they attach to a surface (i). Following this, a yet unmown mechanical signal communicate their PilT motor to retract them (ii - iii). Upon increasing load, a second retraction motor (PilU) is activated. This complement PilT and facilitate pili retraction and cell's displacement in viscous or drag rich environments. Adapted from [66].

bacterial realm.

1-3.2 Bacteria mechanotransductive pathways

The above are but a selected bunch of the most striking and well documented cases of mechanosensitivity in bacteria. While many more evidence exists regarding this, bacteria have also been reported possessing mechanotransductive pathways. These are notoriously harder to elucidate in their fullness since they require the establishment of causal chains that connect mechanical stimuli to behavioural changes. However, if mechanosensitivity is most of the time confined to alter the function of its immediate mechanosensor, mechanotransduction can broadly alter cell behaviour. Usually, the chain

of events in a mechanotransductive pathway rely on the changings in structure or function of some cellular component, most of the time a mechanosensitive element, which transduce the mechanical signal into a chemical one such as protein phosphorylation. Through mechanotrasnduction forces are therefore not limited to alter the function of a specific mechanosensors but their effect on cells can touch on many different physiological outputs such as biofilm formation [67], swarming motility [68] and pathogenicity [69]. Despite not being completed in their causal chains many mechanotransducive pathway have been proposed in the past few years. These fall into mechano-chemical or mechano-electrochemical transduction. The former are pathways where the mechanical information is transformed into a chemical signal without any intermediate step. Electrochemical transductions transduce instead mechanics into chemistry by passing through an electrostatic step. The necessity for a final chemical transduction mostly depends on the fact that, ultimately, bacteria are chemically encoded factories which needs this language to change the program they execute. While the nature of the mechanical input can vary, the most common way mechanotransducive pathways achieve their effect on bacteria is by altering the intracellular concentration of few common chemical, particularly the second messenger c-di-GMP. The effect of this molecule is paramount in bacteria biology as it conveys the signal for the execution of many different biological activities among which those of the same mechanotransducive pathways which influence cells surface colonisation, pathogenicity and biofilm development [70].

At present, *P. aeruginosa* is the species where most of these mechanotransductive pathways have been reported. In fact, its ability to increase intracellular c-di-GMP concentrations has been observed to happen in response to different mechanical stimuli and in conjunction with some of the above mentioned mchanosensitive elements. This

suggest that these mechanosensors are necessary for many of these mechanotransducive pathways.

On this regard rising level of c-di-GMP were observed following increasing liquid shear stress on cells envelope [71] (Figure 9). This was associated with improved cells surface adhesion and was observed to be pili dependent. In fact, when these were removed, cells had lower c-di-GMP intracellular concentration and were no longer capable to increase it under flow. Pili mechanosnsitivity further appeared to be involved in mechanotransducive pathways following increasing tension load upon surface attachment [72] (Figure 10 b). In fact, as this occurs, a yet unclear change in conformation of the pili main component PilA

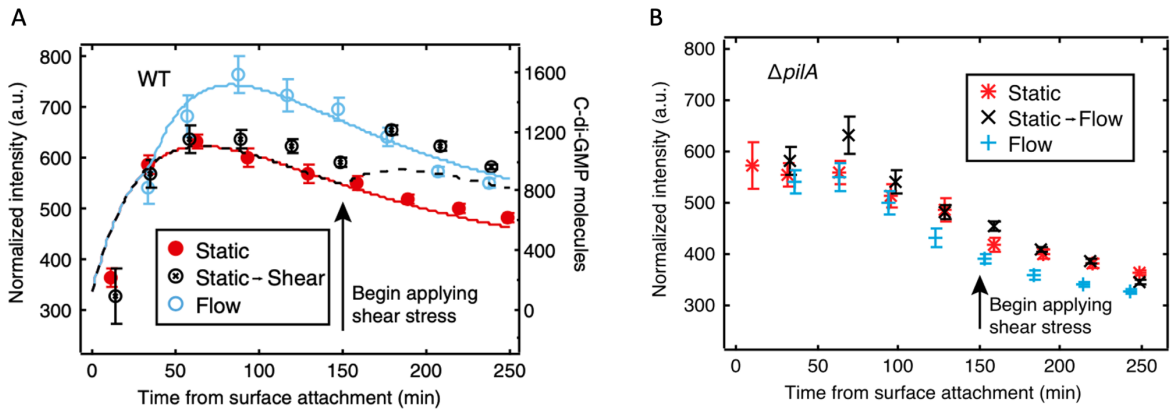

Figure 9: Sensing of shear in *P.aeruginosa* where changings in c-di-GMP intracellular concentration are followed using a fluorescence reporter. A) Over static condition, c-di-GMP levels increase overtime (red). Subjecting cells to hydrodynamic shear further increase its concentration (blue). When cells' adhesion shift instead from static to under flow, c-di-GMP levels adjust accordingly (black). B) Reduced and unaltered response are observed under flow in mutants lacking pili's major component PilA. Adapted from [71].

modulates its interaction with one of its motor components, PilJ. This one in turn activate the chemosensory element ChpA which signal the rising of another second messenger, cAMP. Contrary to c-di-GMP, this is found to increase upon surface contact but it is mostly

responsible for *P. aeruginosa* pathogenic behaviour [73].

Similar results in response to surface contact were observed in connection to another of its mechanosensor, flagella's motors [74] (Figure 10 a). In this case the mechanical signal not only rose c-di-GMP levels, but it also promoted pili activity. This is brought about by the activation of FimW, a highly c-di-GMP sensitive proteins that promotes piliation by promoting their extrusion. Flagella's motors were necessary to observe cells response as when these were removed neither changings in c-di-GMP nor pili activity were observed.

The above mechanotrasductive pathways despite lacking clear start to end mechanisms prove how well adapted *P. aeruginosa* is at sensing mechanical forces around

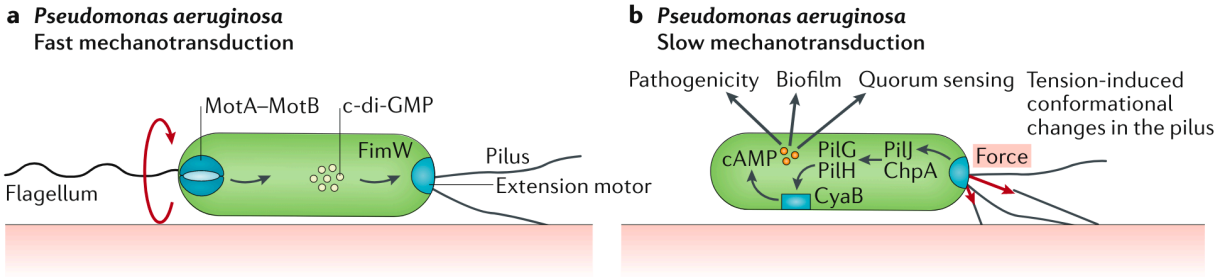

Figure 10: A combination of 'fast' and 'slow' mechanotrasnductive pathways in *P.aeruginosa* help it in at colonising surface and initiate pathogenic commitment. a) Fast surface sensing depends on flagella's motors (MotA/B). In response to increasing torque when near a surface, they send a yet unknown mechanical signal that increases cells c-di-GMP levels. This activates pili through the c-di-GMP dependent activation of FimW, a protein that promotes piliation by activating their motors. b) Slow mechanotransduction happen instead in response to T4P's increased tensile load upon surface adhesion. Through a yet unclear conformational change, tensile load in their filament is sensed by PilJ, a motor binding component that activate the chemotactic element ChpA. This one is ultimately responsible for a signalling cascade that rise cells cAMP intracellular concentration which prime cells to virulent behaviour. Adapted from [6].

it and use them to its advantage. As a pathogenic bacteria used to crawl on its host tissues, the ability to sense shear and use this as a signal to boost surface adhesion and colonisation generate a positive feedback that favour further infection. A nice and fulfilling picture appears then of how *P. aeruginosa* can regulate surface colonisation and its further commitment to pathogenicity. In fact, from the last two examples from above, *P. aeruginosa* seems to have two distinct surface sensing mechanisms. A quicker one based on flagella mechanonsensitivity which through c-di-GMP spikes enhances its adhesion by quickly deploying pili and a slower one that uses cAMP in response to pili load to activate pathogenicity and quorum sensing. The surface act then as a starting clue that prime cells virulence to which they will only commit if enough conspecifics are nearby. Through the use of this AND logic gate, which require both surface and quorum sensing to activate pathogenic behaviour, *P.aeruginosa* is capable to distinguish between peaceful and aggressive surface colonisation [72,74,75].

Mechanotransductive pathways are not exclusive to *P. aeruginosa* as their mutual presence is observed in many other species among which *C. crescenstus*. In this one following surface contact, both flagella and pili have been observed to induce the c-di-GMP dependent secretion of a polar adhesin known as the holdfast [76-79] (Figure 11). This is crucial to the species life cycle as it allows it to quickly colonise surfaces by holding tight onto them.

The mechanotransductive pathways discussed up to this point are all reported to happen as a conversion of a mechanical input (surface, shear or tension) into a chemical output (c-di-GMP or cAMP). However, this is not the only way this could happens as changings in cells electric potential have also been proved to partake the process leading to mechano-electrochemical transduction.

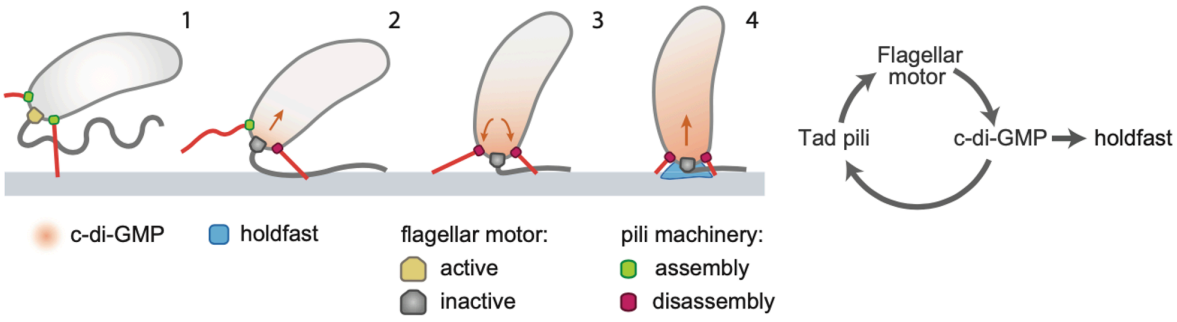

Figure 11: *C.crescentus* uses the joint functioning of pili and flagella to sense and attach to surfaces. Swimming cells use their pili to initiate surface adhesion (1). Following this, through a yet unclear mechanism, mechanical load on their flagella's motors induces c-di-GMP synthesis (2) which further stimulate pili retraction (3). This increase surface mechanical signalling on flagella, initiating a positive feedback which further increase c-di-GMP concentration. As this reach a critical threshold, it finally activates the machinery required for the secretion of their polar adhesin, the holdfast, which consolidate cell's hold on the surface (4). Adapted from [78].

In this one a mechanical input is always transduced into a chemical output but through an electrical intermediate. On this regard, while pathogenic strains of *E.coli* are well known to rely on similar pili and flagella dependent mechanotransduction pathways to induce pathogenic behaviour upon surface contact [69], domesticated strains have shown a more peculiar transductive behaviour. In fact, *E. coli* appears to be able to rise its c-di-GMP concentration following changings in its membrane voltage. Specifically, different studies have highlighted how, in response to surface contact, *E. coli* initiate rapid oscillations in its polarisation known as 'electrical spikes' [80] (Figure 12). Their dependency on mechanical cues was further strengthen observing their frequency, intensity and duration increasing when cells were pressed under agarose gels [81]. Although a clearer connection remained to be established, these sparks correlate with alkaline spikes in cells internal pH and c-di-GMP [82]. This final step is the suggested culprit for the signal

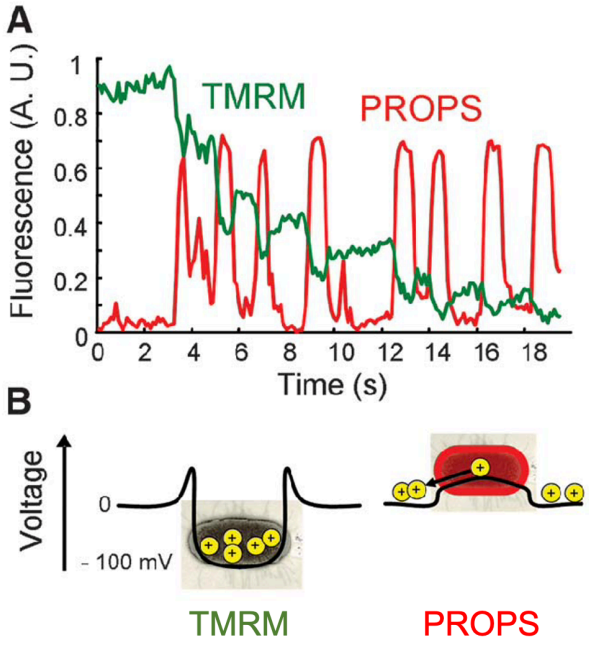

Figure 12: *E.coli* electrical "spiking" behaviour. Upon landing on a surface, cells polarisation fluctuates in time (A). This process is captured from the change in fluorescence of the cationic (TMRM) and anionic (PROPS) dyes (B). Specifically, when cells polarisation decrease (cells interior gets less negative) TREM and PROPS intracellular concentration respectively decrease and increase. This can be seen happening in A from the concomitant drops in TREM and increases in PROPS fluorescence. Adapted from [80].

electrochemical transduction. In fact, while through some yet unknown mechanism surface landing alters cells polarisation, this one is responsible for cytoplasm basification and subsequent c-di-GMP synthesis.

What I discussed in the preceding sections are few insightful examples of the complexity, breadth and vibrant role that cells mechanobiology cover on both mammalian cells and bacteria. From this it can be appreciated how, through both mechano-sensing and transductive pathways, forces appear to play a fundamental role in many aspects of cells biology shaping both their body and behaviours. All of this looks very technologically promising as, similarly to how much chemical cues have been used to control cells behaviour, also mechanical forces could be exploited to the same end. Examples of this already exists as mechanical forces have successfully been used to alter cells behaviour specifically cells differentiation [83-87]. In fact, mechanical forces in the form of surface vibration have been used to induce stem cells differentiation into osteoblast [88]. Despite the

very recent nature of these and other studies on the process, mechanical signals appear effective to direct cells mechanobiology and its many physiological processes.

However, at present, this only holds true for mammalian cells. In fact, to our knowledge, little to no attempt have yet been made to exert the same level of mechanical control on bacteria mechanobiology. Here is therefore where our work is located. In the above-described panorama of bacterial mechanobiology, I would like to explore if what is already true for mammalian cells could also be for bacteria as their mechanobiology is exploited to control their behaviour. To test this point I decided on staying close to the already existing mammalian literature and tested the effect that mechanical stimulation in the form of surface vibrations had on bacteria physiology and behaviour. But which aspect of bacteria's mechanobiology can be influenced? One answer quickly appeared to us: surface colonisation. The above discussion on cells mechanobiology provides some hints on the reasons behind our choice but, to better see how this came to be, we need to dig a little more into cells biology starting from one of its most remarkable and troublesome features, biofilms.

1.4 Biofilms and bacteria surface colonisation

Not later than few decades ago scientists came across something not entirely new but long neglected: biofilms [89]. These are generally and loosely referred to as heterogeneous microbial communities which develop on surfaces and, similarly to mammalian cells, are sheltered by a shared extracellular matrix (ECM) [90]. Specifically, biofilms grow and develop on almost any natural and manmade surfaces, following a process that, despite being species and environmental dependent, it is commonly described as divided into three main stages: *(i) surface colonisation*, where seeding cells or

cluster of cells colonize the surface, *(ii) maturation*, where the main characteristics of a biofilm appear, such as the fully assembled matrix and division of labour, and finally *(iii) dispersion*, where a mature biofilm goes full circle releasing single cells or bundles in the environment promoting further colonization [91,92]. Despite cells lack biofilm specific genes, their development is incredibly well orchestrated both in time and space which, according to recent report, appear akin to even embryo development [93]. From a row number perspective, biofilms are the most common way of life for bacteria as they can be found all over the biosphere, from the height of the atmosphere down to the deepest crevices of the oceanic subsurface [94,95]. What makes them such a successful evolutionary choice capable to occupy so many environmental niches is their peek into social organization [96]. In fact, as microbiological fortresses encased in ECM, biofilms allow the flourishing of heterogeneous and multispecies communities within their walls [97]. Cellular communication [98], differentiation [99], division of labour [96,100,101] and the sharing of genetic material [102], public goods [103] and metabolites [104] are some of the advantages made possible by living within a biofilm. In fact, their conjunction enhances cells resilience and fitness toward many common natural insults such as predation, starvation and both mechanical and chemical stressors [105].

Such biofilm's resilience represents both an opportunity and a scourge from a human perspective. On the bright side, biofilms' ability to function as small multicellular factories capable to withstand harsh environmental conditions have attracted a lot of technological interest. Their most common application sees them used in water implant for their purification and bioremediation [106]. However, more recently, their mechanical and social structures are also under investigation to be respectively exploited as living materials and bio-factories. Specifically, their sturdy mechanical properties and the ability to self-

repair from environmental damage are leading to their preliminary applications as smart concretes [107] and self-healing materials [108]. Moreover, their social structure leading to both cells differentiation and division of labour is receiving a lot of attention in synthetic biology. Here, researchers are trying to capture biofilms social features and create synthetic consortia [109-112]. Within these, genetically engineered cells can grow and interact as if they were in the safety of wild biofilms but with the added twist that they can now serve human purposes. In fact, because of their added social complexity, consortia have the potential to surpass single cells suspensions in all their current applications such as biofuel production [113], drug synthesis [114] and biocatalysis [115].

The above are areas where biofilms and humans meet under a peaceful light but as mentioned, this is only half of the story as biofilms are also seen as a persistent biological threat. In fact, because of their ability to colonise and persist on virtually any surface, overtime biofilms can cause equipment malfunctioning and its failure via a conjunction of biofouling and biodegradation. This has a considerable economical effect on most technological and industrial settings as only few are immune to biofilms reach. Water networks [116-119], ships transports [120,121], solar implants [122], food processing [123-125], fuel storage [126], aviation [127] and space flight [128-130], all to some extent feel biofilms' negative influence. However, where biofilms deleterious impact fall more harshly is on our health care as here they can directly affect or end our lives. What makes biofilm's infections so much hard to deal with is once again their resilience to stress [131,132]. In fact, because of the damage it would cause to tissues, biofilms mechanical removal is out of question in many medical circumstances. Moreover, their encasing matrix, mixed composition, genetic exchange and differentiation into dormant cells makes them recalcitrant to the most common therapeutic treatments, especially antibiotics [133-136]. While we are still poorly

armed against biofilms attacks to our bodies not everything is lost as encouraging results are coming our way, particularly from unexpected allies such as viruses. On this regard, bacteria targeting viruses or bacteriophages have proved effective at dissipating biofilm and limit their infectivity [137]. Furthermore, biofilm social structure while being the source of their success can also contribute to their downfall. In fact, researchers are finding ways to undermine biofilms by targeting their social dynamics [138]. Specifically, the use of chemical that suppress the production of commonly available substances, known as public goods, induces something akin to cheating behaviour in the community reducing cells' ability to cooperatively assemble the biofilm. Promoting this sort of social unrest has proved to cripple ECM formation leaving biofilms exposed to the use of old weapons as antibiotics.

The above discussion shows how hard it is to deal with biofilms when these are fully fledged and formed and it explains why a lot of experimental effort is trying to circumvent the problem by preventing their formation. Central to these efforts is the investigation of biofilm's very first developmental step: surface colonisation. Here, I can finally leave the tangent I have been following on biofilms and go back on our argument of why I aim at influencing surface colonisation using mechanical cues. From its crucial involvement in biofilm formation and its widely reported reliance on mechanotransducive pathways, surface colonisation it's in fact the perfect target that tie together mechanobiology with a great technological urgence. However, until now I kept referring at surface colonisation without giving a clear picture of what this is and how bacteria perform it. Therefore, before entering the details of how others and I aimed at controlling this process, it's time to spend a few words describing how this happens.

Bacteria surface colonisation is a loosely defined terms that applies to all scenarios

where cells attach to surfaces and start growing on it. As we have seen it is a prerequisite to biofilm formation and its usually a step which takes a few hours to complete. The reason behind this time window is dictated by surface colonisation most characterising feature: cells phenotypic transition. Bacteria living in their environment are defined as either planktonic or sessile. These are broad labels that indicated the "gears" or genetic circuits which are active and dictate cells behaviour at any given time. Planktonic refer to the most idealised picture of a bacterium one can have, a single cell swimming and dividing in its environment. However, when bacteria bundle together or attach on surfaces their phenotype drastically change as they turn sessile [139]. This is instead bacteria surface associated lifestyle which sees them non-motile and stickier as they secern adhesins to consolidate their position on the surface.

Several reports exist of abrupt change in gene expression before and after surface exposure with mutually exclusive pathways being selectively activated suggesting that a true phenotypic change is taking place [140,141]. One common feature of this planktonic to sessile transition is the increase intracellular concentration of the second messenger c-di-GMP. As we have seen above, this molecule plays a central role in influencing cells behaviour by activating and suppressing gene expression within the cell. This enable scientist to use c-di-GMP as a chemical tag for cell's statuses where high and low concentrations are identified with respectively sessile and planktonic phenotypes. Despite our still fragmented understanding of the gene's differential expression during surface colonisation and sessile transition [142], from this mosaic experimental evidence a mechanistic description of the process is emerging (Figure 13).

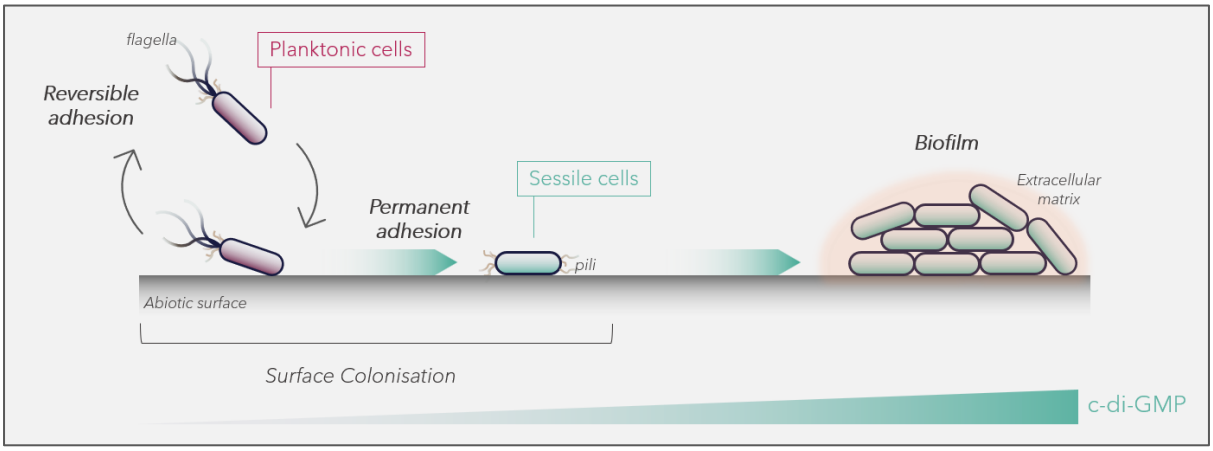

Figure 13: Schematic representation of cells surface colonisation and biofilm formation. From left to right, cells colonise a surface transitioning from *planktonic* to *sessile* phenotypes. In this process cells use their flagella and pili to sense surfaces. Through a series of reversible mechanical interactions this would rise their c-di-GMP intracellular concentration which would improve their adhesion and turn it to permanent. Once firmly established on a surface cells duplication and secretion of an extracellular matrix would then lead to a biofilm.

Above all, planktonic bacteria need to reach the surface which they do through either active swimming or passive Brownian motion and sedimentation [143]. Then cells are assumed to make physical contact with the surface. How quickly and reliably this happen would greatly depends on the affinity between cells physiological state and surface physico-chemical properties [64,144]. Cells that have appendages and adhesins would increase their chances to interact with the surface facilitating their adhesion. Following this, a sequence of mechanical contacts turns cells from surface "naïve" to surface "sentient" while in response to each interaction cells begins to rise their intracellular c-di-GMP levels [145]. As I have discussed, this makes cells 'surface-ready' by promoting adhesin secretion, suppressing flagella motility and allowing them to turn their adhesion from reversible to permanent so completing sessile transition. At this point cells are well adapted to their new mechanical environment, are firmly attach to the surface and, based on the density of

the surrounding colonisers and the nature of the surface, they can initiate different process such as pathogenicity [75,146], swarming [147] or biofilm development [148]. With this picture of cells surface colonisation and its relevance in biofilms development, the stage is set to discuss which strategies have been developed to control the process.

1.5 Physico-chemical techniques to control surface colonisation

As I discussed, because of its key position in biofilm development and their extreme resilience to treatment, surface colonisation shifted the dogma of how these can be controlled. Specifically, many strategies had been developed in the past decades, the most common and well-established of which revolve around the chemistry and physics of bacteria surface colonisation [144,149]. This gave birth to two main approaches, which, depending on the fate of surface approaching cells, are classified as either biocidal or anti-biofouling. The former aim at killing surface colonisers while the latter simply hinder their adhesion. However, despite their different ways of action, they both limit surface colonisation using either destructive or disrupting physico-chemical interactions between cells and surfaces.

For this to be achieve, surfaces are modified either chemically or physically [150] (Figure 14). Specifically, chemical strategies attain antimicrobial effects via various kind of surface functionalization. These can in fact be coated with a plethora of chemicals which can either have antifouling properties or antimicrobial affects upon contact or their release. Biocompatible polymers and polymer brushes are of the most recent and stronger example of surface decorating chemicals showing remarkably good anti-biofouling properties [151].

Different biocides have instead been employed as coated agents capable to kill bacteria that reach surface. Antibiotics [152], lysozymes [153], antimicrobial peptides (AMP) [154] and inorganic nanomaterials [155-157], particularly silver nanoparticles [158], have all proved to be greatly effective in preventing bacteria colonization. In their most recent embodiment,

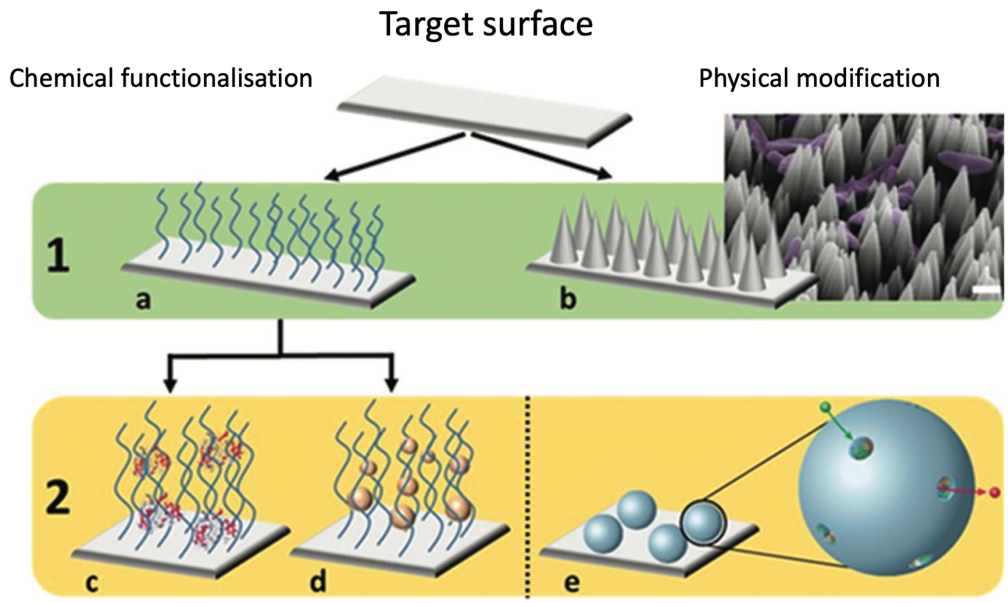

Figure 15: Current physico-chemical strategies to control bacteria surface colonisation. Chemical functionalisation (1a and 2e) decorates the surface with polymers or nanomaterials that can be further functionalised with biocidal chemicals (2c, d). Physical modifications inhibit instead cells interaction with the surface by altering its morphology and topology. This mostly reflects in the biocidal puncturing and killing of surface approaching cells or the obtention or super-hydrophobic surfaces. Adapted from[150]

these are dispersed into a polymer coating which act as an entrapping matrix.

However, rather than being passively released in the vicinity of the surface, these new smart surfaces use bio-responsive polymers that change their conformation following several environmental clues [159-161]. This allow the on-demand release of the biocidal

chemicals which can act on cells only when these are present. Evocative example of this approaches is the use of pH sensitive polymers. Representative of this class of polymers is poly(methacrylic acid) (PMAA) [162] (Figure 15). Because of its abundant -COOH residues it has remarkably different physico-chemical properties at low or high pH. In fact, under acidic conditions (pH < 4), almost all its carboxy groups are protonated and the polymer structure curl on itself.

However, upon increasing the pH, more and more group deprotonates expanding

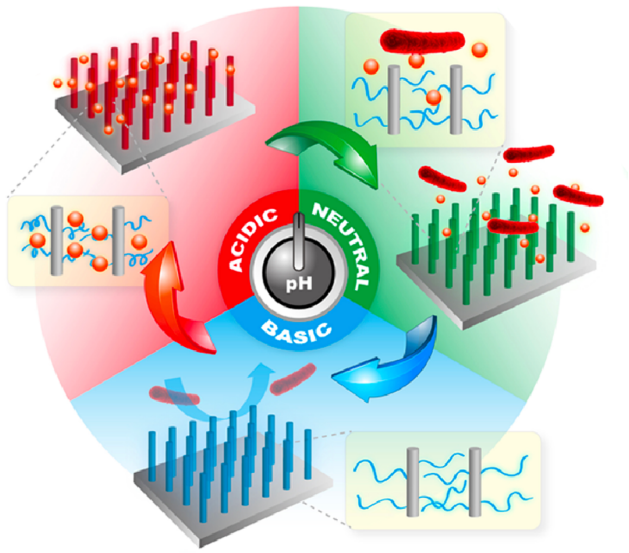

Figure 15: pH sensitive smart bactericidal surfaces. These are functionalised with pH sensitive polymers such as PMAA. At low (acidic) pH these are loaded with biocidal agents (red spheres) whose release is triggered by PMAA conformational change at neutral pH. After these are released, dead cells can be removed from the surface by further increasing the pH. In fact, under basic conditions, PMAA residues are mostly negatively charged allowing them to repel similarly charged cells. Adapted from [163].

its structure. In fact, as more $-COO^-$ appear, this one swallow and stretch to diminish their electrostatic repulsion. As such, while PMAA is curled and electric neutral in acidic environments, this one become stretched, fully hydrated and negatively charged when these turn basic. These properties allowed researchers to trap biocidal chemicals such as AMPs or lysozymes into surface functionalised PMAA at low pH (~ 4). These were then released at physiological pH (~ 7) during cells colonisation with on-demand biocidal

activity. Moreover, because of bacteria negative surface charge, these can also be removed from the surface after killing by further increasing the pH to basic (~ 10). In fact, the strong electrostatic repulsion with the plentiful PMAA's carboxylate groups (-COO^-) appear to successfully clean the surface before reloading this one with a new round of biocidal compounds Figure 15**Error! Reference source not found.**).

Aside from chemical functionalisation, the modification of surface physical properties has also become praxis in controlling bacteria surface colonisation. This field took inspiration from many naturally occurring surfaces such as shark skin, lotus leaves cicada wings and many more which are notoriously resilient to bacteria colonisation [163-165]. Similar nanostructures and topologies had therefore been synthetically emulated on many different materials with the intent of recapturing the success of their natural archetypes [166]. From these, two biomimetic approaches emerged: antifouling and mechano-bactericidal. The first one takes most inspiration from shark skin and lotus leaves and see surfaces manipulated to create micrometric patterns. Thanks to photolithographic and imprinting techniques, these have then evolved into numerous different features among which ridges, cones, pillars, pits and ribs are the most common ones. These can vary in both forms and shapes but all share the same intent of reducing the available area to colonising cells. This is done by hindering their mechanical interactions with the surface through enhanced hydrophobic properties [167]. Specifically, these surfaces achieve super-hydrophobicity through the entrapment of micro- and nano-metric bubbles within their features [168].

This phenomenon greatly hinders bacteria surface interactions with remarkable antibiofouling effects.

Contrary to patterning techniques, mechano-bactericidal strategies limit cells colonisation by killing cells using morphologically controlled nanometric features [169] (Figure 16). These can be divided into rigid features such as pillars, cones or columns

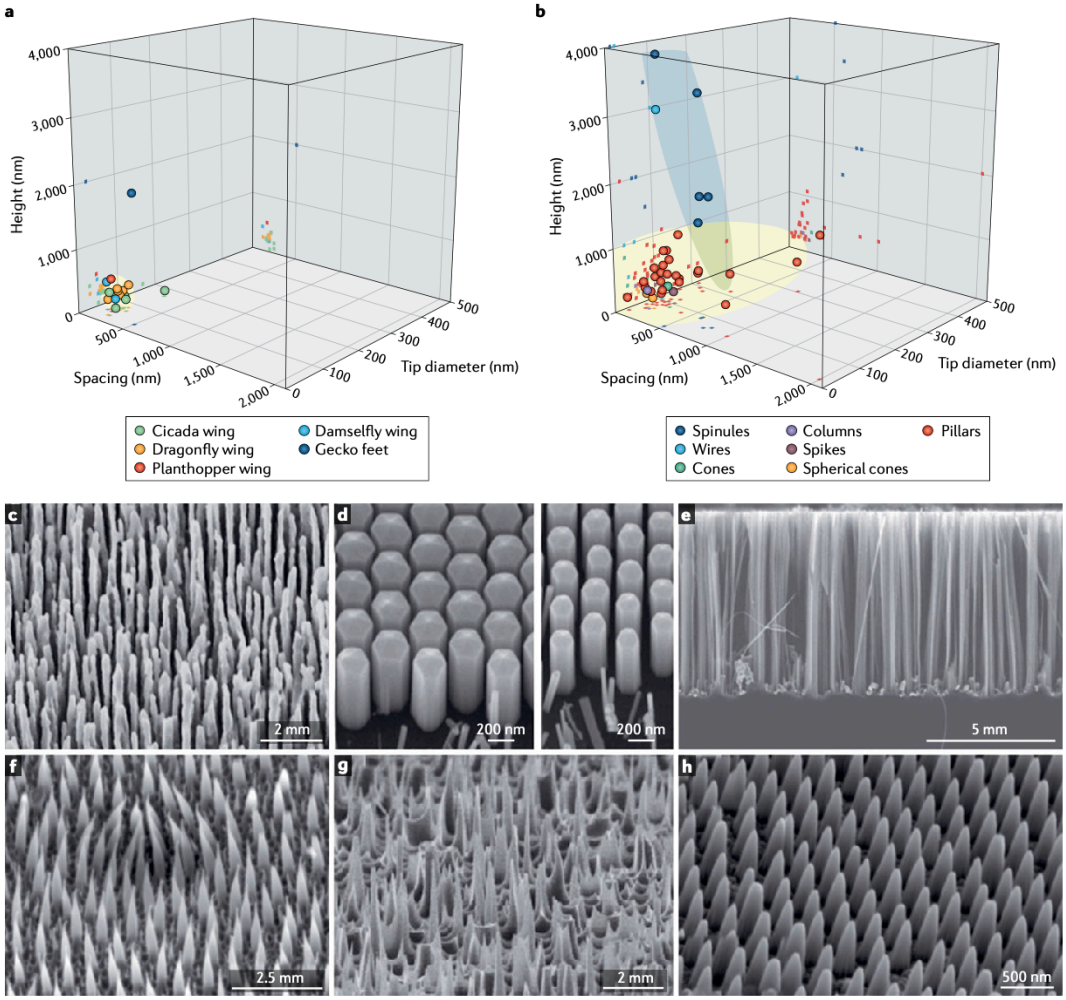

Figure 16: 3D spaces of features diameters, heights and spacing in cicada and dragonfly wings (a) and their synthetic equivalents (b). As can be seen, features need to possess specific values to induce mechano-biocidal effects on cells. These are mostly bound in the bottom left corner of the spaces above, within a fictitious space cube of dimensions 200 x 1000 x 500 (diameter x height x spacing). c-h are SEM images of artificial nanopillars (c), nanocolumns (d), nanowires (e), nanospinules (f), nanospikes (g) and nanocones (h). Adapted from[173].

which do not bend upon cell contact, or flexible features such as nano-spears, spikes or tubes. These techniques are mostly centred around the emulation of the cicada wings' effect which use nanometric spikes to kill surface engaged bacteria [165]. However, not all nanometric features are effective at killing cells. In fact, it has been experimentally and theoretically proved that, for this to be possible, such features need to possess specific aspect ratios without which these won't have any effect on cells [170,171]. However, when these conditions are met, the adhesion force acting between the feature tips and cells membrane cause these to break, leading cytoplasm leakage and the ensuing cell's death [172] (Figure 16).

However, despite their promising experimental success, several drawbacks and unknowns cripple the applicability of physico-chemical strategies, especially in medical settings. First, releasing and functionalising chemicals can get deplenished and biodegraded over-time shortening their lifetime and applicability window. Moreover, when antibiotics are employed as diffusible biocidal, their progressive deplenishment can expose bacteria to sub-inhibitory concentration and promote the insurgence of antibiotic resistances, stressing what already is a worldwide problem [173,174]. When nanoparticles and nanomaterials are used instead, little is known of their long-term cytotoxicity limiting the prospects of their medical applications. Physical approaches, while being intrinsically more durable and not affected by chemical deplenishment, are not immune from drawbacks. In fact, their efficacy has proved to be species specific. Gram positive bacteria are notoriously more resistant to many mechano-biocidal approaches because of their thicker cell wall which limits the application of these approaches to generic, all-rounded scenarios [175,176]. Both chemical and physical biocidal techniques are also affected by the very thing they try to circumvent: biofouling. In fact, over time, killed cells and debris can

cover the surface and, if not promptly removed, could limit its biocidal activity. While this is partially offset in smart surfaces using responsive polymers [177], mechano-biocidal strategies do not have yet a clear way out of this problem.

Medical applications using implants are further complicated by the fact that preventing surface colonisation in implanted materials is not enough. In fact, after implantation a so called "race" for the surface begins between bacteria and tissues cells [178]. Successful functionalisation should disqualify bacteria and allow tissues to win the race. Implant materials while they are carefully selected to allow tissues colonisation, they can seldom prevent bacteria to do the same. As we have seen, the physico-chemical treatment of the surface could solve the issue but not all implant materials can be physically modified and their tissues biocompatibility can be limited by their chemical functionalisation. Despite some attempts proved successful in promoting mammalian colonisation while limiting bacterial [179], finding the right combination of parameters that suit the requirement of a particular medical application remains a challenging task. When the above issues are then compounded by the still high cost of surface functionalisation, it explains why these techniques are not yet widely applied. To compensate for part of the above issues, a newer kind of approaches had developed the past few years. How these aim at influencing surface colonisation is not via its functionalisation but, rather, its own kinetics.

1.6 Kinetic control of bacteria surface behaviour

The above methodologies while being different in their execution shared the same fundamental logic: functionalise the surface to hinder colonisation. However, in all the approaches discussed above the surface played a static role as it needed to do nothing but provide the support required to achieve the desired functionalisation. Opposite to these

approaches are kinetic ones. These new bunch of methodologies shared the same "surface centrism" but invest the surface of a more active role as they influence colonisation using its kinetic properties. Undulatory surface phenomena such as vibrations, oscillations and standing waves all proved capable to alter cells surface behaviour in three main ways: (i) mechanical inhibition (ii) morphological patterning and (iii) hydrodynamic sweeping.

Strong evidence of mechanical inhibition of surface colonisation was observed with *P. aeruginosa* [180]. Within this species, vibrating polystyrene surfaces over 24 hours at 200 Hz to 4 kHz and 30 nm amplitudes suppressed biofilm formation. The observed reduction was frequency dependent with least biofilm forming at 1 kHz (64% reduction in biomass). Similar results were obtained with *E. coli*, *S. aureus* and *S. epidermidis* after 1 hour vibration at 158-168 kHz and ~150 nm [181]. However, this time the response was both strain and material specific as this was stronger in *E. coli* when surfaces were plasma treated before employment while the outcome was opposite for *S. aureus* and *S. epidermidis*. Encouraging result have also been observed when samples were vibrated at lower frequencies and wider amplitudes of respectively 4 - 40 Hz and 1 mm [182]. However, while *S. epidermidis* remained sensitive to the above combinations, these no longer decreased surface colonisation in *E. coli*. Despite the resulting effect on cells colonisation, it remains yet unclear which mechanism could be responsible for the effect that mechanical vibrations have on cells.

Aside from the above mechanical suppression, surface oscillations and vibrations have instead been reported to promote biofilm formation and influence its morphology. On this regard, standing oscillatory patterns between 100 Hz and 1.6 kHz with micrometric amplitudes proved effective at promoting biofilm formation over 48 hours in both *P. aeruginosa* and *S. aureus* [183]. Interestingly, on both species the resulting biofilms

shared the same morphological features of the vibrational pattern suggesting that these can be used to shape their structure. This same morphological control was confirmed and finely controlled when researchers looked at biofilm formation in thin liquid layers [184]. Under such shallow water conditions, vibrational patterns are known to transfer to the submerging liquid and generate what are known as Faraday's waves. Surface acceleration dictates the stability of these patterns and their effect on surface colonisers. For frequencies of 120 Hz, surface accelerations between 2 to 3 g led to stable Faraday's waves which promoted *E. coli* biofilms over 48 h with consistent morphological transfer of the vibrational pattern from surface to biofilm. In contrast, 7 g accelerations disrupted

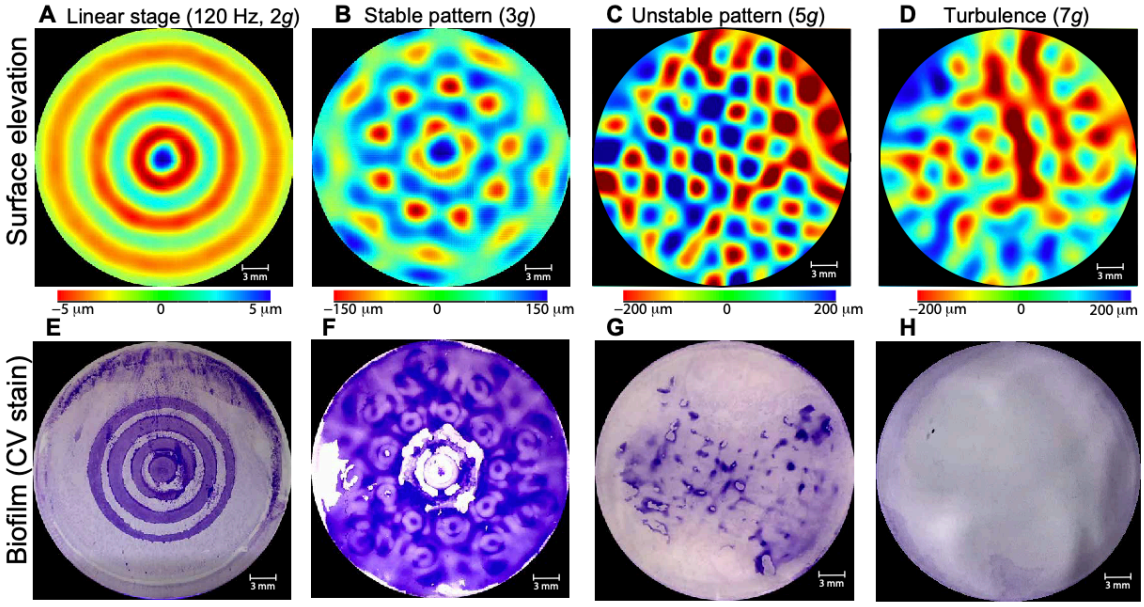

Figure 17: Biofilm development and morphological control in shallow water conditions under different vibrational regimes. Biofilm formation depends on the stability of vibrational patters and their associated Faraday's waves in the liquid. A to B and E to H are the simulated patterns and the resulting stained biofilm after 24 hour for different surface accelerations g. Stable patters (2-3g, A and B) transferred to the growing biofilm and promoted its formation (E and F). Unstable and turbulent patterns, from higher surface accelerations, (C and D) suppressed biofilm formation (G and H). Adapted from [185].

vibrational patterns and hindered biofilm formation via the turbulent motion of the liquid in the samples (Figure 17).

This last observation together with recent findings show how kinetically induced hydrodynamic effects are detrimental to surface colonisation. Specifically, millimetric surface waves can induce vortexes in close proximity to the surface with outstanding anti-biofouling performances in *E.coli* [185]. In fact, when such waves are sent across the surface every 3 s with an amplitude of 0.4 mm, they decreased bacteria colonisation over 18 hours by up to ~ 90%. Under these conditions strong vortexes are created in the liquid by the travelling surface waves which, acting as a hydrodynamic sweep, interfere with bacteria's ability to reach and colonizing the surface.

Together the above shows how kinetic approaches have the potential to overcome some of the issue affecting more consolidated physico-chemical strategies. For instance, they do not need any form of surface functionalisation which entirely remove all the issues associated with their cytotoxicity, biocompatibility and cost. Moreover, the fact that they lack diffusible chemicals and are non-biocidal increases their lifetime applicability and reduce fouling by dead cells, leading instead to potential self-cleaning features. While technical concerns can rise over the feasibility of achieving surface kinetics on any technology relevant material, despite their little number, these studies show how this approach represents a promising way to influence bacteria colonisation.

So far, both physico-chemcial and kinetic approaches described in the preceding sections share a common feature which is their surface centricity. They all aim at influencing cells colonisation by putting the surface on the foreground. So far this had proved a successful strategy but in doing this cells' role and their agency had instead shifted in the background. However, as we have seen, cells can do much more than

passively experience the surface and attach to it. So, it is time to discuss where our approach is different and how this can impact the modern context of both bacteria surface colonisation and more broadly, their mechanobiology.

1.7 The end and the beginning - aim of study

As I mentioned, the aim of my work is to assess the influence that mechanical stimulation has on cells surface behaviour. On this, my approach shares similarities with some of the most recent kinetic strategies, particularly those which use surface vibrations [180]. However, despite the similar tools employed, my approach is prospectively different because of few characterising features, first of which a renewed focus on cells agency.

We have seen in the past sections how rich bacteria mechanobiology is and how it is often employed in surface sensing and adaptation. Consequently, the way I would like to influence these processes is by tickling cells. In fact, using mechanical cues of different intensities and frequencies, I aim to alter cells surface mechanotransduction and understand its impact on their surface behaviour.

How I would like this to be done on an experimental ground bring us to my second characterising feature: the focus on cells stimulation. Not all physical cues when applied to living organism are classifiable as signals or stimuli. For these to be considered as such they need to belong to a scale the organism is capable to sense. For this reason, I used surface vibrations to deliver stimulation intensities that bacteria have been reported to sense and respond to.

The goal of my work is therefore twofold as it has both a narrow and broad one each bringing its own benefits. On the narrow side, intent of my work is mainly what I just

discussed above: to understand *how mechanical stimulation can influence cells surface behaviour and colonisation* (Figure 18). Exploring this question can contribute to the field of surface colonisation in few ways. First, by focussing on cells mechanical stimulation and its physiological effect, my work can help explain the yet unknown mechanism through which some of the kinetic approaches above discussed achieve their effect. This would provide investigators with a conceptual framework that can both elucidate existing findings and help in achieving new ones. Moreover, the ability to control surface colonisation can have immediate benefit in all those applications where biofilm formation is involved.

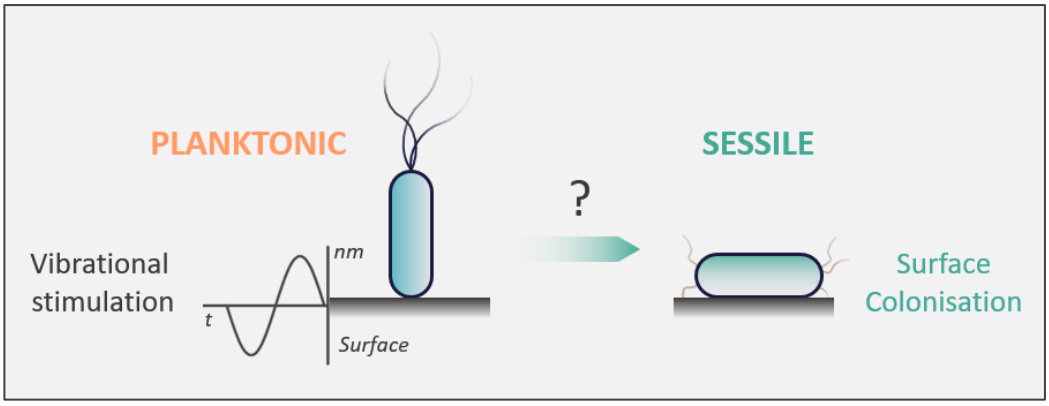

Figure 18: Aim of our work is to understand how vibrational stimulation can influence surface colonisation and cells planktonic to sessile transition.

Finally, on a broader side, my task touches the question: *is bacteria mechanobiology a viable strategy to control their behaviour*? We have seen how much bacteria's mechanobiology has grown and how rich the field has becoming. So, similarly to what has already been done in mammalian cells, I would like to assess whether bacteria mechanobiology can be exploited in much the same way. Finding a positive answer to this question could change our ways of thinking about bacteria. Far from being the sometimes

too familiar bag of proteins, passive to their environment and sensitive to chemical and eventually optical cues only, we could establish mechanics as a new channel to direct and control their behaviour. My work is specifically oriented on surface colonisation but, if successful in its intent, it would open the door to the exploration of how other mechanobiological process and their physiological outcomes could also be influenced through cells mechanical stimulation. Biofilm development, swarming, motility and cells pathogenicity could all become new targets that can be controlled in new ways. To summarise, from a more informal and allegorical point of view, by understanding how bacteria respond to tickling I would like to learn how to better communicate with them.

With a contextual perspective for my work, an appreciation of the richness of bacteria mechanobiology and a hopefully clearly stated intent, it is time to end setting up the stage and begin our journey into bacteria's tickling sensation.

1.8 What to expect — Thesis outline

Above was an introduction and stage setting of the work that will be discussed in the coming pages. However, before blindly dive into this, I offer here a concise synthesis of the overall thesis structure highlighting the chapters' content.

1. **INTRODUCTION:** it provides the context to my work. It summarises the present day 'wall of knowledge' into which I locate the missing brick of my research. Specifically, it discusses the role of mechanical forces in directing both mammalian cells and bacteria behaviour. The argumentation centre around the idea that eukaryotic mechanobiology has led to applications in the way this can be used to control their behaviour. Lacking a similar approach in bacteria, my work set to

compensate for this. Precisely, I aim at using mechanical forces to control one of bacteria force-directed behaviours: surface colonisation.

2. **PROCEDURE DEVELOPMENT:** it presents the preliminary work performed toward achieving our experimental goal. It treats the details regarding growing conditions, stain employment, surface choice and imaging technique required to achieve and quantify surface colonisation on non-vibrated samples.
3. **VIBRATIONAL STUDIES:** it dwells in recounting the main findings of the effect that vibrational stimulation has on cells surface colonisation. It begins with an engineering introduction of the relation between vibrational stimulation and force intensity. Then it shows how pN forces of kHz frequencies can reduce cells coverage on surface. Finally, it expands the understanding of this effect by exploring the negative influence of cells sedimentation, the non-linear dependency with stimulation length and its independency from cells' surface habituation. Finally, the chapter ends on exploring how mechanical stimulation is not harmful to cells' envelope.
4. **MECHANISM HUNT:** this is my last experimental chapter and concludes my work. It explore the work I did to connect vibrational stimulation as an input to reduced colonisation as an output by the mean of a mechanism. If begins by identifying the biological nature of the effect vibrations have on cells. It then identify this as dependent on cells polarisation of which the chapter will discuss its changings upon stimulation. After showing how this hinders cell surface polarisation, it will discuss how it won't affect cells surface motility but it is dependent on their flagella's motors. The suggesting of a mechanism explaining vibrational effect on surface colonisation will conclude the chapter.

5. **CONCLUSION AND PERSPECTIVE:** In this final section I go through the main findings and novel understanding provided by my work. Briefly, vibrational cues of pN intensities and kHz frequencies (ms periods) are an effective stimulant to cells capable to reduce their surface colonisation. This is found to correlate with cells reduced polarisation but not motility on vibrated samples. I suggest that ion fluxes, following vibrational triggering of membrane channels, are responsible for the hindered cells polarisation and reduced surface colonisation upon stimulation. Ultimately, my work suggests that, as it is for mammalian cells, bacteria mechanobiology can also be used to control their behaviour.

2. PROCEDURE DEVELOPMENT

Before studying the effect that mechanical stimulation has on bacterial physiology and surface behaviour, I developed an experimental framework allowing me to consistently quantify these processes without stimulating cells. In fact, it would be useless to follow changings in surface colonisation without developing a reliable way to capture the process when happening undisturbed. Consequently, at the centre of my investigations during the project's preliminary stages, had been the crafting of an experimental procedure allowing me to study surface colonisation while remaining flexible enough to accommodate vibrational stimulation when required.

Such resulting procedure is schematically represented in (Figure 19). From this

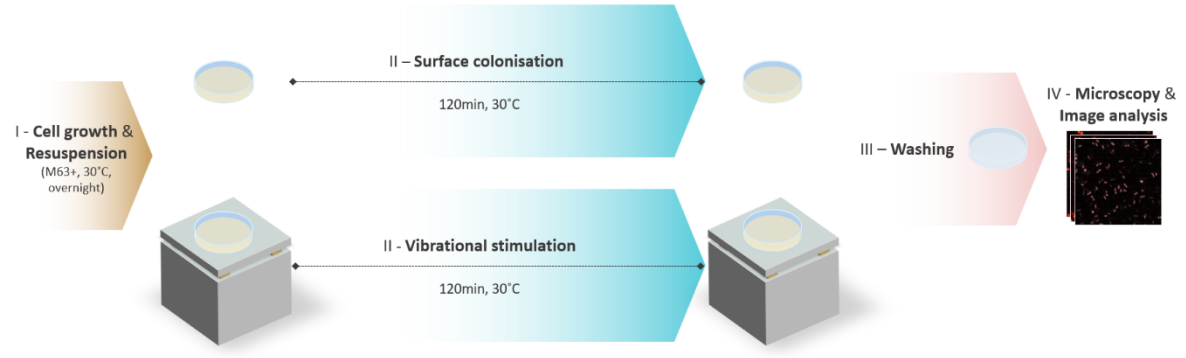

Figure 19: Representation of both non-vibrational (top) and vibrational (bottom) procedure. From the left to the right, *E.coli* fluorescent cells were grown in minimal medium M63+, overnight at 30°C. Cells were then resuspended in polystyrene petri dishes (35 mm) and, to allow surface colonisation, these were incubated for 120 minutes at 30°C. When vibrational stimulation was applied, samples were loaded onto a vibrational device and stimulated during surface colonisation. After this, samples were washed and surfaces imaged using fluorescence microscopy. From the analysis of the resulting pictures I inferred the change in coverage upon stimulation.

one we can see that it requires the growth of fluorescent cells in minimal media, their resuspension in small polystyrene petri dishes followed by their incubation and surface colonisation. Finally, surfaces were washed, imaged with fluorescence microscopy and the extent of surface coverage quantified from the analysis of the resulting pictures. Following this experimental pipeline, I went from cell growth to surface coverage.

However, this was but one specific embodiment among many that would have allowed me to do just the same. Here then is what this chapter will be about. It would provide a rationale and a justification to the question "Why *this* procedure"? It will present and support the choices I did and the constrains I set that shaped its final form. By the end of this chapter, it should be clearer not only what makes my procedure, but also why it is this way. Surface choice, bacterial strain, growing conditions, washing methodologies and quantification methods have all been factors which required optimisation and that the coming sections will discuss in finer detail.

2.1 Surface samples

At the front of my experimental work is the control of cells surface colonisation. As such, the surface itself occupied one of the main roles in my work and it required careful selection to decide which one to employ. Again, such choice was almost endless as bacteria are capable to colonise any sort of man-made or natural material. As such, I let simplicity to guide me.

The goal of my work is to establish new understanding of the effect that mechanical stimulation has on cells surface behaviour. How this can be used to control colonisation on medically or economically relevant surfaces is only incidental and it will make for nice

technological applications but it's a process that needs to be optimised only after the nature of cells response is understood. Consequently, the surface, at this stage of exploration, had only to provide the solid support enabling the reliable transfer of mechanical stimulation to cells and had to little interfere with their colonisation process. Because of this, I tested two commonly available and broadly employed non cytotoxic polymers: polydimethylsiloxane (PDMS) and polystyrene (PS). PDMS samples were made from freshly synthesized polymer (10:1 base to crosslinker ratio) which was cut, plasma-bonded to polystyrene petri dishes (35 mm) and sterilised using UV radiation. Polystyrene samples were instead made from the same petri dishes as above which came in pre-sterilised batches and did not require any further processing (Materials and Methods).

Experimentally I tested cells colonisation on both surfaces resuspending overnight M63+ cultures at 0.4 OD_{600} in 5 mL of fresh medium within the desired surface samples that I then incubated at 30˚C for 1 hours. After surface colonisation, samples were washed, imaged using fluorescence microscopy and cells coverage quantified from the resulting images. These steps will be discussed in the coming sessions and further information can be found under Materials and Methods.

Following these experiments, I observed that surface coverages, both between and within samples, were more broadly distributed on PDMS rather than PS surfaces (Figure 20). I reasoned that, because of its more complex samples assembly, some uncontrolled variable could have been responsible for PDMS broaden variability. I identified one of such variables in the UV radiation. In fact, while this can temporarily turn PDMS from hydrophobic to hydrophilic [186], hydrophobic recovery can vary as it depends on both UV exposure time and PDMS chemical properties. Since surface hydrophobicity impacts both cells adhesion and surface colonisation, I hypothesised that samples with uncontrolled

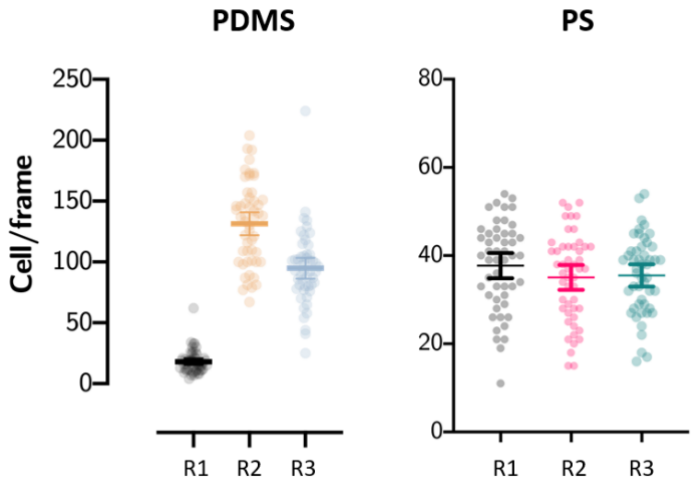

Figure 20: Surface coverage after 1 hour adhesion on both PDMS (a) and PS (b) surfaces. R1 to R3 represents three independent replicates. Data show the mean and SD of the cell count per picture (n > 27 for each condition).

recovery time could differ in their hydrophobicity and have different impact on cells adhesion so explaining PDMS variability.

Because of the added experimental difficulty that would have required to monitor PDMS hydrophobic recovery, I confined my experimental studies to PS surfaces exclusively.

2.2 Bacterial strains and growing conditions

In the above section I discussed cells and their adhesion on surfaces by giving for granted that these were grown at 30˚C in a yet unspecified medium M63+. Purpose of this session is to clarify these points and present where these conditions came from and why I decided on using them.

As stated in the introduction, my experimental question revolved around bacteria surface colonisation which needed to happen consistently before applying any mechanical stimulation. For this reason, I looked closely at two factors which are known to influence this process: bacteria's physiology and their growing conditions. On the bacterial side, *E. coli* MG1655 served as our model organism. The experimental ease of working with this domesticated strain and the vast literature covering its physiology were the main reasons behind this choice. More specifically, I predominantly employed a sub strain of MG1655 named SCC1 [187] which was much simpler to identify on surfaces thanks to its constitutive green fluorescence (Materials and Methods).

Growing conditions and their ability to influence cells physiology through specific environmental clues, also have a prime impact on bacteria's surface adhesion. In fact, in *E. coli*, this process is facilitated by the expression of extracellular adhesins known as curli [188,189]. This depends upon the master regulator CsgD whose activation is triggered by many environmental parameters such as low temperature, osmolarity, oxygen and glucose concentrations [190–192]. To achieve enhanced curli expression and surface colonisation, I then adjusted my growing conditions to meet the above requirements. Specifically, I grew cells at lower temperature (30˚C) in M63+, a low osmolarity medium that I supplemented with 0.2% glucose. Before using these conditions, I tested their effectiveness at promoting both curli expression and surface colonisation.

I confirmed the former by monitoring the changing in fluorescence of a fused curli reporter which, as expected, increased over time leading to robust curli expression passed 18 hours growth (Figure 21 A, Materials and Methods). To prove instead that this could ease surface colonisation on polystyrene surfaces, I grew cells both under the above conditions and in LB at 37˚C overnight. Then, I let them colonise surfaces for 2 hours,

washed them and used fluorescence microscopy to derived pictures from which I quantified surface coverage using image analysis tools (Figure 21 B, Materials and Methods).

Following these experiments, I observed that cells cultured in the curli promoting media M63+ delivered higher surface coverages compared to their LB counterparts. Together the above results confirmed that consistent surface colonisation can be achieved with *E. coli* after 2 hours by adjusting its growing conditions. Specifically compared to rich media at higher temperature, growth in minimal media at lower temperature aimed at promoting adhesin secretion, increased cells coverage on polystyrene surfaces by 97%. For these reasons, I decided on using the above conditions as my default culturing choice, explaining both their appearance in the preceding sections and those to come.

2.3 Microscopy and surface washing methodologies

Fluorescence microscopy was my defined analytical tool to tap into cells behaviour and surface colonisation. The reasons behind its choice over other quantification methods were grounded on its few characterising features: specificity, flexibility, applicability, and self-sufficiency. In fact, different methos exists that could successfully assess surface coverage and cells physiology such as staining or fluorometric techniques which use either crystal violet or plate readers. However, what these provide are mean values and nothing more. They look at the population by gathering cells average behaviour but lose their individuality in the process. Microscopy compensates this as the information provided by recorded pictures and video is cells specific. This makes it far superior to competitive techniques since cells variable behaviour within isogenic population had been proved to be a core feature of their adaptation to new environments [193]. Being able to peak through

this phenomenon makes microscopy less subject to experimental limitation as it can still provide the same population behaviours while preserving cells individuality.

Flexibility gives instead microscopy an edge when compared to similar cell-specific techniques such as flow cytometry. In fact, while this successfully provides cells specific information, its applicability is limited to homogenised suspensions. On the contrary, fluorescence microscopy allows experimenters to study cells coming from a variety of samples which can be imaged either directly, as for microfluidic devices, or by transferring them on agar pads or glass slides. Moreover, the ever-expanding kind of micro-devices, microscopes and objectives sizes makes microscopy suitable to many experimental contexts. However, what makes microscopy truly shine is its almost unlimited applicability which is made possible by its symbiont: image processing and analysis. In fact, per se, microscopy is nothing but image gathering which can only really be used for qualitative estimates. What makes it transit from qualitative to quantitative is the application on its records of the many digital processing tools that together transform images and pixels into data and numbers. This fact is single handily the key to microscopy success in cell biology as any spatio-temporal process that can be imaged can also be quantified. Many complex scientific questions can in fact be boil down to the simpler question of how to image the phenomenon which, most of the time, its answered by the application of few fluorophores.

Together all the above combine to make microscopy an incredibly self-sufficient technique. In fact, its ability to adapt to many experimental needs and to assess many different phenomena in a cells specific manner relieves the need for other analytical techniques to be used. Again, the how to study a new process can be turned into how it can be imaged. A testament to how flexible this technique can be it comes directly from my own work where I used microscopy to monitor changings in surface colonisation,

membrane potentials and cells motility with minimal variations to my experimental procedure. Because of the above it can now be appreciated why I chose this technique as my main analytical tool throughout my work.

This brings us back to my procedure development. Specifically, I left to the identification of the optimal growing conditions which ensured robust surface colonisation on polystyrene petri dishes. Specifically, I let this to happen undisturbed for 2 hours after which I finally used fluorescence microscopy to image my surface and gather the pictures required to estimate cells coverage. However, before this was possible, samples needed to be prepared for microscopy. In fact, despite the above benefits of my methodological approach, this was nonetheless prone to three sources of systematic errors. The primary of them was the appearing in fluorescence pictures of undesired cells such as swimmers. In fact, when these moves in proximity of the surface, they can be wrongly considered as colonisers which would cause to overestimate surface colonisation. A second source of error came instead from surface colonisers themselves. As mentioned, surface colonisation is a twostep process requiring cells to first reach the surface and second to adjust their physiology while transitioning to a sessile lifestyle. Since I want mechanical stimulation to influence this process, potentially impaired colonisers needed also to be removed from the surface before imaging as their lingering on it would underestimate cells response to vibrations. Third and final source of error was due to cells clusters forming on the surface. Their presence in fluorescence pictures would cause unreliable estimation of surface coverage both because of the added complexity required to determine tree dimensional volumes from bidimensional images and because of the difficulty in resolving cells from such clusters.

To address all the above issues, I introduced an extra step in between surface

colonisation and imaging: samples washing. In fact, the moving liquid on the surface would act as a hydrodynamic sweep ensuring the removal of both swimmers and hindered colonisers while allowing to control surface clustering. For these reasons, surface washing played a critical role in our experiments as it limited the introduction of systematic errors, defined the quality of the gathered pictures and the reliability of their analysis. Consequently, I spent a considerable amount of time to meticulously optimise different washing techniques.

Once more, endless methodologies exist to perform this simple task, so I identified the most suitable to my circumstances by fixing three criteria the resulting washing technique had to possess. First, I wanted it to deliver homogeneously distributed cells with no clusters; second, I wanted this to be strong enough to decrease coverage by removing swimmers and feeble colonisers and third, I wanted it to be reproducible and limit technical variability between samples. Under these criteria I tested different washing methodologies that, depending or not on surface exposure to the air, I respectively classified as *Air-loose* and *Air-tight*. I started by testing the former, of which, I employed two techniques: (i) *dipping,* relying on the simple up and down dipping of sample dishes in and out of fresh buffer and (ii) *pipetting,* which flew instead fresh buffer on the surfaces

through a serological pipette (Materials and Methods).

To test whether these techniques met my criteria, I let cells to colonise polystyrene surfaces for 2 hours and judged the quality of the resulting pictures. From these I saw that both techniques suffered from severe cells clustering on the surface (Figure 22). To test if this was a by-product of cells culturing or its processing, I monitored the homogeneity of cells suspension at the onset of surface colonisation using fluorescence microscopy. As I observed no aggregation in the medium (Figure 22), I concluded that washing could have been responsible for surface clustering.

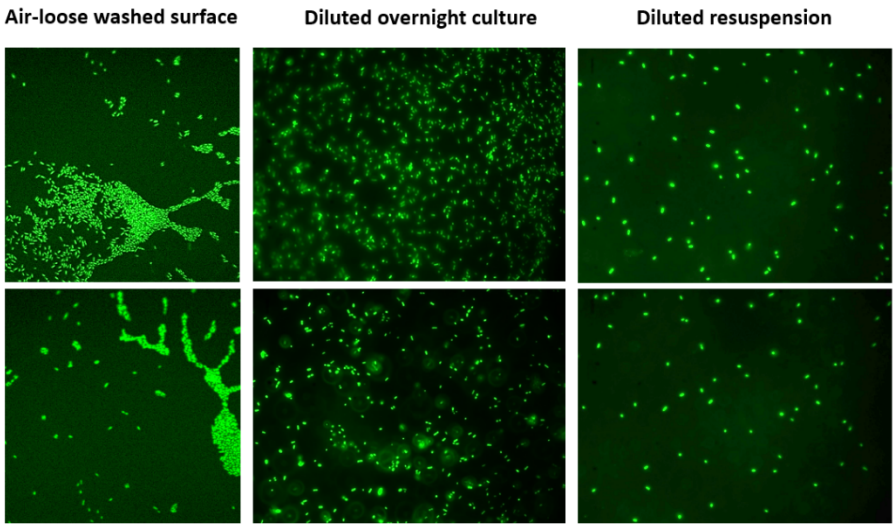

Figure 21: Air-loose washing led to surface clustering on polystyrene surface after 2 hours colonisation. No clustering was observed in either diluted overnight cultures nor their resuspensions.

To assess this point, I imaged stranded cells on glass slides. These were cells that were left on the surface after the retraction of the liquid film between the slide and its supported coverslip (Figure 23 A, Materials and Methods). In these images I observed the same kind of clustering as in washed samples proving that this was involved in their formation. This point was further confirmed by the analysis of video records (Figure 23 B). In these, I observed that the liquid layer first gathered cells upon its retraction and left them stranded on the surface as clusters upon reaching either a critical mass or encountering some surface impurity.

Because of this intrinsic tendency toward clusters formation, I abandoned Air-loose washings and moved toward our second tested methodology: *Air-tight* washing. Building on the above findings, this was centred around the idea of preventing surface exposure to air by keeping it under liquid throughout the entire process (Materials and Methods). To

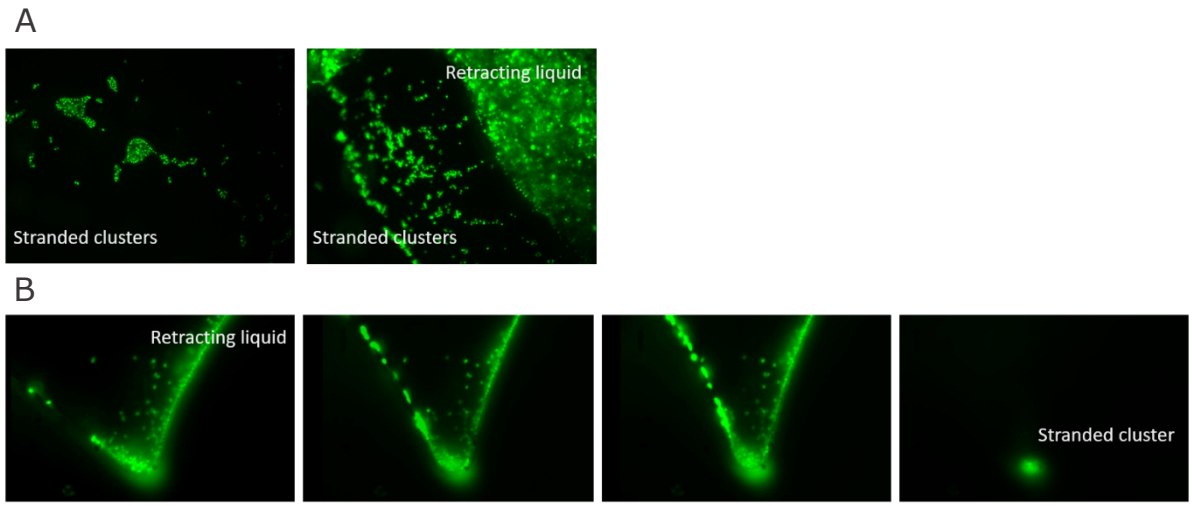

Figure 23: A) Stranded cells and retracting liquid layer in between a glass slide and coverslip. B) Time lapse of the above process (from left to right) showing the formation of a stranded cluster from the retracting liquid suspension.

achieve this, samples containing cells suspensions were entirely submerged in 400 mL of PBS within plastic tips' boxes, held in position at their bottom via neodymium magnets and washed using a mechanical shaker. I then tested the above methodology against our criteria and judged the quality of the resulting pictures, the change in surface coverage and its experimental variability.

From these experiments, Air-tight mechanical shaking successfully met all our criteria. It delivered homogeneous surface populations (Figure 24 a and b) decreased cells coverage and proved reliable upon replication with little experimental variability between samples (Figure 24 c).

This reliable methodology enabled us to perform microscopy without the insurgence of systematic errors, leaving me to enjoy the previously discussed benefits of this technique.

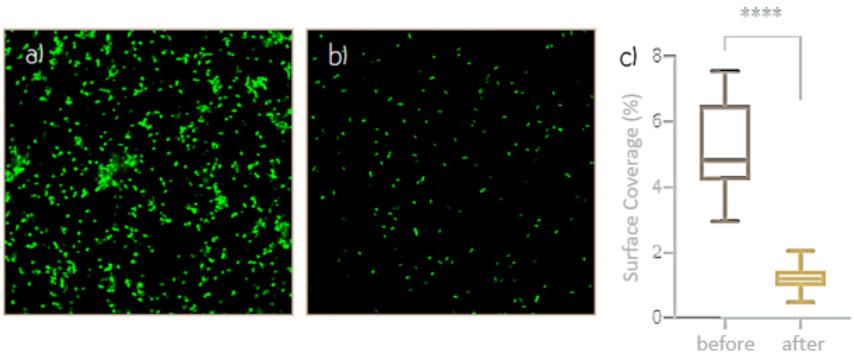

Figure 24: Homogeneously distributed surface cells before (a) and after (b) Air-tight mechanical washing. No cluster is formed using this methodology which also proved effective at reducing surface coverage with limited data variability (c). Box plot represents the surface coverage derived from fluorescent pictures of polystyrene surface after 1 hour colonisation before (brown) and after (yellow) their washing.

This brings us toward the end of my procedure development. So far, I have seen how cells were grown, surface colonisation maximised and microscopy and surface washing used to optimise cells surface distribution. What remains to be described is how surface quantification and its analysis had been performed from the resulting fluorescence pictures.

2.4 Image processing and analysis

As introduced earlier, image processing and analysis makes for the quantitative aspects of microscopy techniques. They can be applied wherever microscopy is used to image cells physiology over both time and space. In my specific conditions, I used image analysis to quantify cells coverage from fluorescence pictures. This quantitative transition from images to numbers was a twostep process made on one side by the digital processing of fluorescence pictures and on the other by the data analysis of the resulting values.

Experimentally I achieved the above by applying different processing algorithms to the gathered pictures and automated this process using customs scripts to decrease the insurgence of operational errors. I did this using FIJI, a freely available image processing software that comes with all the necessary tools to extract cells coverage from fluorescence pictures. Without allowing unnecessary details to cloud the argument and discussing only the meaning of the employed algorithms, our processing workflow is divided in three parts: *(i) processing*, where images are polished from environmental noise, *(ii) binarization*, where features are binarized and distinguished from the background and finally *(iii) detection*, where they are classified as independent regions of interest (ROI) and their

desired statistics derived (Figure 25).

Starting with processing, I corrected image backgrounds for uneven illumination which can vary in the pictures because of imperfection in either the samples or the

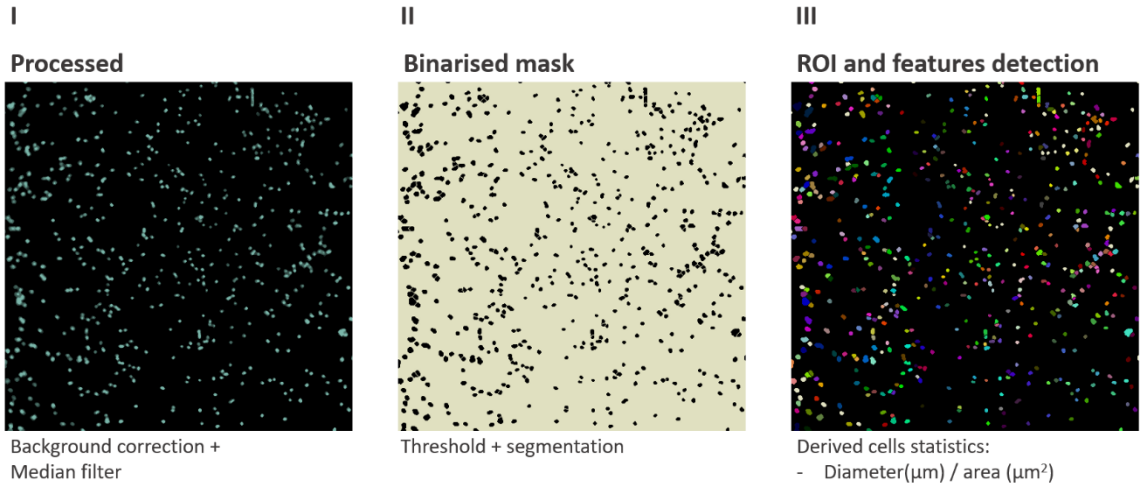

Figure 25: Image processing steps followed to determine cell surface coverage and size. Fluorescence Images were first processed by correcting the background for uneven Illumination and by homogenising cells features using median topological filters (I). Processed images were then binarized and cells resolved using specific threshold and segmentation algorithms (II). Finally, regions of Interests (ROI) were identified and their diameter and surface area determined.

microscope stage. As such, specific algorithms exist that can recognise skewness in pixel intensity and normalise it across the picture. Following this step, I improved cells recognition in the image by first removing the now normalised background and second by applying topological filters. Specifically, background removal is meant to ease features detection by lowering background pixel values to 0. In its essence, this is the same as subtracting the background using a blank sample before any fluorometric measurement.

The used of the topological median filter is instead less intuitive and it requires a little more discussion. Essentially, a topological filter is a mathematical operation (a

convolution) that transform the intensity of every pixel in the image according to a defined law or kernel. In the specific case of median filters, this kernel transforms pixel intensities based on the median values of its eight neighbours in a squared arrangement around it. This has basically three effects on the picture: it homogenises the values of pixel belonging to the same feature such as my cells, it increases the contrast of their boundaries and it finally denoise the image reducing its granularity. The joint combination of background subtraction and median filters improves then cells detection in my images which, to summarise, is achieved by making their pixels more distinct from the background and by homogenising their intensities.

Once the images were processed and polished, I prepared them for detection through binarization. This step is performed first by distinguishing the features from the background using threshold algorithms and then, by resolving them using segmentation algorithms. Finally, once cells/features are distinguished and separated from one another they are detected and classifies as independent regions of interest (ROI). These can be analysed to derive cells specific statistics that can vary depending on experimental needs. For surface coverage quantification, my most characterising features were ROI's diameter, total number and surface area. The latter values are then combined for all pictures coming from three experimental replicates and used to determine cells mean surface coverage.

This last point usher the transition from digital processing to data analysis. Specifically, as I was mostly interested in relative changings in surface coverage rather than its absolute values, for any given condition, the resulting coverage was normalised by the value of its associated control. This way I was able to express variation in coverage between vibrated samples and controls as fractions or percentage of its change.

Closing my analysis workflow, is the statistical comparison between conditions. To

do this, I applied standard statistical tests to the normalised changes in coverage using either parametric or non-parametric tests. Guiding my choice was the nature of data themselves. When parametric tests such as t-test and ANOVA were used, I checked that the data were bell shaped (normality) and had similar spread (homoscedasticity). Where normality failed, I used Welch's variants of the above tests and where also homoscedasticity failed, I moved to non-parametric alternatives such as Mann-Withney U-test or Kruskal-Wallis.

In conclusion, I managed to consistently determine cells surface coverage and infer its changing upon different experimental conditions from the joint combination of image processing and data analysis tools.

2.5 Conclusion

The detour on my experimental procedure and its development has now come to an end. As we have seen from the above sections, I succeeded in crafting a working pipeline allowing me to study cells undisturbed surface colonisation. This was possible through the optimization of several factors, first of which the choice of the colonised surface. On this regard, polystyrene proved more reliable than PDMS because to its almost non-existent sample preparation and the absence of uncontrolled variables. Then cells culturing in M63+, at lower temperature and under limited glucose availability promoted adhesin secretion and enhanced cells colonisation which eased the observation of the process. Air-tight mechanical washing, that prevented surface exposure to the air, proved also fundamental to prepare samples for microscopy as it ensured the removal of swimmer and impaired colonisers while delivering homogenous surface population in a consistent way. Finally, I reliably quantified surface coverage through the automated processing of

fluorescence images. With this procedure, I confidently move my studies further and get to the heart of my scientific endeavour. In fact, if until now I confined ourselves to undisturbed surface colonisation, I can finally change that and direct our attention to the effect that mechanical stimulation has on this process. To achieve this, I simply had to take the above procedure and made room for the centre piece of my studies: vibrational stimulation.

3. VIBRATIONAL STUDIES

In the preceding chapter we saw how I successfully determined cells coverage using an optimised experimental procedure. Now it is time to see how I used this one to tackle instead my project's main scientific question: *can mechanical stimulation influence bacterial surface colonisation?*

Before presenting my findings, it is useful to pause and discuss the nature of such mechanical stimulation. Forces are ubiquitous in nature and so more so are mechanical forces. These follow from Newton's second law which, in their simplest one-dimensional form, define them as proportional to the product of the mass m of an object time its acceleration $a(t)$ or the second derivative of its displacement $x(t)$.

$$F(t) = ma(t) = m\frac{d^2x(t)}{dt^2} \qquad 1$$

From such simple relation, one can estimate the force acting on a vibrating object supporting a weight m. However, how were cells vibrated in first place? Which kind of device I used to do so? What is the relationship between surface vibrations and applied forces and how did I estimate them? All these questions are going to be addressed in the following section which provides a concise guide to the engineering behind my work.

3.1 A detour on the physics

In the previous chapter we saw the nature of my samples: polystyrene petri dishes (35 mm in diameter) containing cellular suspension. Now we need to see how through vibrations, these could be subjected to forces.

To get there, we need to answer two questions: *(i) Which device did I use to vibrates samples?* and *(ii) How vibrations can generate mechanical forces on cells?*

Any experimental effort needs the right tools to meet its purpose and, in my case, this meant the assembling of a device capable to apply mechanical forces on surface approaching cells. The experimental work needed to assemble and characterise such device was performed by Dr. Nasim Mahmoodi and I will now describe it at my best, starting by the device structure and its working. So, which device did I use?

From a structural point of view this was made of a heavy aluminium base on top of which corners four piezoelectric elements were fixed with thermoresistant glue (Figure 26 A). Glued on top of these was a thinner aluminium plate covered with a 1 mm thick steel sheet. This served as a stage for my samples which were magnetically bound to it using a neodymium magnet. To allow this magnetic binding, a steel disk (34 mm in diameter) was glued at the outer bottom surface of my samples which were then gently slide on top of the magnet.

Now how the above vibrates samples? The answer to this question lay within the piezoelectric elements and their ability to mechanically expand when electrically polarised. This allows to control piezos' expansion using electric currents as the flow of negatively charged electrons, near one side, polarises it, expanding and contracting its structure. Since the applied current $I(t)$ is proportional to the voltage V that generates it (Equation 2), a sinusoidally oscillating current of frequency f would therefore cause the piezos to expand with same frequency and an amplitude A (Equation 3). This is what results in samples vibrating. By being glued to the aluminium plate on top of them, piezos' expansion is vertically transferred to the plate itself, so transforming an electric signal into

a vibration.

To make the above possible, the piezoelectric elements were wired in series and connected to a signal generator and amplifier which generated the sinusoidally oscillating voltages and currents. Therefore, by controlling the frequency and magnitude of the applied voltage it is in principle possible to control the frequency and amplitude of the resulting vibration.

Inverse Piezoelectricity

$$I(t) \propto \boldsymbol{V}sin(2\pi ft + \varphi) \qquad x(t) = \boldsymbol{A}sin(2\pi ft + \varphi)$$

2 3

However, while its frequency is the same as that of the current that drives piezos' expansion, its amplitude is expected to linearly depends on the applied voltage and needs to be determined. To do this, Dr. Mahmoodi applied currents of different frequencies and increasing voltages to the piezos and recorded the resulting vertical displacement of the aluminium plate using laser interferometry. From this she then derived the vibrational amplitude that she plotted against the applied voltage for all tested frequencies. What she observed is that for voltages between 0 and 40 V, vibrations had nanometre amplitudes and increased linearly with voltage for all tested frequencies of 0.5, 1 and 2 kHz (Figure 26 B).

While this behaviour confirmed the device intended working, it allowed us to completely describe the amplitude and frequency of the vibration by knowing the voltage and frequency of the applied current. Since these can be set through the signal generator, the above setup allowed me to vibrate samples at amplitudes between 0 to 120 nm and frequencies of 0.5 to 2 kHz.

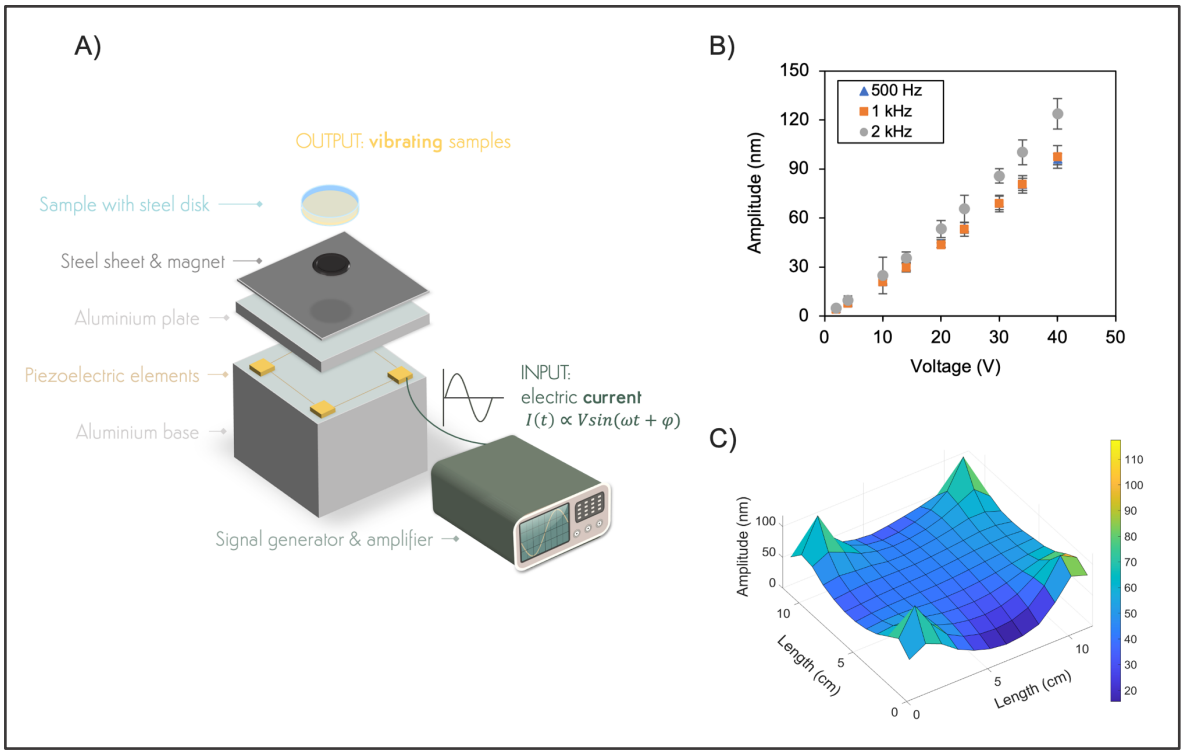

Figure 26: A) Schematic representation of the vibrational device and its functioning. A signal generator and amplifier originate a sinusoidally oscillating voltage which send a corresponding electric current to four piezoelectric elements. Their ensuing periodic expansion causes the aluminium plate, magnet and sample to oscillate as a single body. This generates a vertical vibration the amplitude of which is proportional to magnitude of the applied potential. B) Linear proportionality between applied voltage and vibrational amplitude for frequencies of 0.5, 1 and 2 kHz. Points on graph are laser interferometry data of the amplitude average with standard deviation measured at the centre of the vibrating aluminium plate. C) Laser interferometry data of vibrational amplitude measured at 121 squared tiles on the steel sheet covering the aluminium plate in A. This was vibrated at 1 kHz and 25 V and data are the average amplitude measured at the centre of each tile over three experiments.

Through the above work Dr. Mahmoodi showed that the aluminium plate vibrated with frequency *f* and amplitude *A* upon piezos electrical stimulation but what about the sample on top of it? For cells to experience vibration two more things need to happen: first, vibrations need to be transferred from the plate to the sample dish and second, they

need to be homogeneous across its surface. Let's see how the device met these criteria.

Since both the aluminium plate, the magnet and the sample are rigid bodies, vibrations can transfer unhindered from the former to the latter, allowing the three of them to vibrate as one. However, damping effects happening at their respective interfaces, could hamper this process and lead to the mismatched transfer of vibrational amplitude, frequency or both. To test vibration transmission to the sample dish, Dr. Mahmoodi performed the same experiments she did to characterise the plate's vibration, only this time she monitored the displacement of the sample's bottom surface using laser interferometry. She observed that, for the tested vibrations, the sample oscillated with the same amplitude and frequency as the plate (data not shown). This supported the rigid body behaviour of our setup that can therefore transfer undamped vibrations from the piezo up to the sample.

The second criterion mentioned above is that vibrations must be uniform over the surface of the samples which means that they should oscillate vertically at the same frequency and amplitude. This is a critical step in our vibrational design since, as I'll explain shortly, it permits cells to experience the same force near the surface while preventing the insurgence of hydrodynamic vortexes. In thin liquid conditions such as mine, vibrational patterns can in fact transfer from the surface to the liquid [184] and for non-homogeneous vibrations, these so-called Faraday's waves sweep the surface hindering cells adhesion [184].

Given the rigid body behaviour described above, the homogeneous transfer of vibrations to the dish is only conceivable if the aluminium plate either does not deform while vibrating or if a portion of it, the size of our sample, vibrates homogeneously.

To check which of the above scenarios applied to our device, Dr. Mahmoodi divided the aluminium plate surface in 121 square tiles and derived the amplitude, frequency and phase of their oscillation using laser interferometry. By plotting the resulting amplitudes in 3D, she observes that, while these were greater above the piezos at the plate's corners, a wide region (4 x 4 tiles) at the centre of it, vibrated uniformly (Figure 26 C). We therefore marked this region and used it as the loading position for the magnet and samples it supports.

Through the work above, Dr. Mahmoodi showed that the device she assembled can vibrate samples uniformly by applying oscillating currents of controlled frequency and voltage. Moreover, the uniform vibration of the tiles supporting the samples also ensure that cells adhesion is unhindered by hydrodynamic sweeps and that the forces that vibrations generate are equal across their surface. Talking of forces then, it is finally time for me to explain how these arise in the samples. So, forces is where we are heading next.

So far, we have seen the structure of the device and how this vibrates samples through piezoelectric stimulation. However, vibrations are not enough since my experiments aim at influencing cells behaviour by applying mechanical cues. We are therefore left to question how the above device can generate mechanical forces acting on cells? To see how this is possible, we need first to zoom at the samples' bottom surface and, once there, we'll need to use Newton's second law.

Near the bottom of the samples, cells swim by or engage with the surface. No matter how they move horizontally to it, they always experience the weight of the liquid on top of them. Following piezos' electrical stimulation and during vibrations, we saw that the surface, the cells and the liquid mass they support oscillates as a single body with frequency f and amplitude A (Equation 3). Driving this motion is the force generated from

the piezos' expansion which is transferred to the samples' surface and from there is further transferred through the cells to the liquid weighting on them.

Cells are therefore in analogous situation as the shoulder of a weightlifter. As these are supporting the weight loaded on them, so do cells on the surface with the liquid suspension. When the lifter then pushes with its legs, a force is transferred through the shoulder to the weight which is lifted. Throughout this process, the weight opposes the lifting force with one of equal magnitude but opposite direction which act on the shoulders. Similarly, when the surface exerts an upward force, this is transferred from the surface, through the cell to their supported liquid which once again exert a reaction force on cells.

Therefore, upon vibration, surface approaching cells experience a force which is perpendicular to the surface and of the same magnitude as the one that this transfer through them to the hovering liquid. Such force can be estimated through Newton's second law (Equation 1, rewritten below) by knowing the acceleration $a(t)$ and mass m of the displaced object.

$$F(t) = m\, a(t) \qquad \mathbf{1}$$

Since the force acting on cells has the same magnitude as the one needed to lift the liquid above them, to estimate this force, we determined the liquid acceleration and mass.

By assuming that the liquid in the sample behave as a rigid body and does not deform, its acceleration can be determined by the displacement of the surface itself. For vertical oscillations of frequency f and amplitude A, the acceleration takes then the form below.

$$a(t) = \frac{d^2x(t)}{dt^2} = \frac{d^2[Asin(2\pi ft)]}{dt^2} = -\boldsymbol{A}(2\pi \boldsymbol{f})^2\, sin(2\pi \boldsymbol{f} t)$$

4

From Equation 4 we see how the vibrational frequency and amplitude associated to the sample displacement $x(t)$ can thus be used to determine its acceleration $a(t)$.

I previously discussed how Dr. Mahmoodi showed that the sample vibrates with the same frequency as the applied current and determined a linear relation between its amplitude and the applied voltage. As such, for vibrations occurring between the previously given ranges of 0 - 120 nm amplitude and 0.5 - 2 kHz frequency, we have all the information needed to use Equation 4 and compute sample's acceleration from the frequency and voltage of the applied current.

What we are still missing to estimate the force is the mass of the displaced object. In our case, this is the liquid column cells support near a surface and it can be found from the product of cells' average surface area A_{cell}, the height of the liquid volume h in the sample and its density ρ (Equation 5)

$$m = (h\, A_{cell} \rho)$$

5

Following steps used in similar mammalian studies [194], we determined the above mass by approximating cells suspension density to that of water (998 kg/m^3) and quantifying cells average surface area. For this step I applied the image analysis tools and workflow described in the preceding chapters to fluorescence images of surface attached cells (Materials & Methods 6 and 27 - 1). By substituting the value m of the displaced liquid and its acceleration $a(t)$ in Equation 1 the result is the following.

$$F(t) = -(h\,A_{cell}\rho)\,(2\pi \boldsymbol{f})^2 \boldsymbol{A}\sin(2\pi \boldsymbol{f} t)$$

6

The expression above describes the force that cells experience in vibrating samples (Figure 27). This oscillates with surface's frequency and a maximum magnitude given by

$$F_{max} = |(h\,A_{cell}\rho)\,(2\pi \boldsymbol{f})^2 \boldsymbol{A}|$$

7

On a practical ground, the above description of the force in terms of vibrational parameters *f* and *A* allowed us to control its magnitude through the frequency and voltage of the applied current.

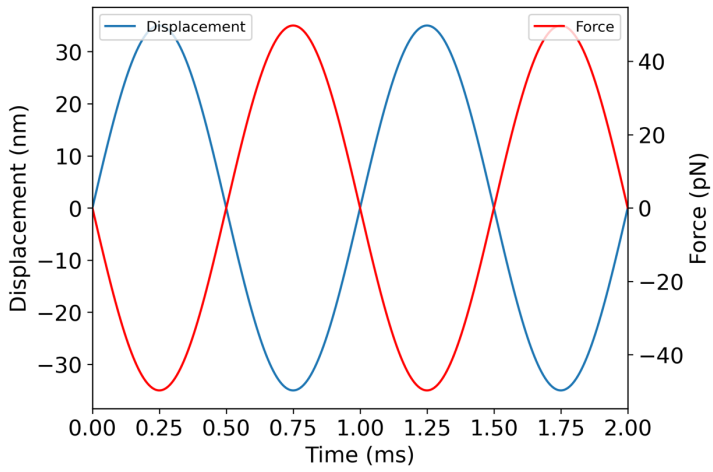

Figure 27: Plots representing the relation between surface vibration and the generated force and pressure acting on cells. From laser interferometry records of a surface oscillating at 1 kHz frequency and 35 nm (blue line), the resulting force can be estimated from Equation 6 (red line). This leads to a force, perpendicular to the surface, oscillating with the same frequency and a magnitude of 50 pN.

From Equations 6 we can now appreciate how critical it is for us to homogeneously vibrate surfaces. Because force is determined by both vibrational frequency and amplitude, if these vary throughout the surface, cells would be subjected to various mechanical loads. However, since the purpose of my research is to study the effect these cues have on

bacterial adhesion, all cells on the surface had to be subjected to the identical stimuli as this is the only way to achieve a bijective relationship between applied these and cell response.

Before proceeding, it is important to acknowledge the elephant in the room, which is pointing to the fact that, while we estimated these forces, we did not monitor them experimentally. The primarily reason behind this was technical. The size of the device, and the nature of the sample are enough to exclude many techniques that would otherwise prove helpful. Take atomic force microscopy (AFM) for example. While this could monitor both the vibrations and forces generated by a single piezo on a cell sitting on it, it would make for an entirely different experimental setup and accordingly different forces applied on the cell.

Despite AFM failure, we could nonetheless experimentally determine our forces using pressure sensors. These are made of piezoelectric components, which send electrical signals in response to applied pressure. While no cell sized sensor is accessible, micrometric ones do. Few such sensors could then be attached to the bottom surface of our sample dishes and submerged in varied liquid heights. Now, if our approximations leading to Equation 6 hold, by knowing the area of the sensors, the density of the liquid and the frequency and amplitude of the vibration, we should observe a linear change in the detected force with the volume and therefore the heigh of the submerging liquid.

These results could solidify both the theoretical assumptions and final estimate of our forces but, because of their complex technical nature, they were deemed beyond the scope of my work and are left for the next round of students to explore.

An alternative to our vibrational strategy could use fluid flow and shear to subject

cells to mechanical loads. Through this approach, forces can be precisely derived by the liquid flow rate, a parameter that is easily controlled and monitored. This would require the engineering of a brand-new microfluidic device, made of a small flow chamber where flow is driven by automated pumps through which flow rate and mechanical load could be controlled. Such a microfluidic device could also be installed under a microscope allowing more information to be available from the recording of time lapses when studying cells response. Unfortunately, while the above alternative has been discussed, the work needed to optimise its proved beyond my time constraints but it would definitely make worth investigating as a new project.

The above discussion closes this section excursion on the engineering which I started by asking two questions: *Which device did I used to vibrate samples?* and *How vibrations can generate mechanical forces on cells?* The answer to the first question is found in the inverse piezoelectric effect, which allows oscillating electric currents to govern the expansion of piezoelectric materials. Because of the rigid body behaviour, vibrations are transferred from these to the samples with no loss of amplitude or frequency which leads to the answer to my second question. In fact, these vertical oscillations subject cells to mechanical forces in the same way that a squatting weightlifter's do to its shoulders. The inertia of the liquid on top of cells applies on these a force which is a response to the lifting one transferred from the moving surface through the cells.

With the procedure discussed in the preceding chapter and the engineering of the vibrational device out of the way in this one, I can return to my scientific question and discuss how bacteria surface colonisation can be influenced through vibrational stimulation. On this regard, I will begin by touching exactly on this point, the need for stimulation.

3.2 Bacteria vibrational stimulation

The way I wanted to influence cells surface behaviour and colonisation was by tackling cells' surface response and its mechanical signalling. As discussed in the introduction, a growing body of experimental evidence is establishing the fact that bacteria can sense mechanical stimuli and forces via specific physiological changings [140]. This process can differ among species and several mechanisms had also been observed to exist within one. Pili, flagella, motility and membrane potential, these are among those physiological components that have been reported to vary due to surface mechanical presence and who's changings help cells in transducing mechanical cues into physiological outputs. These consists of intracellular variation of second messenger levels such as c-di-GMP and cAMP, protein synthesis and genetic expression which together rewire the cell and prepare it for a sessile, surface associated, lifestyle.

I therefore reasoned that, altering any of the physiological responses that usher this transition from planktonic to sessile behaviour, could hinder cells natural surface response and its resulting colonisation. To achieve this, I used the previously described surface vibrations as exogenous force generators and physiological perturbator. Central to the success of my approach was therefore the identification of suitable force magnitudes enabling bacteria mechanical stimulation.

So far, I discussed the physical nature of these forces and how these can be obtained, however, their intensity can vary broadly. Applying a force, any force, to cells it is not enough to achieve their stimulation and trigger physiological changings. For this to happen, a force needs to act as a stimulant and be sent within a precise scale so that it can be perceived and processed. Failing at this not only would prevent us from answering our

question but it would also compromise its answer. In fact, if applied forces exceed beyond physiological sensing range, any observable response they have on cells couldn't be considered as a genuine result of their stimulation since other effects, such as membrane damage, would also be relevant at higher order of magnitudes. Therefore, for vibrations to be effective at stimulating cells they should alter their physiology without affecting their integrity. Moreover, beyond its intensity, stimuli must also have a specific time scale. In fact, they need to be sent with the right timing if these want to be sensed or interfere with the process. As such, for applied forces to act as stimulant they need to possess both the right intensities and frequencies. Before applying mechanical stimulation, I then identified these scales that, starting with their intensities, I did by turning my attention to what bacteria can do with forces.

Every living organism belong to a particular scale and as such, is capable to sense and respond to a plethora of environmental stimuli which are specific to their scale and bacteria are no exception. They live in mechanical environments that encompass a range of forces from the pico- to the micro-newton; 10^6 orders of magnitude and a broad range to begin with [195]. However, within this spectrum, I began my exploration starting with those forces that bacteria are capable to exert and handle with one of their motorised apparatuses: pili. More precisely, type-IV pili are motile external appendages, ubiquitous among bacteria as a versatile tool enabling motility, sharing of genetic information and predation but their involvement in surface sensing have also been recently highlighted [196]. In performing the above activities, a single pilum can generate forces within the tenths to the hundreds of piconewtons [197], which defined the intensity window I also used throughout my experiments. Justifying this choice are two reasons: first, pili retraction forces provide a sensible indication of the force magnitudes bacteria generate at their scale.

Since these forces can trigger sensing and response mechanisms, similar outcomes should be expected upon their exogenous application. Piconewton forces could therefore be of broad applicability within bacteria even when pili are absent as for our own strain.

The second reason behind our choice resides instead on the relatively small magnitudes of pili's forces. These are in fact at least one order below adhesion forces [195] and, because of this, piconewtons stimulation is unlikely to compromise cells' adhesion through simple mechanical effects. Moreover, always because of their reduced magnitude, no significant disruption to cells envelop should be expected, preventing to incorrectly attribute any effect on colonisation to cells damage.

Once I identified piconewtons as a suitable intensity scale for my simulation, I determined the time and frequency of its application. From Equation 6, vibrational forces are not constant but cycles continuously with the same frequency as the applied vibration. Its period represents then the time between two consecutive stimulation peaks which provides the scale of my stimulation. Specifically, I wanted this to be familiar to what bacteria experience and, to find it, I once more let bacteria to guide my choice looking at yet another of their features: flagella. These whip-like structures are mostly used for propulsion which, under high load, can reach frequencies of hundreds and thousands of Hz [31,198]. I therefore decided to stimulate bacteria with kilohertz frequencies.

One last thing remained to be done. I had the desired magnitude and frequency with which I wanted to stimulate cells, so I only had to translate this information in terms of vibrational parameters. Equation 6 is what allowed this conversion. Since the force is a function of both vibrational frequency and amplitude, to generate stimulation forces of piconewton intensity and kilohertz frequencies meant the use of nanometric amplitudes.

This was the ultimate combination needed to subject surface approaching cells with piconewton forces: vibrations of kilohertz frequencies and nanometric amplitudes.

The above discussion should make sense of what, in the previous section, could have otherwise seemed as a murky or arbitrary choice at best. Why to characterise the device functioning at kilohertz frequencies and nanometric amplitudes? Why not megahertz and micrometres? I hope the reason is now apparent.

The work Dr. Mahmoodi did to characterise the device and which I discussed in the previous section involved kilohertz frequencies and nanometric amplitudes because these are needed for piconewton forces to be applied on surface approaching cells.

We now approached the end of what could look like an excessively long intro to my vibrational studies and here, before moving forward, we face one last question; How are said forces experienced by cells? Earlier we saw how these are generated, which direction and magnitude they have but how are these acting on cells? It is a tricky task to put ourselves in the shoes of cells, but we did this before and, although speculative at this stage, cells membrane should come into focus.

As we saw, vibrational forces come from the opposing inertia of the liquid suspension submerging cells on the surface. This means that cells are sandwiched between the surface and the liquid, transferring the lifting force from one to the other. As such they should experience an applied load acting on their outermost feature, the membrane. This would result in cells feeling a pressure. When dividing the force in Equation 6 by cells average surface area one finds the below expression describing the pressure acting on cells.

$$P(t) = \frac{|F(t)|}{A_{cell}} = |(h\,\rho)\,(2\pi \boldsymbol{f})^2 \boldsymbol{A} \sin(2\pi \boldsymbol{f} t)|$$

8

For piconewton forces and micrometres squared areas, Equation 8 estimates periodic pressures spikes of few tenths of pascals (Figure 28).

We foresee such applied pressure to most likely influence proteins or force transducers such as pili and flagellar motors which are conveniently bound to the membrane. Since protein deformation occur mostly under piconewton loads [1], this means that our applied forces could alter protein conformation and interfere with their sensing role without directly affect cells adhesion.

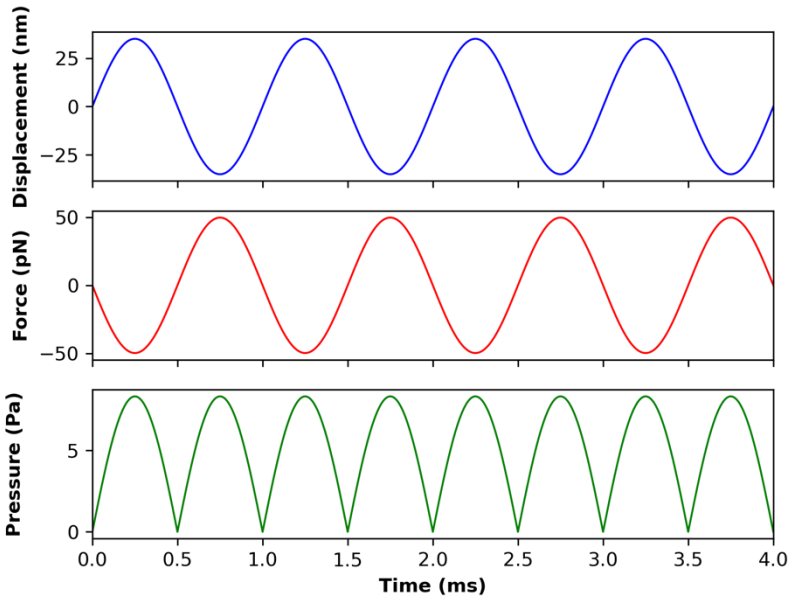

Figure 28: Complete relation between vibrations (top blue), forge (red, middle) and pressure (green, bottom). In this case, surface vibrating at 1 kHz and 35 nm leads to forces oscillating with an intensity of 50 pN. These can then translate in pressure spikes, which, depending on vibration frequency, can solicitate cells' membrane every few millisecond.

One very last question remains on the direction this force needs being applied to affect cells behaviour and protein conformation. Contrary to the force that generates it, pressure is isotropic. This means that surface approaching cells would experience the force as a compression acting homogeneously and normally to their membrane. However, such pressure could also put the membrane under a tension and trigger the deformation or opening of tension sensitive proteins such as mechanosensitive or ion channels. Through the resulting ion fluxes, the applied forces could not only affect protein conformation but also influence other aspects of cells' physiology such as their membrane potential.

The picture we can synthesise of cells experiencing vibrational forces on surface is therefore that of a squashed balloon. When you apply a force on it with your foot it comes both under pressure and tension as its volume is compressed and its surface stretched. Cells are expected to face a similar behaviour by being small, inflated balloon sandwiched between a moving surface and an inert liquid exerting forces on them.

On paper, the above forces, "felt" through the membrane, has the potential to touch and affect several components of cells mechanotransduction; from proteins conformation to cells membrane potential.

This speculation on the how cells could feel the applied force finally conclude our tour on the engineering background of our work. We saw the device, the piezoelectric effect that vibrate our samples and how this is uniform across their surface. We then discussed how force are generated through the inertial response of the liquid which submerges cells and how their intensity can be controlled by the frequency and voltage of the applied current.

We understood the need for piconewton stimulation and the requirements for

kilohertz frequencies and nanometric amplitude to achieve this through vibrations. Then, we reasoned of these forces as putting cells membrane both under pressure and tension, potentially affecting protein conformation and cells membrane potential.

With all this behind our back, we can explore how I used all the above technical and theoretical background to answer my question: *can mechanical stimulation influence bacterial surface colonisation?*

3.3 Vibrational stimulation hinders bacterial surface colonisation

From Equation 6, different vibrational forces can be obtained from specific combinations of frequencies and amplitudes. These, however, could have independent effects on bacteria, so, to simplify my experiments, I begun by holding the frequency constant which, de facto, make the applied force a function of vibrations' amplitude only. I then achieved forces of magnitudes between 15 and 500 pN under the fixed frequency of 2 kHz by adjusting their amplitudes accordingly to Equation 7. The resulting combinations are reported in Table 1.

Dictating this choice was the fact that 2 kHz maximise the range of forces that our device could generate under a fixed frequency, allowing the wider possible experimental window. Moreover, because frequencies above 2 kHz are close to the device own resonating limit, they won't establish a linear relation between applied voltage and vibrational amplitude. This would ultimately prevent me from using Equation 6 to estimate the resulting force making these frequencies useless to my experimental purpose.

Table 1: Combinations of frequencies and amplitudes associated to different stimulation intensities. N.A. represents values not experimentally achievable using our device.

	Frequency (kHz)		
	2	1	0.5
Intensity (pN)	Amplitudes (nm)		
15	3	11	22
30	5	21	42
50	9	36	N.A.
100	18	72	N.A.
200	36	N.A.	N.A.
300	54	N.A.	N.A.
500	90	N.A.	N.A.

The core hypothesis I wanted to test with these experiments was that vibrational stimulation would elicit physiological changings in bacteria that could hinder surface colonisation. To assess this hypothesis, I deployed the experimental procedure which was discussed throughout the preceding chapter with the added difference that samples were now vibrated during incubation (Materials and Methods).

To quickly summarised it here, I grew fluorescent *E. coli* in M63+ overnight, cells were then diluted in fresh medium to 0.4 OD_{600} in polystyrene small samples dishes (35 mm) which I vibrated for 2 hours in the dark at 30˚C. Specific combination of the vibrational parameters A and *f* depended on the intensity of the force that I wished to apply and which ranged from 15 to the 500 pN. Controls were processed in the same way as above but were not vibrated while incubating. All samples were then washed following a Air-tight procedure before using fluorescence microscopy to gather between 30 and 40 pictures of the surfaces. These were then processed and analysed with custom scripts to finally quantify bacteria surface coverage. For every tested force, experiments were

repeated as independent triplets and the average surface coverage obtained from all gathered pictures were used to compute their change between vibrated samples and controls.

Following this experimental workflow, vibrations decreased surface coverage across all tested forces by ~ 21% (Figure 29). For a 2 kHz stimulation frequency, the effect was constant as there was no significant difference in its extent between force points. In fact, changing stimulation intensity did not alter cells response across an entire order of magnitude, from 15 to 500 pN. Consequently, vibrational stimulation influence cells surface colonisation by mitigating its extent.

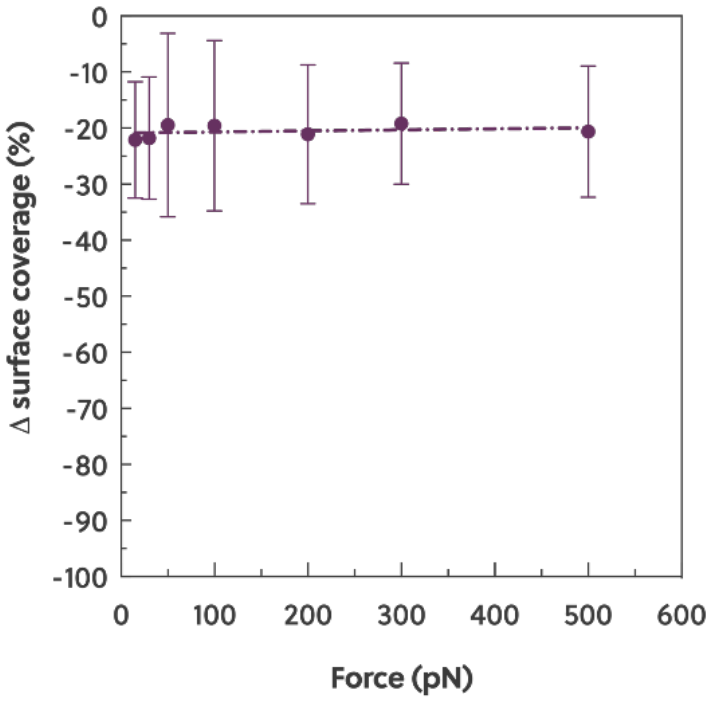

Figure 29: Change in surface coverage after 2 hours stimulation at 2 kHz with intensities between 15 and 500 pN. Data points represents the mean and SD of the difference in coverage between samples and controls across three replicates (n > 110 for all conditions). Dotted line represents interpolation line (R^2 = 0.98).

Knowing that vibrational response was stable at 2 kHz, I explored the effect that on the above observations had varying stimulation frequencies. Using the same procedure as above, I monitored the change in surface colonisation after 2 hours stimulation at both

1 kHz and 500 Hz. The same stimulation intensities were obtained by adjusting vibrational amplitudes in accordance with Equation 7 and the resulting combinations are reported in Table 1. However, because of our own setup limitations, the amplitudes required by forces above 100 pN couldn't be reached with frequencies below 2 kHz. As from Equation 6, these would have required amplitudes which were too high for our device to generate. I therefore limited our exploration to forces between 15 to 100 pN when using 1 kHz and 15 and 30 pN with 500 Hz. Lower frequencies still reduced surface, however, the extent of cellular response diminished when frequencies were lowered from 2 kHz. This reduction was both frequency and force dependent as it was stronger for 500 Hz and toward the "edges" of the employed range. Specifically, relative to 2 kHz, response at 1 kHz (red line in Figure 30) was in fact unchanged for central forces of 30 and 50 pN but diminished respectively by 27% and 34% for side forces of 15 and 100 pN. Frequency reduction to 500 Hz (pink datapoints in Figure 30) further diminished vibrational response by 38 and 31% for both tested forces of 15 and 30 pN.

From these results I concluded that, piconewton stimulation of surface approaching cells reduces their colonisation depending on stimulation frequency. Specifically, reducing its value diminish cells response by up to 38%. This appear to be force dependent as forces of 15 and 100 pN were the most affected while forces of 30 and 50 pN retained the same vibrational response when stimulation frequency was halved to 1 kHz.

Taken together, the above results proved that bacteria vibro-mechanical stimulation in the piconewton and millisecond range can mitigate bacteria surface colonisation. For a give stimulation intensity, this effect depends on its frequency as surface colonisation is most affected when vibrational stimulation is applied at 2 kHz and

decrease upon its reduction to 1 kHz and 500 Hz. This changing is also dependent upon the intensity of the applied stimulation since central forces of 30 and 50 pN appear less sensitive to reduction in frequency.

This dependency suggests that the applied stimulation most effectively elicit a cellular response when it is applied with a period of 0.5 ms (2 kHz). Finally, because of their resilience to changings in frequency, I selected 30 and 50 pN as reference stimulation intensities that I used to explore vibrational effects on cells physiology both in the reminder of this chapter and the next one.

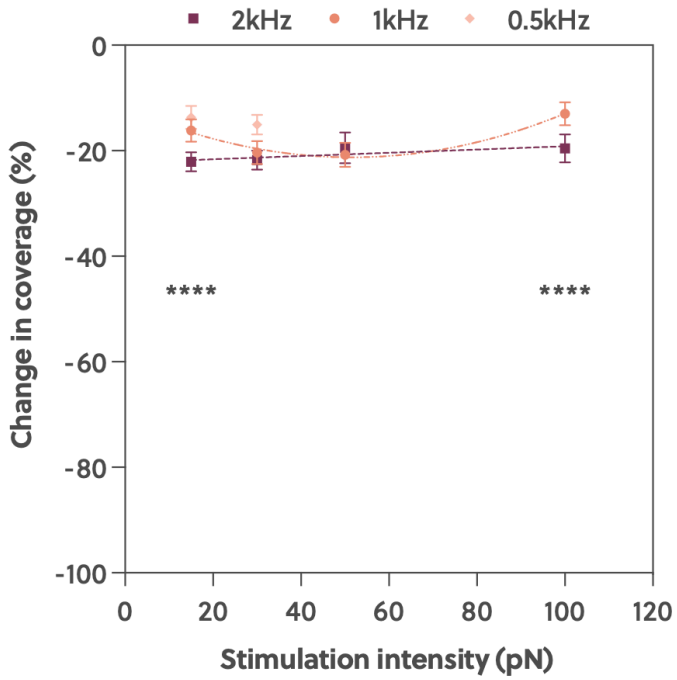

Figure 30: Change in surface coverage after 2 hours vibrational stimulation between 15 and 100 pN and tested frequencies of 2, 1 and 0.5 kHz. For the latter, only intensities of 15 and 30 pN were tested. Vibrational response decreased with stimulation intensity in a force dependent manner. Datapoint represents the mean change in surface coverage with 95% confidence intervals determined as the average change between samples and controls from three independent replicates (n > 120 for all conditions, p.values **** < 0.0001). Dotted lines are simple and non-linear regressions (R^2 = 0.98 and 0.96 for 2 kHz and 1 kHz respectively).

3.4 Cells surface sedimentation decreases vibrational response

Beside surface sensing and physiological transitions, bacteria surface colonisation also benefits from their growth and density in the medium. In fact, as these increase, more and more cells can reach the surface initiating sensing and physiological responses. Aim of the above experiments was to target these components by using piconewtons stimulation to mitigate natural surface colonisation and, although this proved successful, it did not account for the impact that cells density and surface sedimentation have on this process which I then tested. To do this, I increased cells concentration in the samples and monitored how this affected the change in surface coverage once these were vibrated.

Experimentally, overnight M63+ cultures were resuspended in 5 mL of fresh medium at densities between 0.1 and 1.2 OD_{600}. To every suspension, I then applied mechanical stimulation for 2 hours at 30 pN at 2 kHz. During this time cells were incubated at 30˚C in the dark and controls for every condition were processed the same way but were not vibrated during incubation. Finally, samples were washed, imaged and changings in coverage quantified (Materials and Methods).

Following these experiments, a tenfold increase in cells density from 0.1 to 1.2 OD_{600}, diminished vibrational response (Figure 31). In fact, this linearly decreased with cells concentration from -31% at 0.1 OD to no significant difference from controls at 1.2 OD. Consequently, cell concentration in the medium appears to have a detrimental effect on vibrational stimulation and it needs to be accounted for when planning their application. As such, environmental or experimental conditions where cells density is expected to increase could result in diminished response to vibrations. Since these

conditions are met by my experiments, I expected that upon continuous stimulation, their efficacy would decrease over time.

To test this hypothesis, I stimulated 0.4 OD_{600} suspension at 30 pN and 2 kHz between one and four hours when cells were free to grow in the sample. For every time point, I monitored both cells concentration and its change in coverage. As anticipated, this decreased over time with increasing cells growth and suspension density (Figure 32).

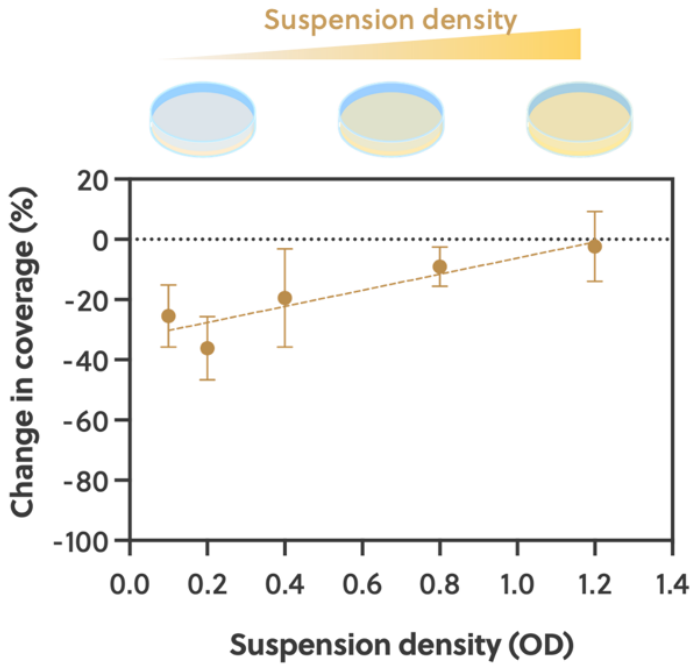

Figure 31: Change in surface coverage after 2 hours vibrations at 30 pN and 2 kHz with increasing suspension density (0.1 to 1.2 OD). Vibrational reduction of surface coverage decreases with cells concentration. Datapoint represents the mean change in surface coverage with its SD determined as the average difference between samples and controls from three independent replicates (n > 110 for all conditions). Dotted lines is simple linear regression (R^2 = 0.95).

Specifically, while cells concentration in samples increased from 0.4 to approximately 1 OD_{600}, the resulting change in surface coverage diminished from -31% after 1 hour to no

significant difference after 4 hours. These results followed the same pattern observed in our previous findings corroborating the idea that increased cells density have a detrimental effect on vibrational stimulation as this is completely negated when densities reach values near and above 1 OD_{600}.

To explain these findings and the inverse proportionality between vibrational response and suspension density, I investigated cells surface sedimentation. In fact, over

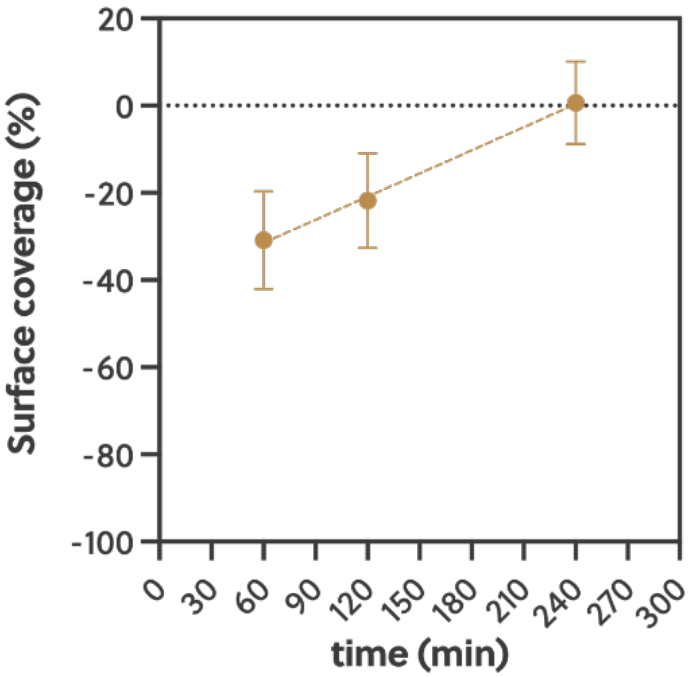

Figure 32: Change in coverage after vibrational stimulation (30pN, 2kHz) applied from 1 to 4 hours. Vibrational response decreases over time in response to cells growth and increasing density in samples (0.42, 0.61 and 0.91 OD_{600} for 1, 2 and 4h respectively). Data points are the mean and SD of the change in coverage between samples and controls. (n > 111 for all conditions). Dotted line is linear regression (R^2 = 0.99).

time, cells can reach the surface through swimming and passive deposition. However, during prolonged exposure and because of cells growth and environmental crowding, clusters would start forming in the medium and fall on the surface as sediments. The

resulting biotic mat can then hamper cells vibrational stimulation because of its different mechanical properties than the hard surface. As a result, clustered and sedimented cells would experience dissimilar forces than those originally applied a fact which would also violate the assumptions required by the approximations I used to estimate them. I therefore hypothesized that extended cells sedimentation would inhibit vibrational stimulation and its effect on colonisation.

To assess this hypothesis, I quantified cells surface sedimentation over time for different suspension densities. These were obtained resuspending overnight M63+ cultures in 5 mL of fresh medium within sample dishes and at variable OD_{600} of 0.2, 0.4 and 0.8. Samples were then incubated at 30˚C in the dark and surface colonisation was allowed for progressively longer times of 1, 10, 30, 60, 120 and 240 minutes. After this I used fluorescence microscopy to gather 10 to 15 pictures of the surface from which I quantified cells' sedimentation following the image processing steps represented in Figure 33.

Aim of my analysis was the determination, for every picture, of a sedimentation ratio expressing the fraction of surface area covered by sediments. To obtain this, I started by quantifying the total coverage in each picture without applying any restriction to the size of the analysed objects in them. Then I determined the coverage due to individual cells by restricting the above analysis only to those objects within our previously determined cell size of 4 $\mu m^2 \pm 0.9$. Finally, I subtracted this cell coverage to the total obtaining the sedimentation coverage that, when divided by the total, resulted in the looked-for sedimentation fraction. For a given suspension density and time point, this approach was applied to all pictures gathered from three experimental replicates and the resulting ratios were averaged and interpolated for graphical comparison.

From the resulting data, sedimentation fraction increases sigmoidally over time for all tested cells concentrations (Figure 34). The higher this is, the quicker and the earlier surface sedimentation happens as more cell clusters can reach the surface. After 2 hours, sedimentation fractions increased with cells density reaching values of 3%, 31% and 78% for 0.2, 0.4 and 0.8 OD_{600} respectively (vertical dotted line in Figure 34). Moreover, when looking at the time evolution of surface sedimentation at 0.4 OD_{600} (mid-line in Figure 34), its increase correlates with the previously observed reduction in vibrational response overtime (Figure 32). From these results, I inferred that increasing surface sedimentation

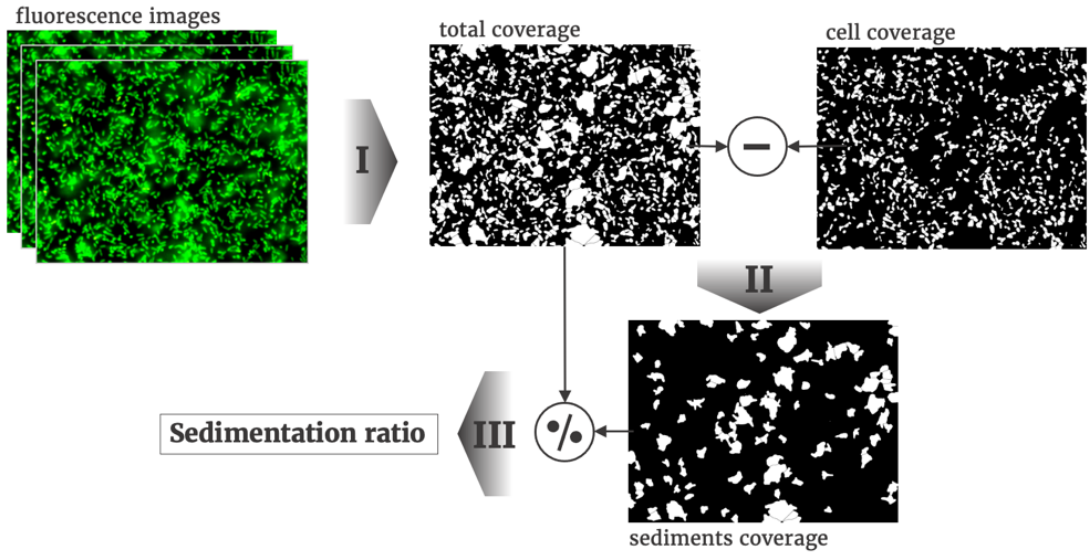

Figure 33: Sedimentation analysis workflow: I) a threshold is applied to fluorescence images and used to determine the total and cells specific surface coverage, II) the two are subtracted to obtain the coverage due to surface sediments only. III) this value is then divided by the total to determine the sedimentation fraction of the area covered by cells sediments.

reduces vibrational influence on its colonisation. Consequently, vibrations appear to better stimulate cells under limited or absent surface sedimentation as this diminishes vibrational

response which completely disappears when sediments saturate the surface.

The onset of their sigmoidal growth represents then the time before vibrational stimulation starts losing its efficacy and it therefore defines its applicability window. In

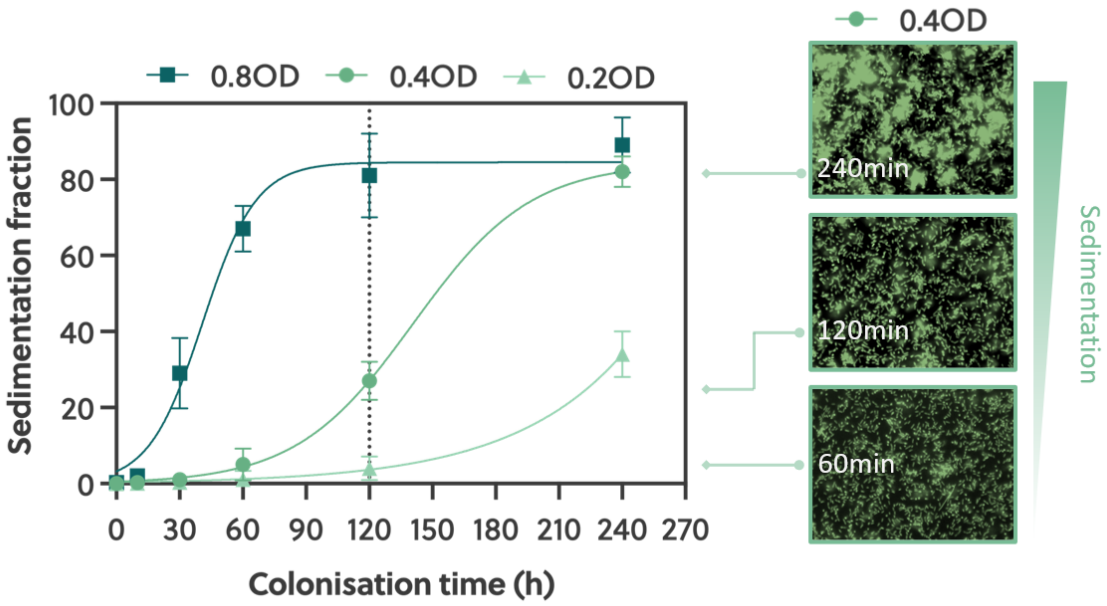

Figure 34: Sigmoidal growth of surface sediments for three different starting cells concentrations (0.2, 0.4 and 0.8 OD_{600}). Data for specific time points represents the mean sedimentation ratios and their SD determined as the average value across three independent replicates (n > 36 for all conditions). Lines are sigmoidal interpolations of the resulting mean values (R^2 > 0.96 for all tested cells densities). Inserts on the right are fluorescence images of surface coverage at 60, 120 and 240 minutes from 0.4 OD growth.

fact, before this time, the process happens with limited to no clustering and mechanical stimulation can effectively be transferred to surface approaching cells. However, passed this point, surface coverage transit from individual cells to sigmoidally growing clusters. These hinder vibrational stimulation through the formation of a biotic mat which, upon saturation, completely inhibit cells response. Consequently, the longer the surface can remain free from sediments, the longer vibrations can limit cells colonisation. This makes

sedimentation curves a fundamental parameter which need to be accounted for before applying vibrations in all those scenarios where bacterial growth could happen unchecked.

I use this newly acquired knowledge to further optimise vibrational stimulation under my own experimental conditions. In fact, the above results predict that greater vibrational response should be expected when these are applied at low sedimentation. Since I were interested in 2 hours stimulations, I looked at minimise this process during this time. Under my initial conditions of 0.4 OD_{600}, sediments covered approximately one third of the surface (33%) but when this was halved to 0.2 OD_{600} this value decreased to only 3% (Figure 34). Looking then at 0.4 and 0.2 OD response after 2 hours stimulation (30pN / 2kHz) I saw that surface coverage on vibrated samples further decreased from -21% to -36% (Figure 32). Guided by this observation, I therefore maximised vibrational stimulation over 2 hours by minimising surface sedimentation by halving cells concentrations to 0.2 OD_{600}.

3.5 Cells response to mechanical stimulation is time dependent

From the above, I learned about the importance of suspension density in planning vibrational experiments and how surface sedimentation can negatively affect their outcomes. I also saw that, for the same reasons, vibrational response decreases over time if cell growth is left unchecked. However, this information left open the question of when and how vibrations influence on cells colonisation changed with the length of their application. To answer this question, I stimulated cells at 30 pN and 2 kHz over

progressively longer times from 10 to 120 minutes. Moreover, to prevent sedimentation to influence my results the longer vibrations were applied to cells, I minimised its impact by adjusting the starting cells concentration based on stimulation length. Specifically, when this was shorter or longer than one hour, I respectively used suspension densities of 0.4 and 0.2 OD_{600}. In fact, as I saw in the preceding section, sedimentation is of little

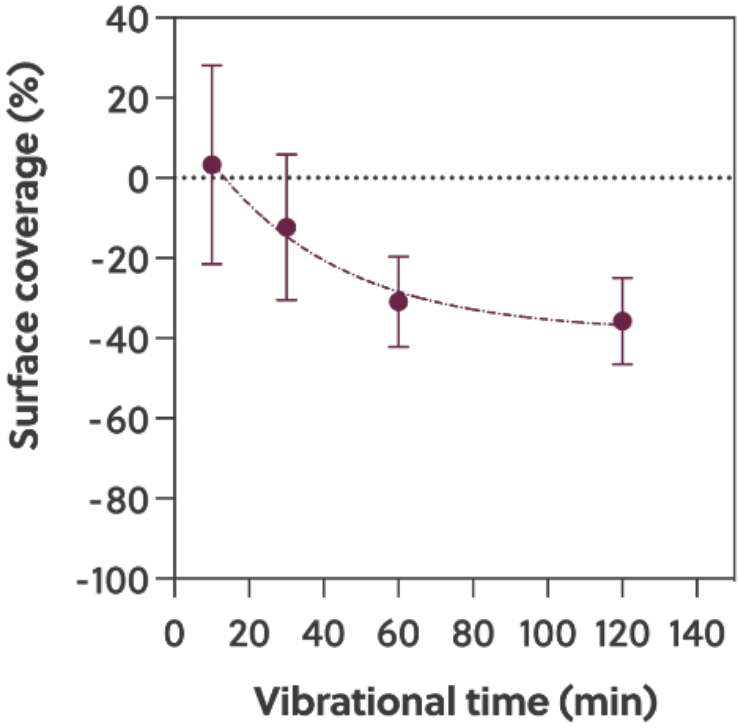

Figure 35: Change in surface coverage following longer stimulation length (30 pN / 2 kHz) under minimal surface sedimentation (less than 5% for all conditions). This was achieved using cellular suspensions of 0.4 and 0.2 OD_{600} for experiments respectively below and above 60 minutes. Datapoint represents the mean variation and its SD determined as the average value across all fluorescence pictures among three independent replicates (n > 105 for all tested times). Dotted line is non-linear interpolation of the mean values (R^2 =0.89).

extent and similar for colonisation times below 60 and 120 minutes respectively (Figure 34). From the above experiments I observed that surface coverage on vibrated samples

decreased with increasing stimulation time until it plateaued when this was applied beyond one hour (Figure 35). Specifically, vibrational stimulation began affecting cells colonisation after 30 minutes (13% coverage reduction) and then, after one hour, its effect more than doubled (31%) and remained nearly constant afterward (36% at 2 hours).

These results proved that cells response to vibrational stimulation is both delayed and non-linear in time. In fact, vibrations require a minimum of 30 minutes to elicit an effect on cells and one hour to approach their full efficacy. This suggests that stimulations do not have an immediate effect on cells but that it rather unfolds within the first hour of their application. This delay and its origin present two non-mutually exclusive hypothesis: (i) vibrational stimulation takes time to induce a physiological effect or (ii) this happens quickly but its response is slow to unfold. No matter which one of the above scenarios prove to be correct, the presence of such a delayed response strongly points toward a physiological process that needs time to be activated and initiate a response.

I will explore what such process might be in the following chapter when discussing the involvement of protein synthesis and membrane potential in transducing vibrational stimulation but for the rest of this chapter the focus is set on the second characterising feature of the above findings: their non-linear response. In fact, while their effect on surface colonisation kept increasing with time, its change decreased until the effect remained constant when the plateaux was reached. This loss of efficacy suggests that some process is counteracting vibrations making them less and less effective at mitigating colonisation. Having excluded sedimentation as a lurking variable given its limited extent within these experiments, I thought instead that one such countering effect could come from cells colonisation itself.

3.6 Surface colonisation do not affect vibrational response

In the experiments above, vibrational stimulation reduced surface colonisation when these were applied from the onset of this process. However, during the early colonisation stages, cells transition from a planktonic to sessile lifestyle which leads to their improved surface adhesion [144]. Consequently, over the course of 2 hours, cells become better colonisers, a fact that could counteract vibrational stimulation and explain their decreased efficacy with time. In fact, as surface adhesion improve with colonisation time, I expected that the longer this could happen before stimulation the less it would be hampered by it.

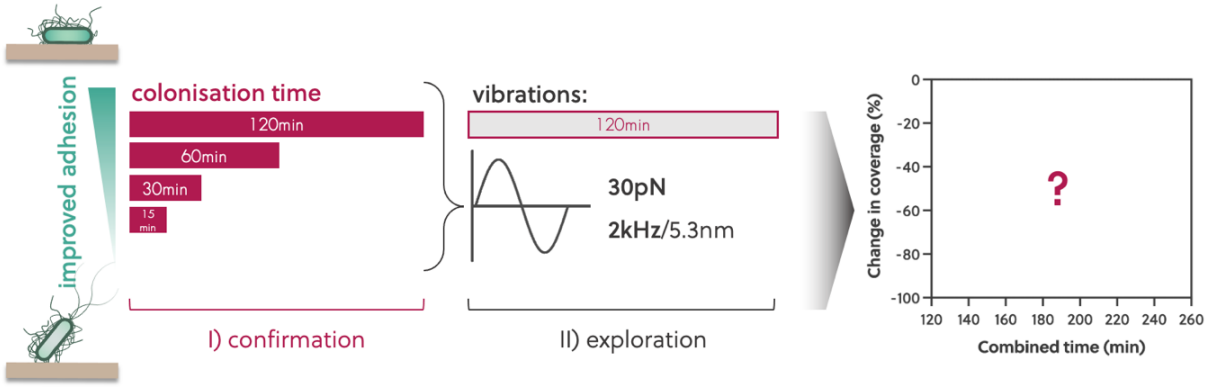

Figure 36: Experimental strategy I used to assess the effect of surface colonisation on vibrational response. From the left to the right, I first confirmed that cells surface adhesion improves with colonisation time (I) and, second, I explore the influence that this has on cells response to vibrations when these are stimulated for 2 hours at 30 pN and 2 kHz (II).

In an unexpected turn of events where the acted upon became the agent, I therefore investigated the effect that surface colonisation had on vibrational stimulation. I did this following a two steps approach which is depicted in Figure 36. First, I confirmed that

surface adhesion improves with colonisation time and then I determined how this process could affect cells response to vibrations.

To address our first point, I let cells to colonise surfaces from 10 to 120 minutes and then compared their changes in coverage after these were washed. My prediction was that, as colonisation times increase, so would cells' adhesion leading to more and more cells remaining on the surface after these were washed. However, longer colonisation times can lead to increasing surface coverage not only via improved cells adhesion but also through sedimentation as over time more cells reach the surface. This can be seen happening in Figure 37 A where the green line shows that surface coverage of a 0.2 OD_{600} suspension increases over 2 hours.

Consequently, longer colonisation times would lead to broader surface coverages also because of longer cells deposition. If left uncheck this phenomenon would then bias my results as it would prevent to link changes in coverage to improved adhesion. For this to be possible, I blocked the effect of cells deposition by equalising all samples coverages before washing (Figure 37 A, red dots). This way, differences in surface coverage after washing can only be explained by changes in cells adhesion.

Having successfully blocked sedimentation from biasing our results, I assessed the effect of improved adhesion by resuspending overnight M63+ cultures into 5 mL of fresh medium within polystyrene sample dishes at variable concentrations (0.33, 0.28, 0.25 and 0.20 OD_{600}) according to colonisation length (15, 30, 60, 120 minutes respectively). This was then allowed by incubating the samples in the dark at 30°C, after which these were washed and 30 to 40 pictures of the surfaces gathered per sample using fluorescence microscopy. Change in coverage were finally quantified from the resulting images

(Materials and Methods).

Applying the above procedure, I observed that, surface coverage after washing increased with cells colonisation time (Figure 37 B). Specifically, between 15 to 120 minutes the fraction of remaining cells on the surface after washing increased from 0.34 to 0.78. During this time, more cells are assumed to have transitioned from planktonic to sessile phenotype, allowing more of them to withstand washing.

These results re-establish the correlation between surface colonisation and improved cellular adhesion under my experimental conditions. I used this fact to assess my second point from above and check the effect that colonisation and improved cells adhesion has on their vibrational response. The way I approached this was by letting cells

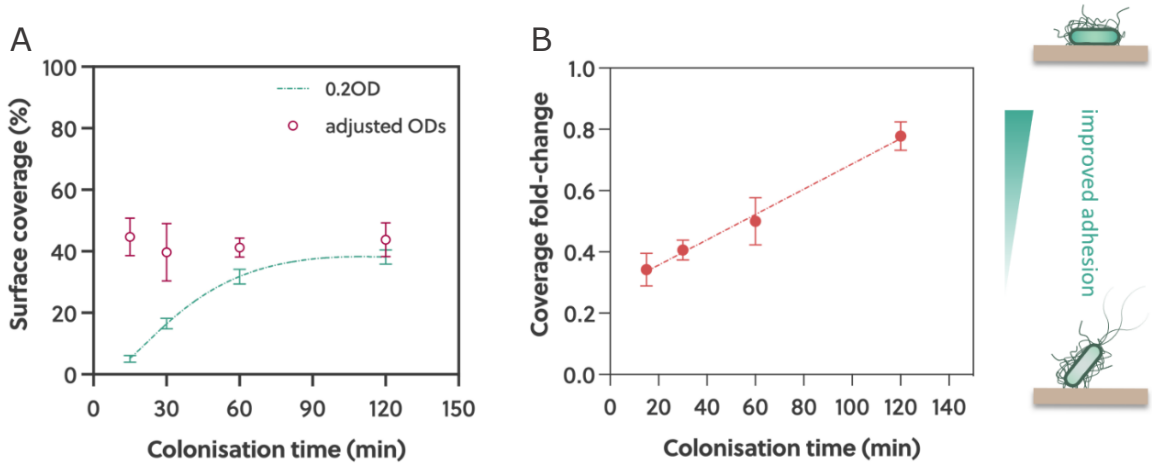

Figure 37: A) Surface coverage for a 0.2 OD cellular suspension increases with colonisation time (green line). Similar coverages (red dots) are obtained by adjusting cells concentration (0.33, 0.28, 0.25 and 0.20) with colonisation length (15, 30, 60, 120 minutes respectively). B) Change in coverage after samples with longer colonisation times were washed. Datapoints represents the mean surface coverage (A) and its fold change (B) with associated SD. For all conditions, these were determined as the average value across all fluorescence pictures from three independent replicates. Dotted lines are mean non-linear (A) and linear (B) interpolation lines ($R^2 > 0.91$ for both).

undisturbed to colonise surfaces for variable times before applying vibrations and compare the resulting change in coverage. I expected that, as surface adhesion improve with colonisation time, the more this was allowed to happen before stimulation the less vibrations would decrease cells coverage.

Experimentally, I tested the above resuspending overnight M63+ cultures in 5 mL of fresh medium within small polystyrene petri and allowed surface colonisation to happen in the dark at 30°C between 15 and 120 minutes. As for the previous experiments, to minimise differences in surface coverage to bias the results, I adjusted cells concentration based on colonisation length. After this one, I then diluted the samples 1 in 25 to isolate cells surface populations and prevent that difference in cells suspension would influence vibrational stimulation. This was finally applied for 120 minutes at 30 pN and 2 kHz after which samples were washed and fluorescence microscopy was used to gather 30 to 40 pictures from the surface. From these I finally quantified surface coverage through automated image processing and analysis (Materials and Methods).

Contrary to my expectations, I observed that, following longer colonisation times, vibrational influence remained constant, decreasing surface coverage by an average 23% across conditions (Figure 38). Improving cells surface adhesion through increased surface residence time prior to stimulation appears then to have little to no effect on vibrational response.

These results marked two important points: first, they reject the hypothesis that increased cells adhesion decreases the effect stimulation has on colonisation over time. Second, they show that vibrations do not need to be applied from the onset of surface colonisation to be effective.

In fact, vibrations can still mitigate adhesion even when this has been happening for up to 2 hours before stimulation. This allows vibrations to also be applied in those scenarios where surface colonisation had already taken place.

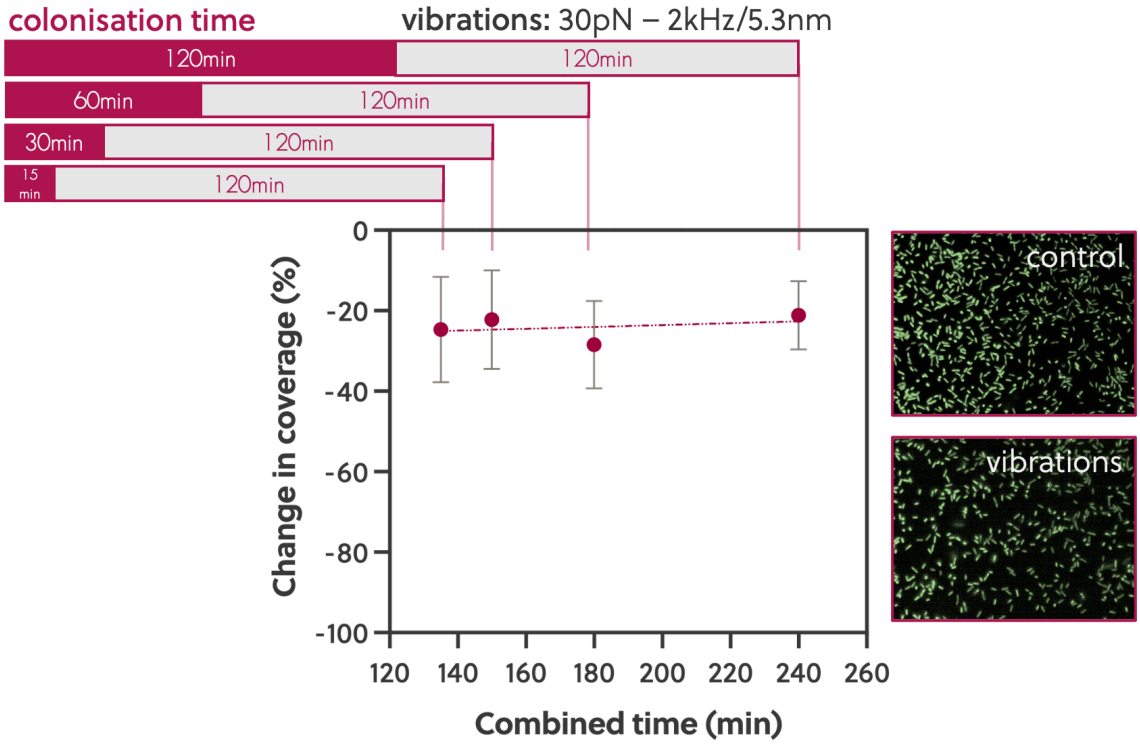

Figure 38: Effect of colonisation time on cells response to vibrations. Samples were let to colonise surfaces for different times (from 15 to 120 minutes) after which they were diluted and stimulated for 2 hours at 30 pN / 2 kHz. Changes in surface coverage remained constant with longer colonisation times with an average reduction of 23%. Inserts are fluorescence images of cells from the surface. Datapoints represents the mean change in coverage and their SD determined as the average value across all fluorescence pictures among three independent replicates (n > 120 for all conditions). Dotted line is simple linear regression ($R^2 = 0.93$).

I began this section looking for an answer to the non-linear change in vibrational response I observed with time, hypothesising that this could have derived from the very same process vibrations were hindering: surface colonisation. Specifically, as this is

happening during stimulation, cells adhesion would improve and counteract the effect of vibrations. As stated, the above results proved this is not the case as cells variation in surface coverage varies little between samples with longer colonisation time. This finding, while reject my hypothesis, it also strengthened its competitive one: that only a fraction of cells population could be sensitive to the applied stimulation.

To explain this phenomenon and find a reason for vibrations effect on surface colonisation, I carefully peaked into cells physiology and its change upon mechanical stimulation. I will discuss my efforts on this regard in the next chapter but before going there and try to find a biological explanation to my findings, I first exclude that these were deriving from damaging effects vibrations had on cells.

3.7 Vibrational stimulation does not damage cells envelope

To exclude harmful effects vibrations could have on cells I used a fluorescence microscopy technique known as live/dead assay. Despite cells death can be a daunting task to define, the loss of their membrane integrity can act as a proxy of their viability. Specific dyes pairs take advantage of this fact and assess for its loss using different combinations of dyes permeabilities and fluorescence.

One of such pairs, and the one I used, is Syto9 and propidium iodide (PI). Both dyes bind to nucleic acids, but the former is membrane permeable and has green fluorescence while the latter is impermeable and has red fluorescence. Because of its non-permeability, when used in combination with Syto9, PI can only stain cells with damaged or instable membranes. However, once inside the cell, it would compete with Syto9 for binding sites

but, because of its higher binding enthalpy, its prevailing would cause cells fluorescence to turn from green to either yellow or red depending on the extent of permeability loss and membrane damage. This can then be quantified by computing the ratio of damaged (red) to healthy (green) cells in fluorescence pictures; the bigger the ration, the more severe the damage caused by the process under examination is.

To assess this occurrence in our vibrational experiments, I stimulated cells for 2 hours (0.2 OD_{600} starting concentration) at 30 pN and 2 kHz and stained them according

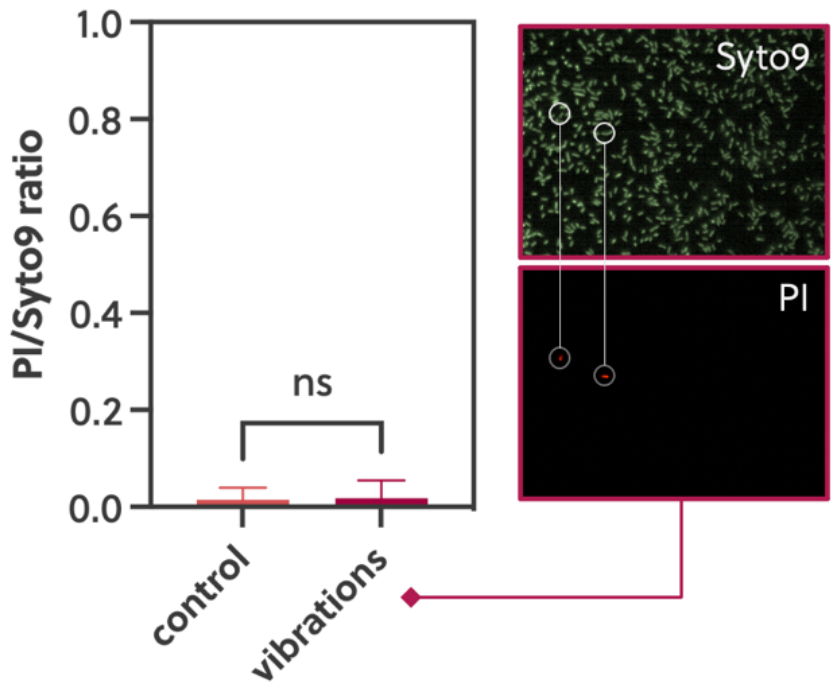

Figure 39: Ratios of red (damaged, PI stained) to green (healthy, Syto9 stained) cells with and without vibrational stimulation (2 hours at 30 pN and 2 kHz). The same red/green ratios were observed for vibrated samples and controls (< 0.2%). Inserts are samples images from vibrated surfaces - damaged cells in the red channel are highlighted in white. Data represent the mean and SD of all ratios coming from pictures among three replicates (n > 134 for both control and vibrations).

to manufacturer instructions using Syto9 (3.5 μM) and propidium iodide (18 μM) for the remaining 20 minutes of vibrational stimulation (Materials and Methods). This was then stopped, samples were washed and 30 pictures gathered from the surface as pairs on both the red and green channels. From these I finally derived the total number of cells that was used to determine the extent of cells damage from their red to green ratios.

Following these experiments, I observed that less than 0.2% of cells on the surface were positive to red fluorescence and that this value was not statistically different for non-vibrated controls (Figure 39). This shows that vibrations are not harmful to cells when these are mechanically stimulated and that this cannot be responsible for their effect on surface colonisation. Therefore, vibrations appear to act as a genuine cells stimulant that can mitigate surface colonisation without interfering with their physical integrity.

3.8 Conclusion

Before venturing forward and explore the experiments I did to find a mechanistic explanation to the above findings, it is beneficial to stop and recollect what these are.

When applied for 2 hours, vibrational stimulation with piconewton intensities decreases bacteria surface colonisation by 21% (Figure 29). For stimulation frequencies of 2 kHz, this effect is independent from the applied intensity as the response is constant across all tested forces between 15 pN and 500 pN. This force non-specificity is a most welcome result as it makes vibrational stimulation more flexible to meet different experimental needs as cells can be stimulated within a range rather than using specific values. However, the interplay between stimulation intensity and cells response become more complex as their frequency is reduced to 1 kHz and 500 Hz (Figure 30). In fact, this

diminishes vibrational response in an intensity dependent manner where central forces of 30 and 50 pN are less sensitive to this change while with side forces of 15 and 100 pN cells response decreases by up to 38%.

Changings in stimulation frequencies rather than intensity appears then to have a greater impact on vibrations ability to alter cells behaviour suggesting a deeper connection to their millisecond time scale. Specifically, 0.5 ms periods (2 kHz) between consecutive stimulation peaks, proves the most effective at reducing surface colonisation. I will explore this point further in the coming chapter where I will discuss its connection to changings in cells polarization following vibrational stimulation.

I then observed that increasing cells concentration in the medium decrease vibrations effect on surface colonisation. Specifically, for cells concentrations beyond 1.0 OD_{600}, 2 hours stimulation at 30 pN and 2 kHz stopped having any inhibitory effect on cells surface colonisation. I explained this observation with the sigmoidal growth of cells sediments on the surface as their different mechanical properties compared to the hard polystyrene can damp cells stimulation. In fact, this is retained until sediments start growing sigmoidally on the surface, a process that depends on cells concentration. The lower this is, the more it takes for sediments to appear allowing mechanical stimulation to be effective over longer times.

Accounting for this phenomenon, when I halved cells concentration from 0.4 to 0.2 OD_{600}, surface sedimentation over 2 hours decreased from 33% to 3% (Figure 34) allowing vibration to further reduce cells coverage from -21 to -36% (Figure 31). Surface sedimentation and its sigmoidal growth appear then as prime factors that need to be accounted for when vibrationally stimulating cells. More generally, these results suggest the deleterious damping effects that on this process could also have other forms of surface

crowding and impurity such as conditioning layers and cells secretions. Conditioning layer is a term loosely employed to identify the result of chemicals that passively attach onto surfaces due to their non-specific physical interactions [143]. Cells can then partake to the formation of such layers via the secretion of their own wastes and by-products. Furthermore, once on surfaces, cells can alter their mechanical environment via the secretion of extracellular polymeric substances or EPS [199]. These are a mixture of polysaccharides, proteins and DNA that cells use to glue themselves in and that could damp their mechanical stimulation.

I expect the above processes to have little influence on my results as our experimental conditions proved unfavourable to the formation of a conditioning layer. This was in fact limited by using pristine sterile surfaces and minimal media that respectively reduced the incidence of surface impurities and, contrary to rich media, had no debris, proteins or other chemical chunks in suspension. Moreover, influences from cells secretions were limited by resuspending them in fresh minimal media that prevented any by-product from overnight cultures to be carried into samples. However, under less controlled environments, the influence of conditioning layers and cells secretion can't be overruled and its damping effect on vibrational stimulation would require further investigation. Nonetheless, I suggest that, because of the nanometric scale of the resulting layers, these would have a smaller effect on vibrational transfer than cells sedimentation, making them a less relevant variable to account for.

Following the above experiments, I also observed a complex interplay between stimulation time and altered surface colonisation (Figure 35). In fact, cells response appears after 30 minutes and this non-linearly increases with time as it double after 60 minutes and plateaus to a constant value between 60 and 120 minutes. This lag suggests

that some physiological feature needs time to translate the vibrational input into an altered colonisation output. As similar delays are common in transcriptional response, which require the activation and transcription of new proteins, I will investigate its involvement in my findings through the coming chapter. Moreover, this non-linear response suggests that while vibrational effect on colonisation keep increasing with time, it does so with less and less efficacy. This presented the hypothesis that either a fraction of the population is sensible to the applied stimulation or that cells could counter stimulation through a yet to be discovered mechanism.

I thought one of such mechanism could have been surface colonisation itself that, by improving cells adhesion over time, would have made them more resilient to stimulation. However, when cells with longer surface residence times were stimulated, vibrational response did not decrease but remained constant instead (Figure 38). Consequently, improved adhesion during colonisation did not explain the non-linear change in cells response with stimulation time. While weakening my second hypothesis from above, these results strengthen the former, suggesting that only a fraction of cells residing on the surface could be sensible to mechanical stimulation.

This view is supported by the fact that vibrations only have a limited effect on surface adhesion. In fact, at ideal conditions (0.2 OD, 30 pN, and 2 kHz), the coverage loss never exceeded 36%. (Figure 35). This behaviour could be explained by two phenomena: population bet hedging and cell surface orientation.

Bacterial bet hedging refers to the ability of bacteria to cope with unexpected environments by stochastically altering gene expression. This permits a previously homogeneous population to become heterogeneous. Subpopulations of the resultant cells express various sets of genes, causing them to respond differently to mechanical stimuli.

This mechanism is also more likely to occur under stationary phase and starving conditions, both of which our experimental settings satisfy.

Alternatively, the orientation of cells on the surface can influence how they respond to stimulation. As we saw from Equation 6, the force and pressure that cells feel on their membrane are proportional to their surface area. This value, as well as the force acting on them and their mechanotransduction, changes with different orientations.

The above hypothesis could be tackled in the future by either monitoring cells heterogeneity using flow cytometry pre and post experiment. Since different gene expression is often correlated to different phenotypes, the comparison between forward and side scattering of cytometric data could eludicate cells' population homogeneity in samples and during vibrational experiments. Alternatively, the impact of cells' orientation can be assessed through a thorough investigation of fluorescence images. From these, several algorithms can be applied to determine the angles cells form with the surface. By comparing the fraction of upright and flat standing cells between vibrated samples and control one can infer which population could be more sensitive to vibrational stimulation and therefore less likely to appear on the gathered pictures.

Finally, I tested for vibrational damage on cells membrane and observed that stimulation is harmless as the fraction of damage cells on vibrated samples was both minimal (< 0.2%) and non-significantly different from non-vibrated controls (Figure 39). This is an important confirmation which allowed me to exclude cells damage as an explanation of cells behaviour and consolidated vibrations role as cells stimulants.

To summarise, my results shows that vibrational stimuli mitigates surface colonisation when these have piconewton intensities and kilohertz frequencies. The extent of cells

response reaches max effect within 2 hours of stimulation and, while it is independent of adhesion strength or previous surface colonisation, it is negatively affected by cells sedimentation. These findings ultimately provided me with a round understanding of the effect that vibrations have on cells surface behaviour and which experimental parameters needed to be accounted for its optimisation.

With this knowledge at my back, I investigated how vibrations effect on cells surface behaviour could be brought about. I tailored vibrational stimulation to elicit physiological changings aimed at disrupting cells natural surface sensing and colonisation. Having achieved this, I explored which physiological changings could have been responsible for it; a search that I began by confirming physiology as a necessary condition to my findings. This is where we are heading next.

4. MECHANISM HUNT

In the preceding chapter, I established a connection between vibro-mechanical stimulation and reduced bacteria surface colonisation (Figure 29). I achieved this by applying forces of piconewton intensities to elicit physiological changings in bacteria. Understanding the nature of such changings was fundamental step in bridging the knowledge gap laying between our input (vibrational stimulation) and our output (decreased colonisation). In fact, a connection between these two phenomena in a causal

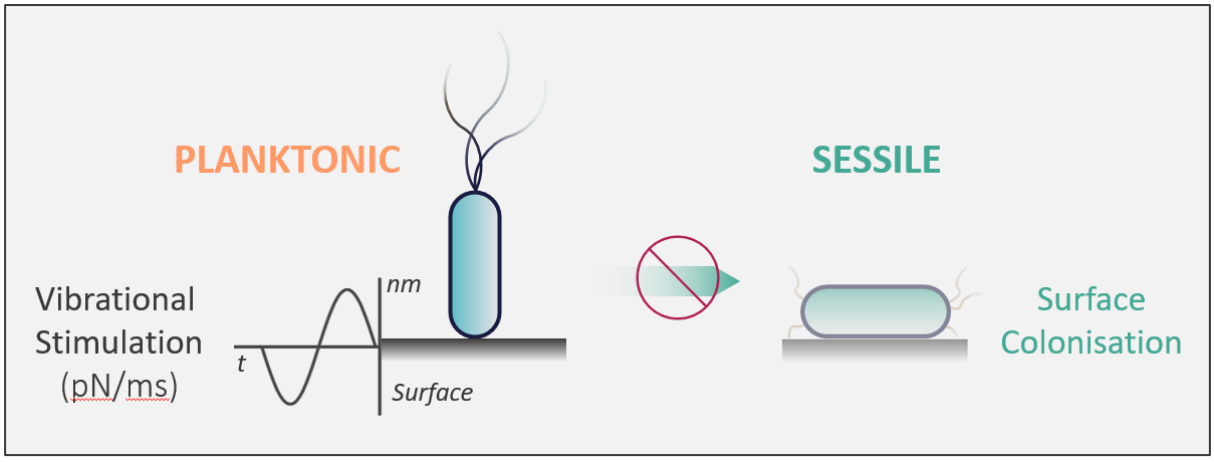

Figure 40: Schematic representation of the existing connection between vibrational stimulation and surface colonisation. Specifically, when surface approaching planktonic cells are mechanically stimulated with piconewton intensities and over milliseconds periods (kHz frequencies), surface colonisation is decrease suggesting their delayed transition to a sessile state. The reminder of this chapter would be to identify what connects vibrational stimulation to hampered surface colonisation.

chain would enable to explain my findings through the proposition of a mechanism. Therefore, clarifying such a connection and identifying such mechanism occupied the remainder of my experimental efforts and the following of this chapter.

4.1 Vibrational effect and its nature

The previous chapter ended by excluding cells damage from being responsible for the observed reduction in surface coverage, but it did not prove that vibrations elicited physiological changings responsible for my findings. In fact, these could have been explained using entirely physical, physiological or mixed arguments. Indeed, vibrational response might have been caused by changing in cells physiology, such as flagella motility or protein synthesis, but they might as well have been explained by purely physical effects such as mechanical repulsion or other unforeseen physical phenomena. These would not have involved any aspect of cells biology as they would apply to any physical object given its correct size. Therefore, to explain my results and fil the gap between vibration and colonisation, my first step was to identify the nature of its mechanism. This information would have guided my search either on the physical or physiological side of the cell to surface interaction.

As any other living organism, bacteria perform biological tasks while retaining general physical properties through their body and shape. Both sides of their nature influence and account for the complexity of their surface interactions which are mostly categorised as passive or active. Passive interactions are exclusively physical in nature and do not require any involvement of cells metabolism and functioning to be performed; they are, in this sense, passive. These are further divided into generic and specific; the former, as the name suggest, are those broad and average physical properties defining cells outer membrane such as its charge, hydrophobicity and overall chemistry. These are generic since their existence rely on fundamental physical forces and are non-exclusive to cells as any microscopic objects interacting with the surface would be characterised by them.

Specific interactions are instead cell specific or even strain specific and account for the ensemble of their outer membrane features. External appendages and adhesins such as pili, flagella, curli and cellulose along with the peptidic or lipidic nature of the outer membrane fall into this category. Despite being fundamentally physical in nature, these interactions are distinct from their generic counterparts because they are shaped into features that serves specific biological purposes. Balancing these passive and mostly physical surface interactions, are active and exclusively "biological" ones. Active here stands for physiological activity as these represent all behavioural responses bacteria perform when interacting with a surface. While some of these modulate pre-existing generic and specific interactions, others genuinely internalise mechanical signals from the environment and generate unique responses such as changing in motility, membrane volage, gene expression and protein synthesis [141].

The concerted combination of the above interactions account for the complexity of cells surface adhesion and early colonisation [143]. Since vibrational stimulation hinder this process, vibrations effect on cells should derive from the disruption of one or more of such interactions. To understand which one was the most relevant to explain my findings, I assessed their involvement independently.

As in mutational studies a lack of function link to a lack of response, in the same way I approached my investigation. I removed an interaction at a time and observed how this impacted vibrational response and the associated reduction of surface coverage. If such a removal would have diminished vibrational response, then the removed interaction was a necessary condition. Since no easy mutation exist to suppress either passive or active surface interactions, I studied instead the response to vibrations of other systems as abiotic particles and dead cells (Figure 41).

As purely physical objects, abiotic particles can interact with surfaces only through physical generic interactions. Selecting beads where such properties were similar to my cells would have accounted for their involvement in vibrational response. In fact, since such system can interact with the surface only through generic interactions, their lack of

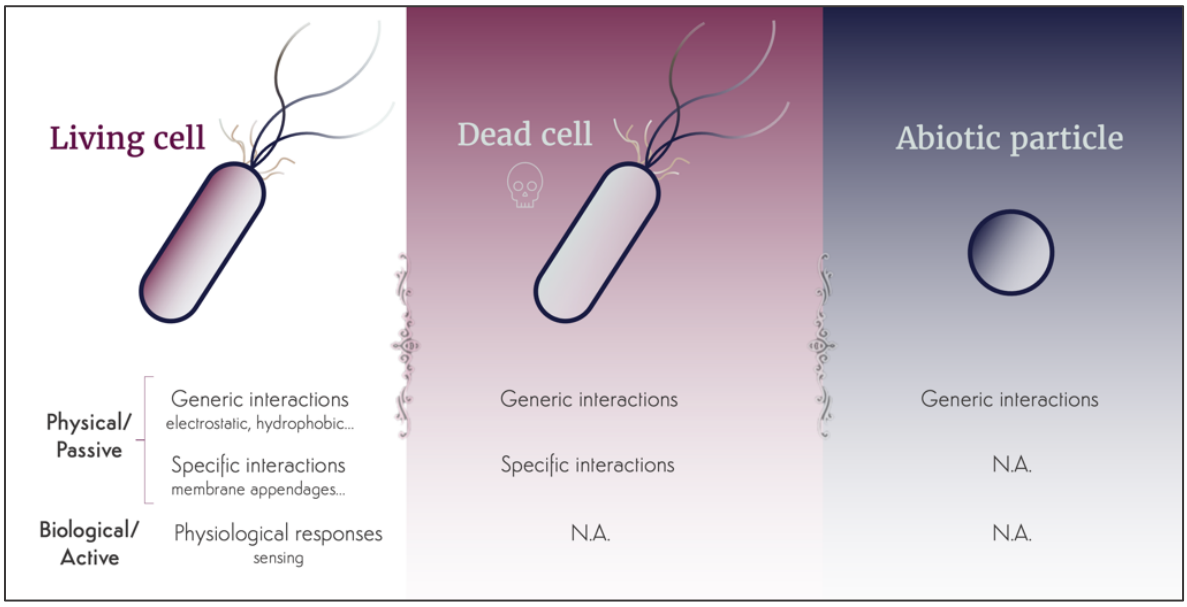

Figure 41: Schematic representation of surface interactions available to different systems. Living cells (left) possess a full interaction spectrum with both passive "physical" and active "biological" interactions. Dead cells (centre) by the lack of both an active metabolism and physiological function cannot make use of biologically active interactions with the surface. Abiotic particles (right) are limited instead to generic physical interactions only.

response to stimulation would suggest that these are not the mean through which vibrations influence cells colonisation. Moving one step further, dead cells, could rely instead on both generic and specific interactions because of their shape and the presence of a cell membrane. However, lacking a working metabolism and the ability to physiologically respond to stimuli, they are not able to actively interact with the surface. As such, their failed or diminished response to vibration would suggest that active

biological interactions are necessary for cells response to vibrations. Following this approach, I then dissected the nature of the vibrational effect by looking at the response of these new systems with reduced surface interaction complexity.

4-1.1 Vibrational response relies on physiologically active interactions

I began these investigations using abiotic particles. For these to be effective at capturing cells passive generic interactions with the surface, they needed to share similar physical features such as: hydrophobicity, size and charge. Similarly to other studies on bacteria surface colonisation [200], I met most of these requirements utilising fluorescent polystyrene microscopic beads, 1 μm in diameter and functionalised with either ammine (PS-NH_2) or carboxy groups (PS-COOH). This functionalisation and the establishment of their respective weak acid (-NH_3^+) and base (-COO^-) was necessary to generate surface charges and Z-potentials encompassing the reported range of *E. coli* and therefore mimicking its electric properties [201]. I then stimulated both kind of particles with vibrations at 30 pN intensity and 2 kHz frequency for 2 hours and monitored the resulting changing in surface coverage between vibrated samples and controls. Experimentally, this was achieved using my vibrational procedure (Materials and Methods) with the only difference being the use of beads rather than cells suspensions. Under my experimental conditions, I observed that, for all tested beads, their surface coverage did not change when samples were vibrated (Figure 42). The same lack of response was also shared by both kind of particles with no statistically significant difference between them. Since general passive interactions are the only mean through which beads could interact with the surface, from these results

I concluded that passive interactions are not involved in cells response to vibrations.

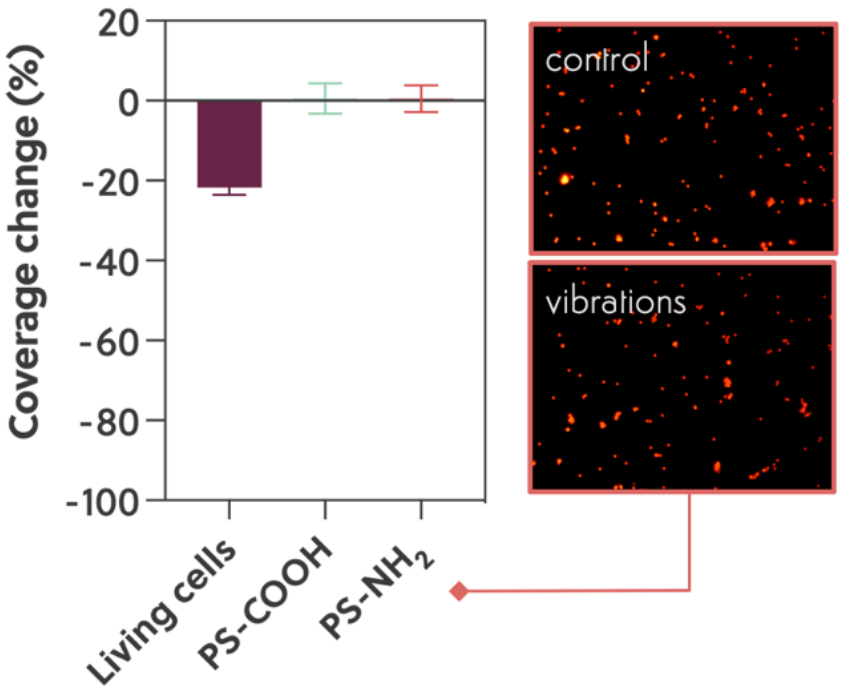

Figure 42: Surface coverage did not change when both carboxy and amine functionalised polystyrene beads were stimulated for 2 hours at 30 pN and 2 kHz. Data represents the mean change in coverage with 95% confidence intervals ($n > 130$ for all conditions, $p^{****} < 0.0001$). Insert are fluorescence pictures from the surface representing ammine functionalised beads on both control and vibrated samples.

Specific interactions were studied next and dead cells were the mean I used to investigate them. As mentioned earlier, their lack of an active metabolism and physiological functioning would prevent dead cells from actively interact with surfaces. However, they would capture both generic and specific surface interactions via their shape and envelope. For this to be possible, membrane and its features needed to be preserved as much as possible upon cells death. Since most of the chemical and physical methods

used to kill bacteria rely on severe membrane damage, I reasoned about the employment of antibiotics instead. Specifically, I opted for the ribosome targeting kanamycin that, by preventing protein synthesis, could kill bacteria with no direct damage to their envelope.

I then treated overnight M63+ cultures with inhibitory concentration of kanamycin (50 µg/mL) and incubated them over 24 hours at 30˚C. I confirmed cells death by plating 100 µL of treated cultures on LB agar and checked for colony formation at 37˚C overnight. Among three replicates, no colony formed on plates (data not shown), confirming our procedure to be effective at making bacteria non culturable, a condition that I associated

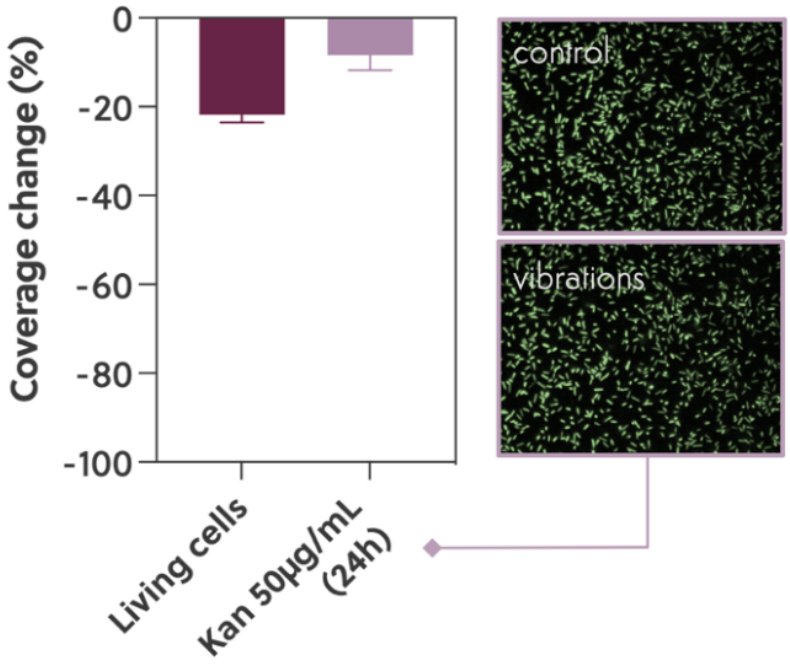

Figure 43: Vibrationally induced change in surface coverage is reduced by ~75% after 2 hours stimulation at 30pN and 2kHz of dead cells. These were treated with 50ug/mL of kanamycin for 24 hours prior to employment. Data represents the mean change in coverage with 95% confidence intervals ($n > 140$ for all conditions, $p^{****} < 0.0001$). Insert: fluorescence pictures from the surface representing dead cells on both control and vibrated samples.

to cells death. Having identified suitable conditions that used antibiotics to obtain dead cells, I tested how these responded to vibrations. To do this, I used the above overnight cultures treated with kanamycin to prepare my experimental suspensions. These were then vibrated for 2 hours at 30 pN and 2 kHz and their effect on surface coverage was quantified following the analysis of the resulting fluorescence images (Materials and Methods).

Treating cells with 50 μg/mL kanamycin reduced the difference in surface adhesion between vibrated samples and control to 8 % (Figure 43). The implications of this finding are two folded: first, dead cells' lack of active engagement with the surface significantly reduces their response to vibrations. However, as this partially persists, vibrational disruption of specific interactions with the surface cannot be ruled out and, together with active interactions, contributes to cells' vibrational response.

Vibrations effect on cells' adhesion appear then to have a mixed nature. In fact, while this mostly depends on cells actively engaging the surface, it also relies on the disruption to their specific interactions with it.

What allow the above results to be inferred is that living and dead cells share the same envelop properties which allow them to interact with the surface through the same mixture of generic and specific interactions (Figure 41). While this assumption is sensible as kanamycin action on ribosomes kill cells by preserving the integrity of their envelope, this could nonetheless change over 24 hours because of passive protein degradation. Because of this, dead and living cells' specific interactions with the surface could differ and with it their response to vibrations.

Therefore, to dig deeper into the role that specific interactions play on cells vibrational

response, the difference in cells' envelope between living and dead cells should be monitored. Fluorescence cytometry would allow such comparison as it can reveal both cells' cells size and shape. Specifically, the greater the overlap in light forward and side scattering of living and dead cells populations, the more they would share similar envelopes.

Unfortunately, because of time constraints, I have not been able to perform these experiments as I directed instead my experimental effort toward understanding how active interactions could mediate cells' vibrational response. In fact, since both abiotic particles and dead cells response to vibrations was either absent or greatly diminished, the above results imply that their effect on cells adhesion mostly depends on the changing in cells' physiology. Having established that the nature of mechanical stimulation is biological, I pursued the search for a mechanism by exploring which aspect of cells physiology vibrations would act upon.

4-1.2 Membrane potential but not ribosome activity is necessary for cells vibrational response

Confident in our believe that the nature of vibrational effect resided in cells biology, I needed to determine which aspect of their physiology vibrations would affect. To achieve this, I once more recurred to the use antibiotics, this time to suppress desired metabolic activities and looked at cell's vibrational response. In fact, vibro-mechanical stimulation would have two effects on cells physiology: it would either induce the synthesis of new proteins or alter the functioning of pre-existing cellular machinery. Using a more technical jargon, the cells response would either be transcriptional or post-transcriptional. To investigate which of these was responsible for my findings, I targeted two of the most

fundamental aspects of cells physiology: ribosome activity and membrane potential.

Ribosome activity is necessary for protein synthesis as they translate nucleotides into aminoacidic sequencies. Because of this central role they are therefore indirectly involved in those surface responses that require new proteins to be synthesised.

Membrane potential might be instead a less well understood or known entity surrounding bacteria's physiology but, as protein synthesis, it is one of their fundamental features if not the oldest and life defining one [202]. From a physical perspective, this electric potential is originated from charged imbalances across cells membrane which are caused by their selective permeabilities to different ions. These resulting charge discrepancy between inner and outer membrane generates a faint electric field that in turn is responsible for the resulting potential. As in a gravitational field, bodies would move from higher to lower values according to their mass, so they would according to their charge in an electric one. Depending then on its sign, this would make either cations or ions to more easily to "fall" from outside to within the cell or vice versa. At its essence this is the fundamental role behind membrane potentials as cells can perform different tasks from these resulting ion fluxes [203]. From a more biological stand points, membrane potential is so ancient, so well conserved across organisms and so fundamental to their functioning that it has even been suggested as our geological ancestor which first formed across the membranes of lithic debris in oceanic vents [202]. The reason why life played around it so extensively lay behind its malleability as a tool. In fact, by controlling ion fluxes cells can also control their metabolic activities and those very same fluxes can also serve as energy source, which is capable to power many different physiological functions, the most important of which are cells motility and energy production. I will explore these in finer details in the coming sections but, to conclude our discussion here, because of membrane

potential critical role in cells physiology, bacteria tend to strike a balance between two opposite conditions: depolarisation and hyperpolarisation. The former happens when ions imbalance across the membrane is resolved and perfect chemical equilibrium is reached. On the opposite side, hyperpolarisation correspond to an increase in ion imbalance and membrane charge. Under normal circumstances in stationary phase, cells aim at maintaining a polarised state known as resting potential that in *E. coli* has a value of about ~150 mV [204]. Because of its central role in cells activity, membrane polarisation appeared as a good candidate to monitor during cells vibrational response, a fact that is further supported by reports of its changings upon surface landing [80].

Because of the above reasons, I tested both the transcriptional and post-transcriptional nature of cells response by observing how this changed when suppressing either ribosome activity or membrane polarisation using antibiotics. Specifically, for the former I used kanamycin and chloramphenicol which target ribosome complexes and prevent peptide bonds formation. For the latter, I used carbonyl cyanide m-chlorophenyl hydrazine (CCCP), an ionophore that suppress membrane voltage by permeabilising H^+ ions. Since their electrochemical gradient in living cells is the principal component to bacteria overall membrane potential, its suppression leads to cells depolarisation. I therefore treated cells with the above antibiotics, suppressed necessary aspects of their physiology and looked at the effect this had on their response to stimulation.

4-1.3 CCCP depolarisation of membrane potentials

Since both kanamycin and chloramphenicol are of broadly and routinely applied in microbiology and genetic engineering, I did not question their effect on cells under my experimental conditions. However, CCCP is more context dependent, particularly in the

way cells polarization is quantified. Therefore, before using it to study membrane potential involvement in vibrational response, I confirmed CCCP depolarising effect on cells. To do this, I treated cells with increasing concentrations of CCCP and quantified their effect on membrane potential using fluorescence microscopy and the voltage-dependent dye: $DiOC_2(3)$. The nature of this dye, along with its electrophysiological response, will be described shortly and in finer detail in the following section. Here it would suffice to know that using this dye, variations in membrane potential can be monitored via changing in both its fluorescence frequency and intensity. Specifically, the dye's fluorescence Stoke-shifts from green to red when its intracellular concentrations increase in response to potential-driven electromigration. This cause polarised and depolarised cells to respectively appear in fluorescence pictures as red/yellow or green. To assess the extent of cells depolarisation, I quantified the ratio of red to green cells in pictures after these were treated with CCCP. What I expected from these results was to observe these ratios to diminish with increasing CCCP concentrations as less polarised red cells would appear in fluorescence images.

Experimentally, I resuspended overnight M63+ cultures in sample dishes to which I added CCCP at working concentrations of 2, 5 and 20 μM. Samples were incubated in the dark at 30˚C for 2 hours then washed, imaged and the polarisation ratios determined from the resulting pictures. Specific image analysis tools and script have been used and these are now going to be described (Materials and Methods).

Briefly, 5 to 15 pictures were gathered from surfaces after 2 hours of incubation. For a given location, images were acquired as pairs on both the red and green channels then automatically processed by a script to quantify their number on both. For every pair, I used the resulting values to compute the ratio of red over green cells which represented

the fraction of polarised cells on the surface.

Following the above procedure, red/green ratios of surface attached cells stained with $DiOC_2(3)$ decreased exponentially with increasing CCCP concentrations (Figure 44). Values above 5 µM strongly decreased membrane polarisation as this was retained by less than 7 % of the imaged cells. These results confirm that, under my experimental conditions, CCCP depolarises cells which make it a suitable choice, together with kanamycin and chloramphenicol, to respectively suppress cells polarisation and protein synthesis.

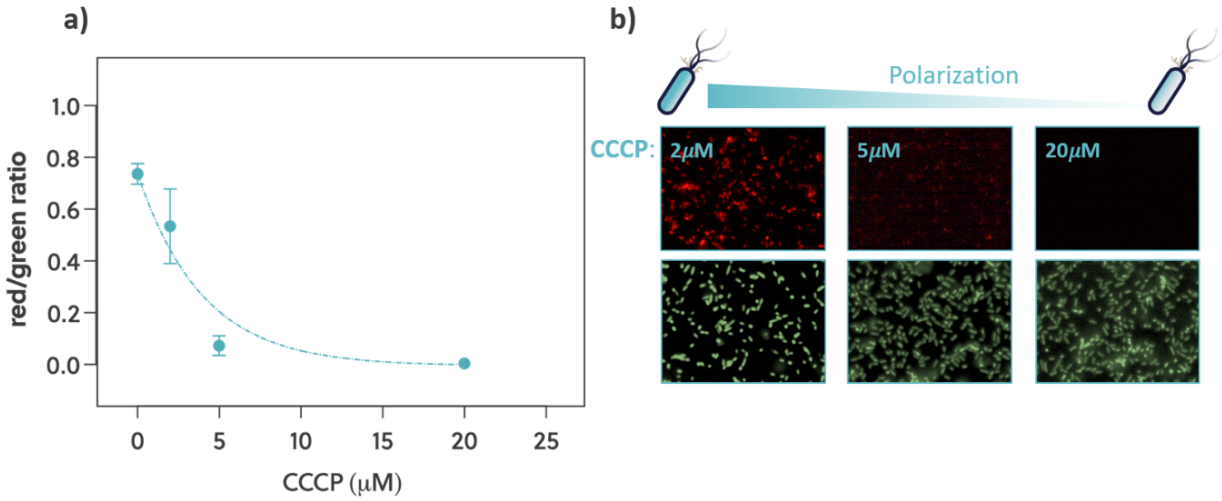

Figure 44: Depolarising effect of CCCP on cells. a) Fraction of polarised cells (red) over total (green) decays with increasing CCCP concentrations. Data are the mean and SD of the resulting ratios from all pictures across three independent replicates. Dashed line is exponential decay interpolation (R^2 = 0.94). b) Inserts of fluorescence images from surface attached cells stained with $DiOC_2(3)$. The number of polarised (red) cells decrease with increasing concentrations of CCCP.

4-1.4 Vibrational response of antibiotic treated cells

To understand if either protein synthesis or membrane potential were involved in

cells response to vibrations, I once more played the game of associating a lack of response to a lack of function. In this case, I was interested in observing reduced vibrational response following the suppression of either protein transcription or cells polarisation. To do this I respectively treated cells with variable concentrations of ribosome targeting kanamycin and chloramphenicol or the proton ionophore CCCP and compared their change in coverage to untreated samples after stimulation. Since in the preceding section I saw how killing cells with antibiotics reduced their response to vibrations, to prevent this from biasing my results, in these experiments I limited cells exposure to antibiotics to 2 hours while also testing sub-inhibitory concentrations.

Experimentally I employed my vibrational procedure with the added difference that samples were supplied with the required amount of antibiotics. These were 10 and 100 μM for kanamycin, 6 and 60 μM for chloramphenicol and 5 and 20 μM for CCCP. Samples were then vibrated for 2 hours at 50 pN and 2 kHz and their effect on surface coverage determined from the analysis of fluorescence images (Materials and Methods). Treating cells with ribosome targeting antibiotics had little to no effect on cells response to vibrations (Figure 45 A and B). In fact, inhibitory concentrations of chloramphenicol (60 μM) and kanamycin (100 μM) respectively caused a 0.87-fold-change and no significant variation in response relative to untreated cells. When these were instead depolarised with CCCP, vibrational response linearly decreased with its concentration (Figure 45 C). Specifically, after 2 hours exposure at inhibitory concentration (20 μM), cells response was almost halved to 0.56 of its original extent.

Taken together, these results show that limiting protein synthesis have little to no effect on cells vibrational response. As such, this seems to be independent from the transcription of new proteins suggesting instead a post-transcriptional nature. Moreover,

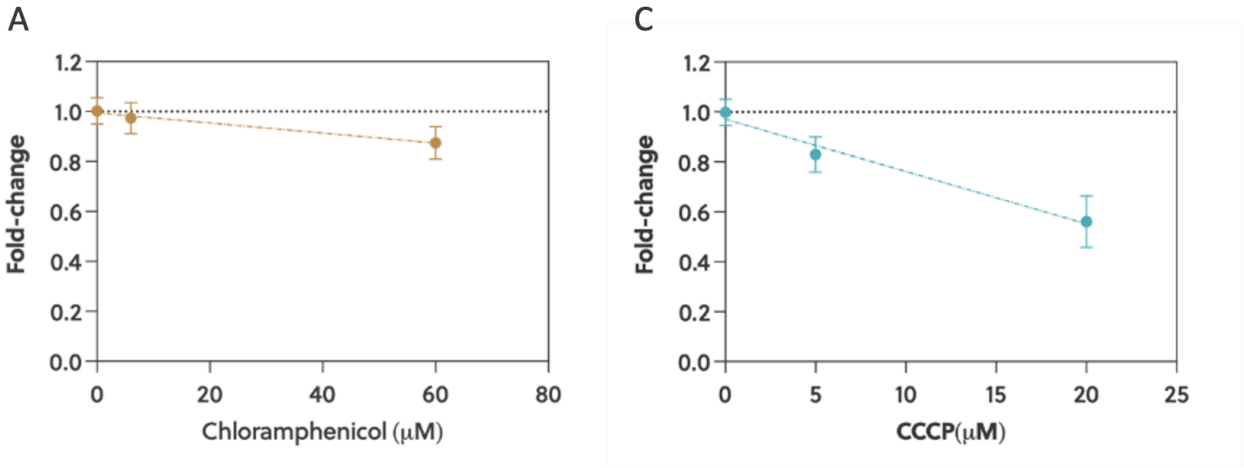

Figure 45: Change in vibrationsl response of antibiotic treated cells stimulated for 2 hours at 50pN and 2kHz. Data represents the fold change in coverage after stimulation of antibiotically treated cells relative to their control. Ribosome targeting antibiotics (A and B) had little effect on cells response that decreased instead by 0.56 when these were depolarised with CCCP (C). Dashed lines are simple linear regressions ($R^2 > 0.91$ for all cases).

when cells were depolarised with CCCP, their response to vibrations decreased. This proved instead that membrane potential is necessary for vibrations to affect cells behaviour during surface colonisation. Such a connection between these two phenomena presents the hypothesis that vibrational stimulation could affect cells polarisation and, through it, their ability to colonise surfaces. I therefore explored this hypothesis by studying the physiological effects that vibro-mechanical stimulation has on cells membrane potential.

4.2 Vibrations hinders cells surface hyperpolarisation

The above results confirmed that cells membrane potential is necessary for vibrations to inhibit surface colonisation as this was reduced when cells were depolarised. These findings started filling the gap between vibrational stimulation and hampered surface colonisation suggesting they could be linked by cells polarisation. Since membrane voltage is not known to directly influence colonisation, this also suggest that some other aspect of cells' physiology should transduce polarisation into colonisation changings.

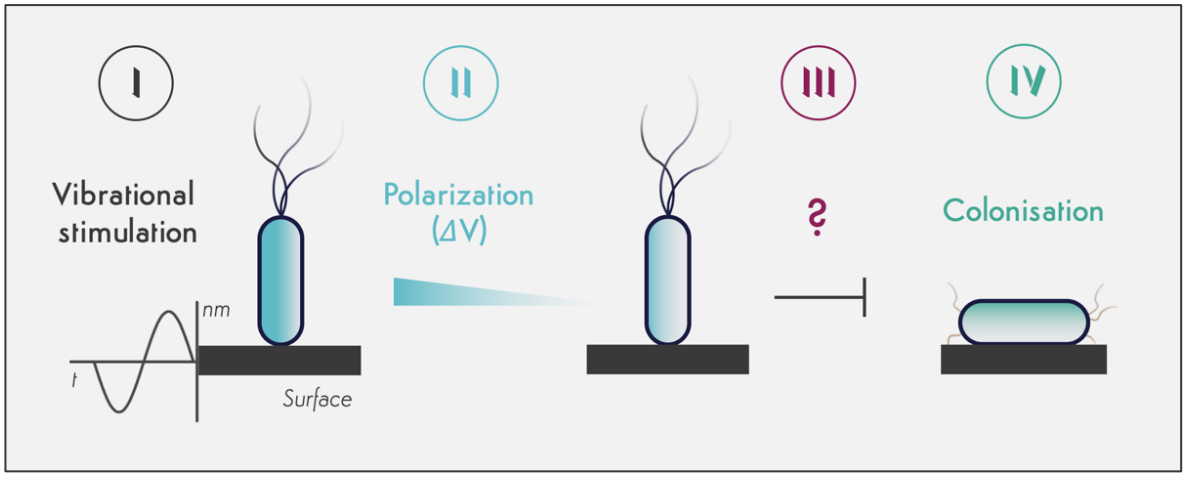

Figure 46: Schematic representation of vibrational effect on cells. Stimultaions of pN intensities and kHz frequencies over 2 hours (I) proved effective in decreasing cells colonisation (IV). The previously uknown connection between the two appears to be dependent on cells physiology and their polarisation (II). To fill the knowledge gap between stimulation and colonisation, I explored how membrane potential change in reponse to vibrational stimulation and how this could influence other aspects of cells physiology which are relevant to surface colonisation (III).

In the following sections I will explore these connections in further detail and I will present the work I did to clarify their influence on surface colonisation. The steps I followed are schematically represented Figure 46. In going from vibrational stimulation to reduced surface colonisation, first I elucidated the effect that vibrations have on cells

membrane potential and second, I determined how its changings would influence other aspects of cells' physiology which are linked to surface colonisation. Central to the above exploration is the concept of membrane potential. This is the first link in transitioning from vibrational stimulation to surface colonisation and it would therefore benefit my argument to briefly discuss why it is important and how it changes upon surface contact.

4-2.1 Membrane potential and its role in cells physiology and surface response

As introduced earlier in the text, cells membrane potential is fundamental for their functioning mostly because of its involvement in energy production and motility. Being living organisms, cells need energy to perform work and stay out of deadly equilibrium with their environment [205]. The most basic energy currency cells use to perform these tasks is adenosine triphosphate or ATP. This is synthesised with apposite watermill-like membrane machinery known as ATPase. As a watermill use water's gravitational gradients to do work, so ATPase uses electro-chemical gradients from H^+ ions to do the same. These are actively pumped out of cells membrane which results in a charge imbalance that generates an electrostatic potential across it. Flowing as water through the wheel of a mill, protons then travel back to the cytosol across the ATPase machinery which transform the potential energy of their gradient into chemical energy of ATP bonds.

Similar to the above process, bacteria transform proton gradients into motion through their flagella. In this case, the energy from such gradients is transformed in kinetic rather than chemical energy [206]. This derives from apposite trans-membrane proteins which rotate in response to the H^+ ions flowing through them. Such motion is then transferred to external whip-like structures, whose rotation propel cells in liquid environments.

Despite arising from the complex interplay of different factors, cells membrane is mostly dictated by the above H^+ gradients [207]. Because of the above role in energy production and motility, membrane potential has been thought to be constant in cells as its changings would hav dare consequences to their fitness. However, abundant evidence has been recently gathered supporting the opposite. Membrane potentials are mostly dynamics, changing over time in response to different stimuli and expanding what cells can do with them [203,208]. Following this experimental evidence, polarisation dynamics are found involved to many physiological processes such as antibiotic resistance [209], inter and intra species signalling [210,211], growth control [212], spore formation [213], surface response and mechanical sensing [80,81]. Particularly relevant to our investigation are these last two points that provide a link between membrane potentials and mechanical stimulation. Specifically, when *E. coli* cells land on a surface, their membrane potential goes through polarisation-depolarisation cycles. This leads to the so-called *electrical spiking* behaviour with longer and more frequent spikes observed when surface attached cells were mechanically stimulated [80,81]. I therefore hypothesised that vibrational stimulation could cause similar changings to cells polarisation when these approach the surface.

Proving the above hypothesis would have strengthened the connection between membrane potential and vibrational stimulation and laid the foundations for a mechanism capable to explain their effect on colonisation. I then set out to test this hypothesis which I did using vibrations to stimulate cells and quantify their effect on polarisation.

Because of bacteria small sizes, once more, the way I wanted to approach this was by using fluorescence microscopy. In fact, different dyes exist that relate fluorescence intensity to polarisation changings. These are known as voltage-dependent dyes as they redistribute across cells membrane following their electric potentials. Following this

approach, before studying such changings in polarisation, few preliminary works needed to be sorted: first, I identify a suitable dye to be used in *E. coli* and second, I optimised its staining under my conditions. Such preliminary exploration preceded by the working mechanism behind such dyes are about to be discussed.

4-2.2 Voltage dependent "Nernstian" dyes

As introduced above, fluorescence microscopy can be employed to follow changings in membrane potential using apposite dyes that relate fluorescence intensity to cells polarisation and for which they are referred to as Nernstian dyes [214]. In fact, unsurprisingly, the way they works is by following the Nernst equation below:

$$\Delta V = -\frac{RT}{F}\ln\left(\frac{[X^{+/-}]_{in}}{[X^{+/-}]_{out}}\right) \quad 8$$

In this one, V represents the voltage (mV), R and F are respectively the ideal gas and Faraday ($\sim$ 8,31 J $\cdot$ K^{-1} $\cdot$ mol^{-1}) constants, T is the temperature (K) and X stand for the intra or extracellular concentration of a give ion (mol/L). This equation describes the equilibrium distribution of permeable ions across a membrane in response to an external electric potential.

As we have seen, in cellular environments, this potential is mostly provided by the proton gradients across the membrane. Cells actively pump H^+ ionss to generate a charge imbalance between the inner and outer side of the membrane. External ions would then experience this potential and adjust their intracellular concentrations accordingly to Equation 8. Because of the negatively charged inner membrane, ions response would differ

according to their charge. Anions would tend to be repelled and accumulate outside the cells while cations will be dragged within, increasing their intracellular concentration. Because of this mechanism, ions gradients would form across cells membrane and their extent directly depends on cells potential ΔV.

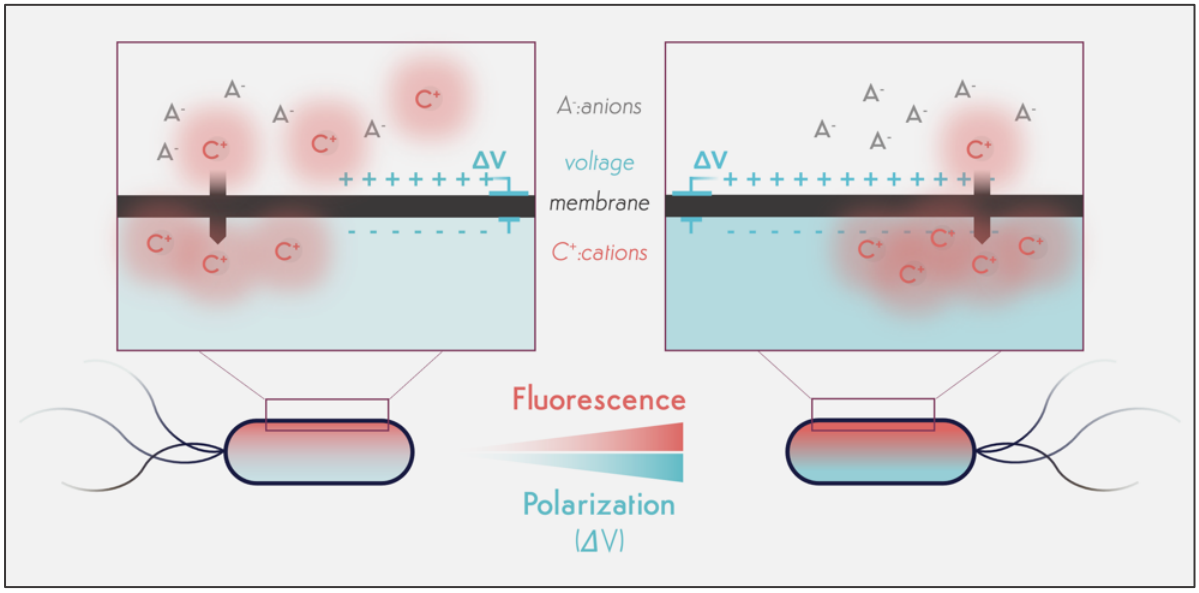

Figure 47: Cationic Nernstian dyes are ionic organic chemicals where either the cations or the anions in the pair can act as fluorophores and that can relate fluorescence changings to membrane potential. Depending on the cationic or anionic nature of the fluorophore, increases in cell polarisation (more negative cytoplasm) will be respectively associate with increase or decrease in their fluorescence. In fact, with cationic dyes, when membrane potential increase and become more negative, more fluorophores are driven within the cells increasing its fluorescence. The reverse scenario is true for anionic dyes.

Nernstian dyes rely on this very phenomenon to connect fluorescence to membrane voltage (Figure 47). In fact, these are organic ions in which either the cations or anions in the pair can be fluorescent. Their ionic and organic nature is what enables them to adjust their intracellular concentration following Nernst equation. Being ionic they can redistribute across cells membrane according to its potential, a process that is eased by

their organic nature and increased permeability.

The ionic component of the dyes will then dictate the kind of fluorescent response following polarisation changings. In the case of cationic dyes, when potential increases so does cells fluorescence as more fluorescent cations are dragged into cells. This state is typical of hyperpolarised cells where membrane potential is increasing. Contrarily, when this is dissipated following cells depolarisation, fluorescence would diminish as less fluorophores are dragged into the cell. With these dyes, depolarised cells display little to no fluorescence, which would sharply increase during polarisation or hyperpolarisation. Where anionic dyes are employed, the above picture is reversed, with fluorescence decreasing with cells hyperpolarization and vice versa for depolarisation. Despite not being able to quantify the actual millivolts variation in membrane potential, the fluorescent measurements of these dyes can nonetheless monitor polarisation changings caused by different treatments.

Moving forward, in the rest of our discussion I will only consider the cationic scenario from above as this is the behaviour followed by my dye of choice: the cationic $DiOC_2(3)$.

4-2.3 $DiOC_2(3)$ and its staining optimisation

3,3'-Diethyloxacarbocyanine iodide, or $DiOC_2(3)$, is a permeable organic dye that is positively charged and follow Nernstian behaviour with added capabilities (Figure 48). Not only it accumulates in cells following their polarisation state, but the colour of its fluorescence is also dependent on their voltage as it changes from green to red. Specifically, in its diluted form, the dye fluorescence is green with emission centre at 510 nm. However, when cells are polarised, it will electromigrates within them increasing its intracellular

concentration and shifting its fluorescence to red (> 600 nm). This process is brought about by the π-stacking of the dyes aromatic rings which aggregate and form clusters whose fluorescence emission is red. The extent of clusters formation and fluorescent shift is proportional to the dye electromigration within the cell following polarisation increases. This cause polarised cells to have variable degrees of red/yellow fluorescence while depolarised one are characterised by green fluorescence only.

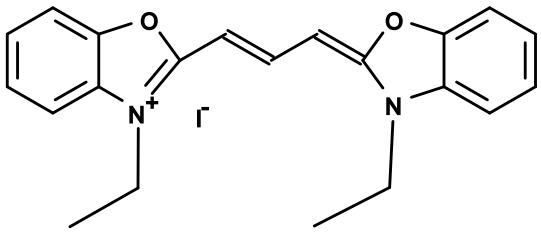

Figure 48: $DiOC_2(3)$ chemical structure. The stacking of the aromatic wings is responsible for the formation of molecular clusters that shift its fluorescence emission from green (510 nm) to red (670 nm).

These chemical properties of $DiOC_2(3)$ make it suitable not only for fluorometric but also ratio-metric determination of membrane voltage. In fact, the fraction of polarised cells can be determined from the ratio of red to green cells in fluorescence images. When such ratio decreases, less cells turn red which indicate a reduction in their polarisation. Because of this flexibility, and its previously attested Nernstian behaviour in *E. coli* [215], I chose to use $DiOC_2(3)$ for monitoring changings in membrane potential caused by vibrational stimulation.

Before proceeding and discuss the relevant experiments, few conditions needed to

be optimised regarding $DiOC_2(3)$ employment such as: strain selection and staining conditions. So far I used SCC1 [187], a mutated strain of *E. coli* MG1655 constitutively expressing Gfp (Materials and Methods). However, its intrinsic green fluorescence would have likely compromised both the fluorometric and ratiometric determination of its polarisation. To circumvent the problem and follow membrane potential responses upon vibrational stimulation, I employed its unmodified parent strain, MG1655.

I then optimised $DiOC_2(3)$ staining conditions. Specifically, I wanted to achieve bright red and green fluorescence emission which would have facilitated both ratiometric and fluorometric measurements. To achieve this, two factors required my attention: dye concentration and membrane permeabilization. As mentioned above, dye diffusion across cells membrane happens with relative ease, however this might not always be the case. In gram-negative species such *E. coli,* their outer membrane impose severe limitations on the diffusion of many chemicals being these antibiotics or fluorescent dyes [216]. To circumvent the issue and permeabilise the membrane during staining, different compounds are used, the most common of which is ethylenediaminetetraacetic acid or EDTA [217,218]. This destabilises cells envelope via the complexification of divalent cations such as Mg^{2+} and Ca^{2+} which decrease the electrostatic repulsions among charged lipids heads forming the membrane.

I therefore used values from the literature to test different dye (30 μM and 150 μM) and EDTA (2 mM and 11 mM) concentrations that would have achieved bright cells fluorescence [215,219]. Figure 49 reports these values along with the experimental procedure I followed to test and optimise $DiOC_2(3)$ fluorescence in MG1655.

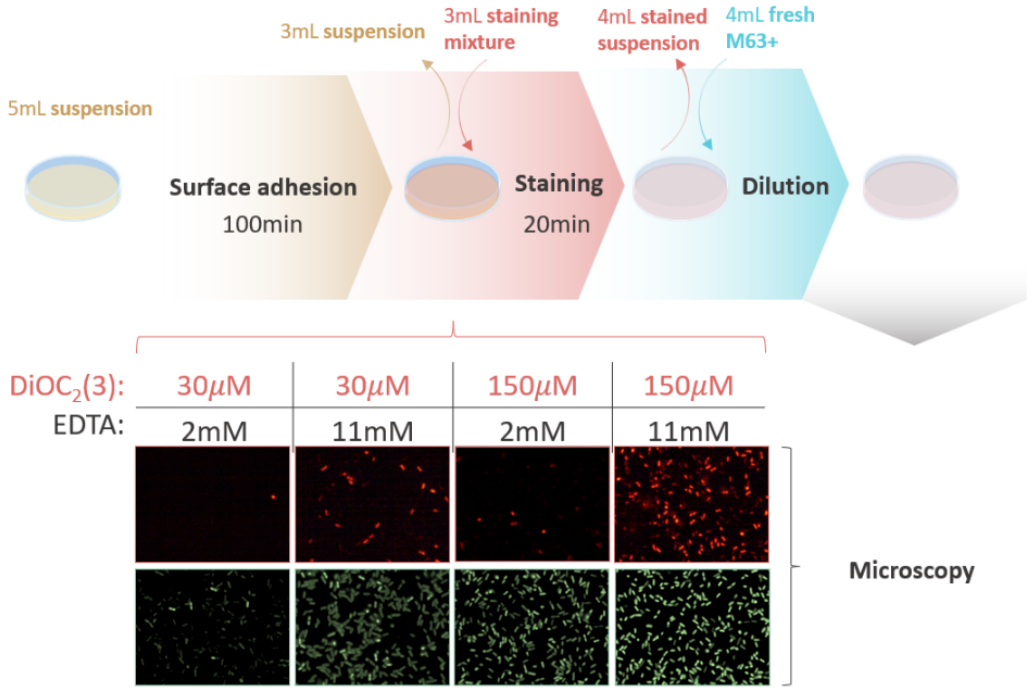

Figure 49: $DiOC_2(3)$ staining optimisation procedure. From left to right, overnight M63+ suspensions of MG1655 are left to attach to polystyrene surfaces for 100 minutes. These are then stained for 20 minutes by replacing 3 mL of suspension with the same volume of a staining mixture in M63+. This contained the required amounts to achieve the above reported combinations of $DiOC_2(3)$ and EDTA. Dyes concentration in samples was diluted 1 in 25 replacing twice 4 mL of stained suspension with fresh M63+. Finally, samples surfaces were imaged using fluorescence microscopy and pictures were gathered as pairs in both the red and green channel.

Briefly, I resuspended overnight M63+ cultures to a 0.05 OD_{600}. Cells were then allowed to attach to the surface for 100 minutes and then stained for 20 minutes using different combinations of $DiOC_2(3)$ and EDTA. This was done by replacing 3 mL of suspension with the same amount of staining mixture in M63+. After staining was completed, samples were diluted 1 in 25 with fresh medium using a serological pipette and finally imaged using fluorescence microscopy to gather between 15 to 20 pictures of the surface for both the red and green channels (Materials and Methods).

Following the inspection of these images, I observed brighter fluorescence when cells were stained with 150 μM $DiOC_2(3)$ and 11 mM EDTA (Figure 49). Consequently, I picked these values to be my reference staining conditions and used them to study cells change in membrane potential upon mechanical stimulation.

4-2.4 Vibrational stimulation hinders cells hyper-polarisation during surface colonisation

Before discussing the effect that vibrational stimulation has on bacteria membrane potential, it could be beneficial to quickly summarise the results that led to this point. First, in the previous chapter, I established a connection between vibrational stimulation and surface colonisation. In fact, stimulating cells with mechanical forces of piconewton magnitudes and kilohertz frequencies, reduced surface coverage and its colonisation. I saw that such an effect was proper to living cells as it was absent or greatly diminished in non-living equivalents such as abiotic beads and dead cells. Therefore, the observed response to stimulation had to be meditated by active interactions between the cells and the surface suggesting its biological nature and the involvement of some cell physiological feature. I then identified one of such features as the bacteria membrane potential. In fact, when this was dissipated with the ionophore antibiotic CCCP, vibrational change in coverage was almost halved suggesting this is necessary for vibrations to influence cells surface behaviour. Finally, I resolved on monitoring polarisation changings upon vibrational stimulation using the voltage dependent dye $DiOC_2(3)$. Of this, I optimised its staining conditions under my experimental needs. Everything is set now to describe the effect of vibrational stimulation on cells membrane potential, presenting both the relevant experiments and their results.

From an experimental perspective, I achieve the above by stimulating cells at a desired frequency and intensity, then I stained them with $DiOC_2(3)$ and use fluorescence microscopy to determine both fluorometric and ratiometric changings in fluorescence that I used to infer cells variable polarisation.

This was achieved by adjusting my procedure, the result of which is depicted in Figure 50. Overnight cultures of MG1655 in M63+ were resuspended in 5 mL of fresh medium at an OD_{600} of 0.05 within small polystyrene petri dishes that were then vibrationally stimulated for 120 minutes at 50 pN and 2 kHz. To prevent any delay between the stop of vibrations and surface imaging, I stained cells during the remaining 20 minutes of their stimulation. Specifically, after 100 minutes, I paused vibrations and stained cells with 150 µM $DiOC_2(3)$ and 11 mM EDTA. I did this by replacing 3 mL of suspension with a staining mixture in M63+ which had the required components to reach the desired working

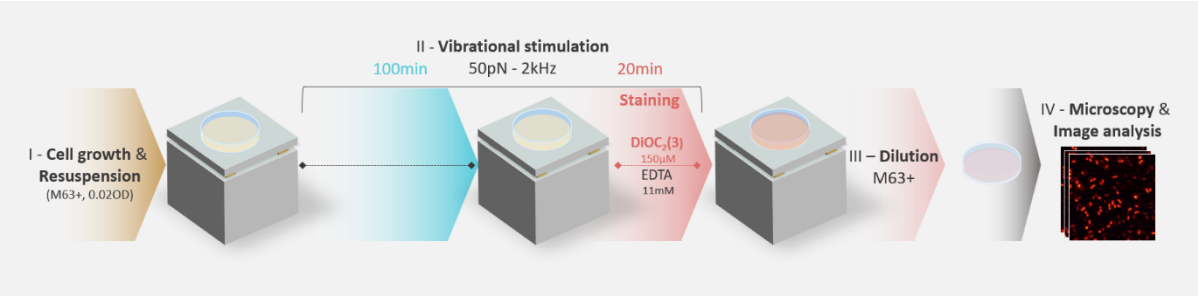

Figure 50: Vibrational procedure used to study the effect of mechanical stimulation on cells membrane potential. I, cells from M63+ overnight cultures are resuspended in 5mL fresh medium within polystyrene sample dishes. II, these are loaded on vibrational device and stimulated at 50pN and 2kHz for 120 minutes. After 100 minutes, samples are stained for the remaining 20 minutes with a mixture of DiOC2(3) and EDTA (150µM and 11mM working concentrations respectively). III, stained suspension is diluted 1 in 25 and IV, fluorescence pictures are recorded.

concentrations in the samples. Vibrations were then resumed for 20 more minutes which

coincided with staining time. Before imaging, to reduce dye background fluorescence, I diluted the samples 1 in 25 by replacing twice 4 mL of stained suspension with fresh M63+. Once diluted, contrary to previous vibrational experiments, I did not wash the samples but immediately imaged them using fluorescence microscopy. The reason behind the absence of a washing step was justified by the desire to quantify changings in cells physiology as a response to vibrations. Specifically, washing would have compromised the results by removing cells from the surface and therefore preventing me from monitoring population wide changings in their polarisation. Finally, from the gathered pictures I quantified variations in fluorescence from which I inferred changings in membrane polarisation.

To do this I relied on two quantification methods: ratio-metric and fluorometric. Turning from green to red in polarised and hyperpolarised cells, $DiOC_2(3)$ can in fact be used to monitor changings in membrane potential by simply comparing the ratio of red to green cells in fluorescence images. Fluorescence intensity was instead derived from the average pixel values of cells in the pictures. Specifically, I limited the analysis to red fluorescence as it is the only one that can vary depending on the degree of cells polarisation. To do this, I first identified cells in red images using segmentation algorithms and second, for each of them, I determined its fluorescence from their average pixel intensity. I then plotted these values as normalised frequencies distributions of the total imaged population and compared these between conditions.

From the above experiments and plots, I observed two interesting phenomena. First, upon vibrational stimulation, the extent of depolarised cells increased from 15% to 24% (Figure 51 B). Second, in both control and vibrated samples, cells polarisation on the surface were bimodally distributed indicating two coexisting sub-populations: one at a

lower peak representing polarised cells and a second one, peaking at 2σ of the former suggesting the presence of hyperpolarised cells (Figure 51 A). Interestingly, these

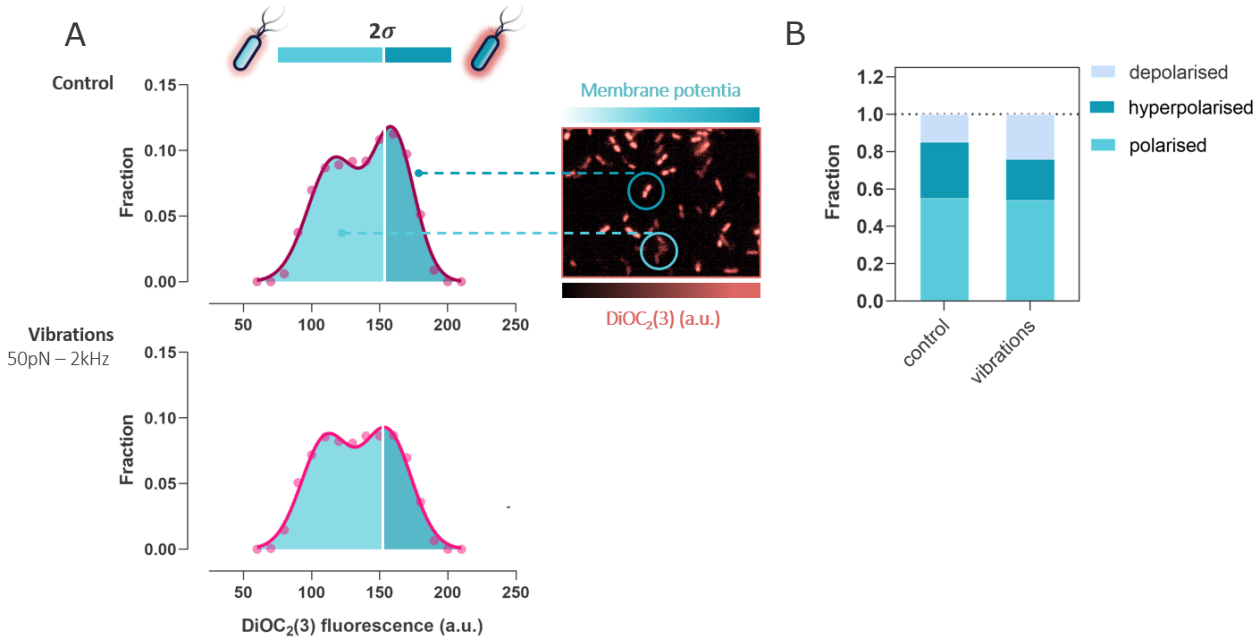

Figure 51: A) Frequencies distributions of $DiOC_2(3)$ red fluorescence in cells with and without vibrational stimulation at 50 pN and 2 kHz. The number or red fluorescence cells was normalised by the total number of cells for both conditions. Imaged populations were bimodally distributed with a first peak at 116 a.u. and a second hyperpolarisation peak centred at 2 SD from the first one (153 a.u.). Solid lines are the gaussian interpolation of the data ($n > 1.6 \times 10^4$ and $R^2 > 0.98$ for both conditions). Shaded areas are the integrals under the interpolating curves. Insert are fluorescent red cells on the surface on control sample. B) Fractions of cells polarisation on gathered mages for both vibrated and control samples derived from the frequency distributions in a and ratio-metric measurements. Values for polarised, hyperpolarised and depolarised cells respectively are 55%, 30% and 15% for control and 54%, 22% and 24% for vibrations.

distributions differed between vibrated samples and controls in the proportion of hyperpolarised but not polarised cells. In fact, integrating the curve below and above 2σ, I observed that vibrations decreased the fraction of hyperpolarised cells from 30% to 22%

while the number of polarised cells remained almost unvaried to about 55% of the imaged population (Figure 5 B). This indicate that vibrations could interfere with cells hyperpolarisation on surface, increasing cells depolarisation by decreasing their hyperpolarisation.

Taken together, the above results proved that during surface colonization cells adjust their membrane potentials which are bimodally distributed indicating the existence of hyperpolarised sub-populations. Moreover, mechanical stimulation in the form of surface vibrations, disrupts this process particularly by limiting cells hyperpolarisation. Interestingly, this changes in membrane voltage also appear to precede and correlate with the reduction in surface coverage, presenting the hypothesis that vibrations could hinder surface colonisation by interfering with these polarisation dynamics.

To test this hypothesis, I artificially disrupted cells membrane voltage and observed how this impacted surface colonisation. I already saw how polarisation can be disrupted by the ionophore antibiotic CCCP, however this severely depolarise cells causing a much more drastic effect than vibrational stimulation. To find a methodology enabling the gentler tuning of cells membrane voltage, I directed my attention to cations and their fluxes across cells' membrane.

4-2.5 Magnesium influxes limit cells polarisation and decrease surface colonisation

One-way cells can regulate their membrane potential is through the efflux of cations. Magnesium effluxes and subsequent hyperpolarisation have been shown to occur when cells are under stress from sub-lethal concentrations of ribosome targeting antibiotics [220,221]. I reasoned that a similar response could be shared by other cellular

stressors such as the membrane strain coming from the surface during its colonisation. Increasing magnesium extracellular concentrations could then inhibit such effluxes and prevent cells from hyperpolarise in response to stress which would provide the mean needed to suppress this process and study its effect on both cell colonisation and response to vibrations.

Consequently, I monitored the effect that increasing extracellular Mg^{2+} content has on cells hyperpolarisation by rising its concentration in the samples by 10-fold (from 1 mM to 10 mM) and quantified its effect on polarisation using fluorescence microscopy.

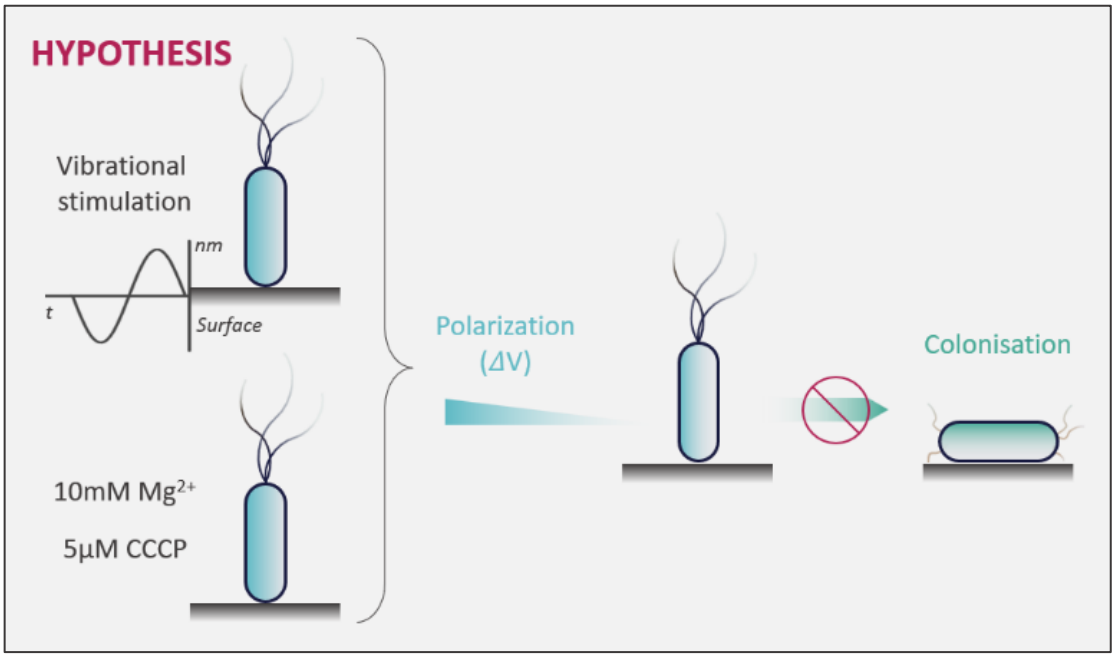

Figure 52: Schematic representation of our experimental hypothesis. Vibrational stimulation leads to cells limited polarisation which is assumed responsible for their reduced surface colonisation. To confirm this hypothesis, I treated cells with known polarisation disruptors (10 mM magnesium and 5 µM CCCP) and observed their effect on surface colonisation.

To do this I used the same procedure as for the above experiments with the added difference that samples magnesium content was enriched and these were not vibrated

(Materials and Methods).

From these experiments, I observed that increased concentrations of extracellular magnesium decreased the fraction of hyperpolarised cells to 7 % while increased that of depolarised to 54 % (Figure 53 B and C). Magnesium fluxes appeared then to influence

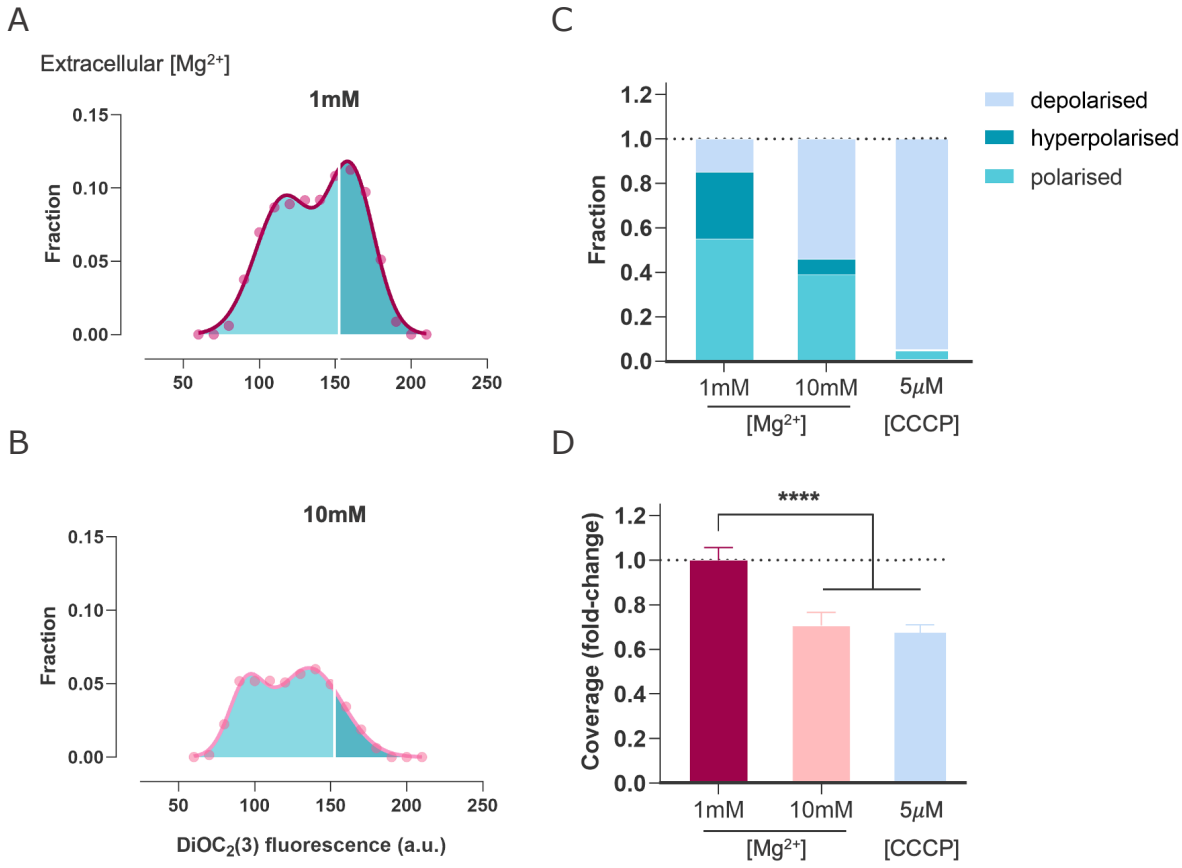

Figure 53: A and B) Frequency distributions of $DiOC_2(3)$ red fluorescence with 1 mM and 10 mM magnesium extracellular concentrations. The number of red fluorescent cells was normalised by the total count from the green channel for both conditions. Solid lines are gaussian interpolations (n = 1.6×10^4 and 4×10^3, R^2 = 0.99 and 0.84 for 1 mM and 10 mM respectively).C) are the fraction of polarised cells in the population for Mg^{2+} and CCCP treated cells. D) Is the change in coverage after 2 hours colonisation for cells treated with 1 mM, 10 mM, 5 µM CCCP. Data are normalised to 1 mM control and represents the mean with SD (n > 118 for all conditions, p.values**** < 0.0001).

cells polarisation dynamics on the surfaces, particularly inhibiting hyperpolarisation without causing population wide depolarisation as from CCCP treatment.

Along with CCCP, I then used increased magnesium contents to disrupt cells surface polarisation and study its effect on colonisation (Figure 52). As such I treated cells with either 10 mM magnesium or 5 μM CCCP, let them to colonise surfaces for 2 hours and compared the resulting coverages to untreated cells. Experimentally, I resuspended cells from M63+ cultures in 5 mL of fresh medium within polystyrene petri dishes (35 mm). I then supplemented the samples with either 10 mM of $MgSO_4$ or 5μM CCCP. Control samples and CCCP treated ones had the normal amount of Mg^{2+} (1 mM). Colonisation was then allowed for 2 hours while samples were incubated in the dark at 30° C. After this they were washed and change in surface coverage relative to the control determined from the analysis of fluorescence pictures (Materials and Methods).

From these experiments I observed that treating cells with either CCCP or 10 mM magnesium decreased surface colonisation by respectively 31% and 34% (Figure 53 D). Interestingly, depolarisation with CCCP was not statistically different to magnesium treatment, suggesting that the reduction in coverage is mostly dependent on the diminished hyperpolarisation rather than population wide depolarisation. To summarise, these findings show that disrupting cell polarisation dynamics on the surface hinders colonisation, supporting the hypothesis that the same mechanism could explain cells' reduced adhesion upon vibrational stimulation.

A sensible explanation of this behaviour involves the uncontrolled opening of mechanosensitive or ions channels as a response to mechanical stimulation. The piconewton forces that this applies on cells envelope could in fact generate enough pressure to open such channels so allowing ionic species to leak the cells thereby altering

their membrane potential on the surface.

Given that the peak-to-peak action of acceleration forces on cells occurs in milliseconds and the typical conductance of *E. coli* ion channels is in picoamperes, the opening of a single channel might leak between 10^3 and 10^4 ions/ms [31,38,207]. Because the most abundant ions have millimolar concentrations in cells, these can lose 0.1 to 1 % of those species every millisecond, generating a significant change in membrane potential.

Aside from expanding the understanding of cells surface polarisation, the above work consolidated the connection between cells polarisation and surface colonisation by establishing membrane potential at the front of the causal chain connecting these two phenomena. However, cells voltage is not known to be directly involved on both cells adhesion and colonisation which ask for some other physiological aspect to complete the connection. On this matter, two closely related features of cells biology came to the rescue: motility and flagella mechanosensing. In fact, they both are linked to membrane potential by the flagella's motor, a protein machinery the functioning of which depends on cells polarisation, and they have also been recently associated with cells ability to attach and colonise surfaces [79,206,222,222-224]. As such, I reasoned that these two physiological aspects of bacteria and their Janus connection to both membrane potential and adhesion, could have provided the missing link between changings in polarisation and colonisation. It is therefore time to discuss how these were both involved and influenced cells response to vibrations.

4.3 Cells motility and its relevance to vibrational response

Bacteria ability to swim is a fundamental aspect of their physiology as this enable them to find nutrients and colonise their environment. However, because of their small sizes, this is very viscous as ordinary water changes when looked up closely at the microscopic scale. There, the same weak bonds between hydrogen atoms among molecules which are responsible for its macroscopic liquid behaviours, are no longer so weak for bacteria the size of few microns. For them, water is a viscous medium which is as hard to pierce through as it would be for human to swim in pitch[205].

Nonetheless bacteria do this and they do it well. In fact, when foraging for food during chemotaxis, they can propel themselves to speeds up to 30 μm/s or, considering an average 2 μm size, 15 body length per second; the equivalent of a human running 110 km/h [31,205]. How they achieve this is through the employment of specific extracellular structures: flagella. These whip-like filaments rotate in a mixed clock and counter-clockwise rotation that make bacteria stop (tumble) and resume swimming based on newly acquired environmental information such as nutrients gradients.

Why flagella are relevant to this discussion is because of the energy source cells use to fuel them: the electrochemical proton gradient that make their membrane potential. In fact, through specific transmembrane proteins known as *mot*A/B, about a 10^5 H^+ ions are used every second to power their rotation which, depending on the viscosity of the surrounding medium, can happen between the hundreds and thousands of times a second [31,198,206], faster than modern jet turbines. As these are powered by electric currents travelling into their circuit, flagella are fuelled instead by ions flowing across their membrane. This

ability of membrane potential to act as a charged capacitor providing the current required for their functioning define a strong connection between cells polarisation and motility enabling changing in the former to influence the latter.

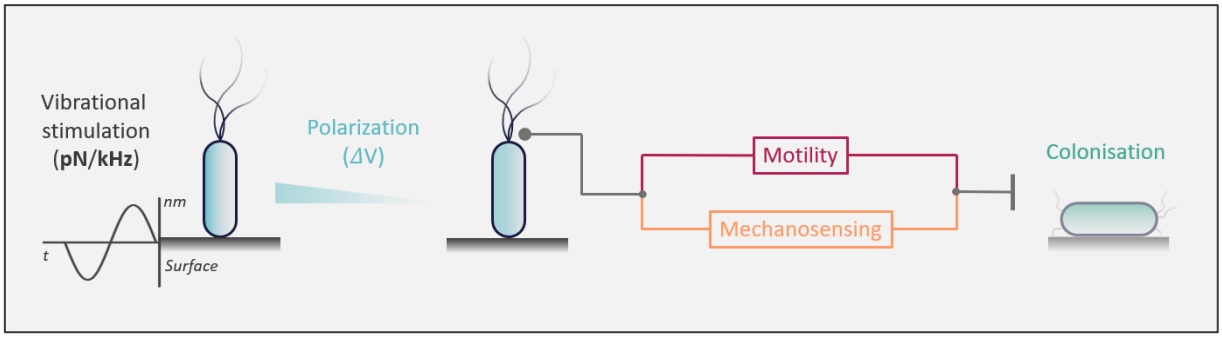

Figure 54: Hypothetical causal chains connecting vibrational stimulation to reduced surfece colonisation. Vibrations hamper cells polarisation on surfaces which can lead to hindered colonisation either via altered flegalla motility or mechanosensing.

But what is even more relevant to our discussion about flagella, is not only their connection to cells polarisation but also to surface colonisation. In fact, flagella are well known to be under-regulated when cells transition from planktonic to sessile behaviour as they found little to niche uses when cells are attached to hard surfaces or bundled into biofilms [225,226]. However, during the early stages of this transition and within few hours of surface exposure, the situation is reversed and flagella are fundamental for their adhesion.

First, they can bias cells swimming toward the surface. The conditioning layer forming on them make so that surfaces carry positive nutrients gradients, activating cells chemotactic machinery which direct them toward the surface. Second, once this is reached, cells further utilised flagella as tools to improve their adhesion and colonisation. The way this happen is via two major mechanisms: flagella mechanosensing and motility driven adhesion [79,224,227,228] (Figure 54). Recent findings support the idea that flagella's motor

could partake in sensing of mechanical stimuli coming from the surface during adhesion via some yet unclear chain of events that would transduce them into cells response. The details are varied and species dependent, but the results is all the same: improved cells adhesion and increased intracellular concentration of second messenger such as cAMP and c-di-GMP [140]. Surface colonisation is also directly dependent on the degree of cells motility. Specifically, cells motion can influence their ability to attach and colonise the surface [143,224]. In fact, when cells approach it, they can decrease their speed to ease their adhesion facilitating the contact with the surface in what results as a motility driven adhesion.

Because of these connection to both surface colonisation and cells polarisation, flagella motility can serve as the missing link in our findings and bridge vibrational stimulation to surface colonisation. In the following of this chapter I will explore how motility is both involved and influenced by vibrational stimulation discussing the experiments I performed to gauge how motility driven adhesion and surface sensing are entailed in cells vibrational response.

4-3.1 Tracking cells motility on polystyrene surfaces

As a first step in connecting changings in membrane potentials to flagella motility, I tested our ability to monitor this process on polystyrene surfaces using fluorescence microscopy. Specifically, by applying tracking algorithms to video records I derived spatio-temporal trajectories that I used to classify surface motion and follow its changings across different experimental conditions.

To test the reliability of my methodology, I recaptured the variable motility between fast and slow growing cells. In fact, a correlation exists between duplication rate and cells'

flagellation as both their assembly and functioning are upregulated in growth promoting environments [229]. Consequently, flagella activity is stronger when cells are fast dividing in rich media during exponential phase at physiological temperature and it decreases when growing rate slowdown at lower temperature, in minimal media or upon entering stationary phase.

The reasons for this behaviour are still debated but an explanation relies on cells energy management during growth. In fact, flagella are very inefficient machines as every rotation contributes only 0.1% of the energy required to propel the cell which make investing resources in their functioning detrimental when nutrients are scarce and metabolic energetic output limited [230]. To achieve different growing rates, I therefore varied the culturing medium, temperature and time. Specifically, fast growth was achieved by culturing cells in rich medium (LB) at higher temperature (37˚C) for shorter times (3 hours) while for slow growth I used minimal media (M63+) at lower temperature (30˚C) overnight (~18 hours).

Complementing this preliminary methodological tests, I also accounted for influences arising from Brownian motion. This random movement is typically encountered in liquids for objects smaller than few microns and it depends on the stochastic anisotropy of their collision with the surrounding water molecules which would set them in motion. To determine the impact of this effect, I studied the displacement of negatively charged abiotic particles 1 μm in diameter. Lacking any form of self-propulsion, their only source of motion would in fact derive from such random influences.

From an experimental perspective, I compared cells and beads surface motility using the following procedure (Figure 55): when cells were employed, their growing conditions differed from fast and slow growers: fast growth was achieved culturing cells

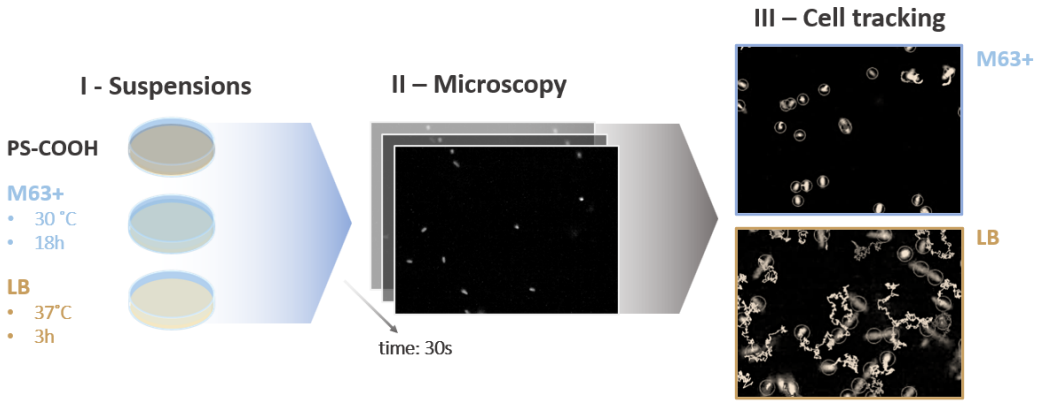

Figure 55: Schematic representation of the procedure used to assess differences in surface motility among abiotic particles and cells under both slow (M63+, 30°C, 18 hours) and fast (LB, 37°C, 3 hours) growing conditions. Both beads and cells were resuspended at 0.1 OD_{600} in 5 mL motility buffer (PBS + 0.2% glucose) within petri dishes (35 mm) (I). For each condition, video records (20 s) were recorded (II), converted into image stacks and object specific trajectories were derived analysing them with track algorithms (III). All experiments were performed as independent triplets recoding 3 to 4 videos in each.

overnight in rich LB medium at 37°C and then re-inoculating them (1 % volume) in fresh medium for further 3 hours growth at 37°C. Slow growth was achieved instead culturing cells in minimal M63+ medium overnight at 30°C. After growth, cells from both conditions were then resuspended within polystyrene petri dishes at a 0.1 OD_{600} in 5 mL of motility buffer (PBS + 0.2 % glucose).

Where beads were used the same suspension as above were prepared by simply diluting the required amount from a stock solution. To facilitate the detection of both cells and beads, I used a green-fluorescent *E. coli* strain (SCC1) and particles (1 µm in diameter, Materials and Methods). Samples were then imaged under the microscope, surface motility recorded as four videos (20 s, 30 fps) and the experiments performed in independent triplets for a total of 9 records per condition. These records were then

analysed using a TrackMate, a tracking algorithm plugin freely available in FIJI [231].

Every video was first converted into image stacks which the program used to derive spatio-temporal tracks of surface moving cells. From these, I then computed the total trajectory length and the farther distance between two points in a track, known as its max displacement. To account for differences in size between tested objects, the above statistics were converted from microns to body-lengths. This conversion was based on the average diameter of the tracked objects which, in the case of beads, was readily available from the manufacturer label. For cells instead, I experimentally determined this value from the analysis of florescence pictures under both rich and minimal growth and rounded their value to one significant digit. The conversion factors were therefore 1 μm for beads, 2 μm ± 0.2 SD for cells grown in M63+ and 3 μm ± 0.5 SD for LB growers. I then used these quantities to classify motion as either stationary, rotating or travelling [232]. *Stationary* were those objects which moved less than half a body length, *rotating* moved between half and one while *travelling* moved more than one body length (Figure 57 A). Finally, I compared these fractions and their underlying populations across experimental conditions.

Following the above experiments, I first observed that all conditions were characterised by some degree of surface motion although its extent greatly varied between them (Figure 56). For example, looking at the frequency distributions of the trajectory lengths, beads travelled the less with an average of approximately 1.5 body lengths. These were followed by slow growing cells in M63+ which travelled an average total distance of 11 body lengths while fast growers in LB displayed a bimodal distribution with two sub-populations moving respectively an average of 7 and 20 body lengths.

I observed a similar trend when looking instead at the populations' distributions of cells and beads max displacement (Figure 56 B). This shared the same averaged and population trends as trajectory length with beads moving the less (0.30 body lengths ± 0.31 95 % C.I.), followed by slow growers in M63+ (0.80 body length ± 0.16 95 % C.I.) and fast-growing cells in LB moving the farthest (1.40 body length ± 0.34 95 % C.I.).

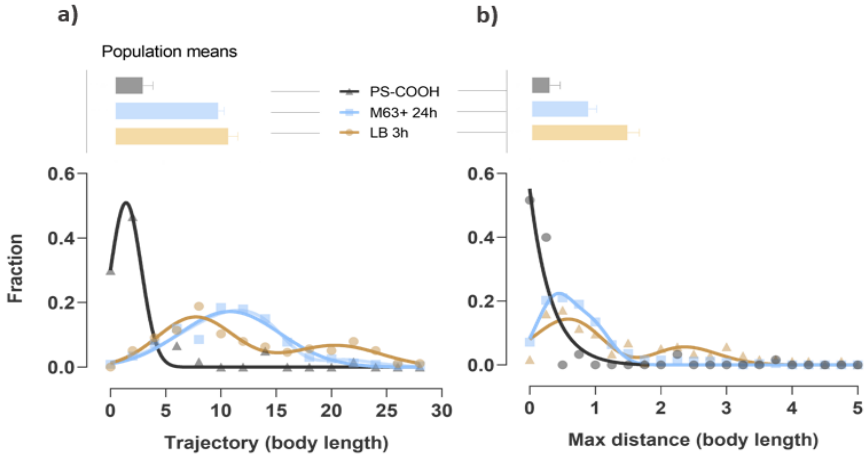

Figure 56: Population averaged and underlying frequency distributions of both the total trajectory length (a) and max displacement (b) for tracked polystyrene carboxy functionalised beads (PS-COOH) and slow and fast-growing cells in either minimal M63+ or rich LB. Bars plots show the mean and 95% confidence intervals of the total tracked objects per conditions (n = 60, 233 and 175 for PS-COOH, M63+ and LB respectively). Solid lines are gaussian interpolations ($R^2 > 0.85$ for all conditions).

Despite travelling trajectories of several body lengths, the above values proved that all objects are relatively confined on their motion. This is particularly true for beads and M63+ cultured cells that, despite an average trajectory length of respectively 2 and 11 body length, did not moved further than a quarter or half a body length indicating a mostly static surface behaviour. This was partially explained when looking at the classification of

beads and cells motion from which a clearer picture appeared (Figure 57 B). In fact, the almost entirety of the imaged beads population (92 %) was stationary on the surface as they moved within a confined radius of less than half a body length.

This picture was reversed for both slow and fast-growing cells where the fraction of static cells respectively decreased to 39 % and 29 %. Interestingly, for cultured cells in M63+, rotation between half and one body length proved to be the most common surface

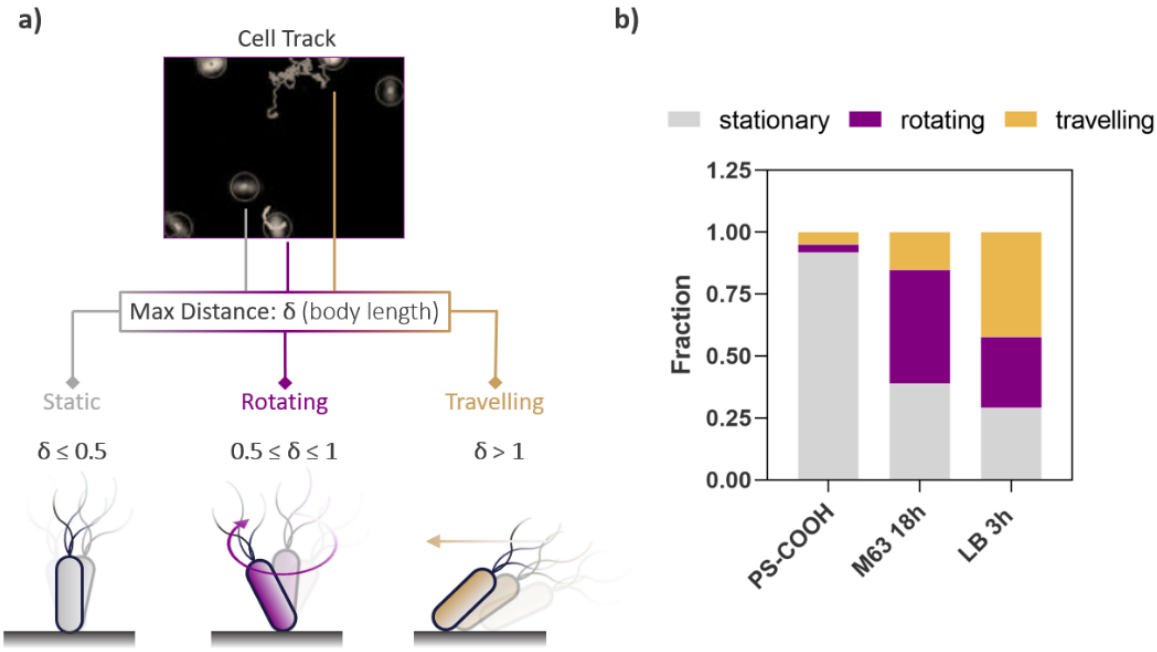

Figure 57: Classification of different motions from analysed trajectories (a). For every tacked object, the max displacement (δ) in their trajectory was computed in body lengths and used to classify their motion according to this value. Fraction of stationary, rotating and travelling objects classified for each condition (total number of tracked objects = 60, 233 and 175 for PS-COOH, M63+ and LB respectively).

behaviour which contributed almost half of the imaged population (46 %). In opposition,

fast growing cells in LB, most of the population (42 %) travelled beyond one body length.

Together, the above results confirmed greater surface motility in fast growing cells and accounted for the limited influences of Brownian motion in our experimental conditions. In fact, cells cultures in rich LB medium showed the highest fraction of travelling population on the surface (42 %) which, in average, moved 1.40 body lengths. Moreover, the almost entirety of polystyrene particles in our record moved less than 0.3 body lengths they were standing stationary on the surface. Brownian motion had therefore negligible influence on the observed cells movement which is to be the results of their genuine self-propulsion. In summary, the above confirmed that my tracking methodology can correctly identify differences in cells motility and can be used to explore how this is influenced by vibrational stimulation.

4-3.2 Vibrational stimulation has limited effect on cells surface motility

In the paragraphs above I saw how membrane potential influence flagella motility by providing the energy required for their rotation. Consequently, when cell polarisation changes in response to mechanical stimulation I would also expect this to indirectly affect cells motility. Given its strong connection to surface colonisation, proving such influence could explain the reduced coverage observed on vibrated samples.

To tackle this experimentally, I used my vibrational procedure to stimulate cells at 30 pN, 2 kHz for 2 hours (Figure 58, Materials and Methods). After stimulation, samples were not washed for the same reason discussed when determining changings in their polarisation. In fact, washing would have removed cells with altered motility and reduced adhesion capabilities. Samples were instead diluted by replacing 4 mL of cells suspension

with motility buffer (PBS + 0.2 % glucose) and subsequently imaged using fluorescence microscopy to record three 20 seconds videos of surface moving cells. This was repeated for three independent experiments and, as described in the preceding section, from the analysis of the resulting video records I derived cells trajectories that I used to classify cells surface motion.

From these experiments I observed little variation in the fraction of moving cells between vibrated samples and controls (Figure 59 A). In fact, the population distribution of cells max displacement was mirrored in both conditions where most of the imaged cells for were standing stationary on the surface as only 15 % and 11 % were either rotating or travelling (Figure 59 B). Responsible for this change was the population of travelling cells that almost quadrupled in vibrated samples increasing from 0.6 % to 2 %. This small increase also led to a significant difference in cells average max displacement that increased from 0.43 to 0.54 µm (Figure 59 C).

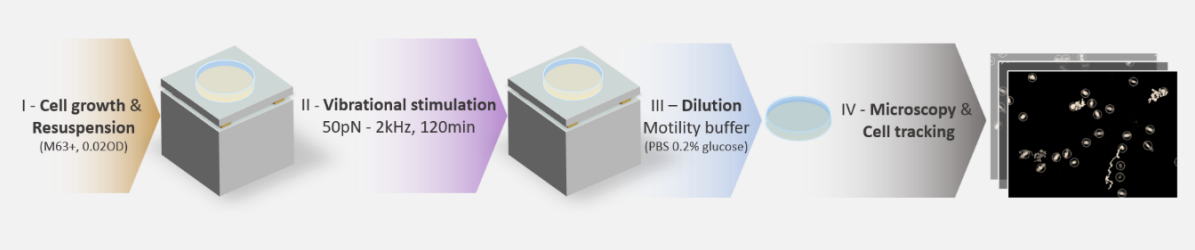

Figure 58: Experimental procedure used to determine the effect of vibrational stimulation on surface motility. Cells from overnight cultures in M63+ were resuspended in 5 mL fresh medium at 0.02 OD_{600} within petri dishes (35 mm) (I) and then vibrated for 2 hours at 30 pN and 2 kHz (II). Samples were diluted by replacing 4 mL of suspension with motility buffer (PBS + 0.2% glucose) (III) and three to four videos of surface moving cells recorded using fluorescence microscopy (IV). Three independent experiments were then performed for both samples and non-vibrated controls.

Vibrational stimulation appears then to cause a limited but nonetheless statistically significant increase in cells surface motility. However, these results should be handled with care before inferring any meaningful effect to surface colonisation. In fact, these might be more informative of the accuracy of the analytical method rather than providing any biological insight. Despite the higher proportion of motile cells on vibrated samples, the effect is small as it increases the number of motile cells and their max displacement by

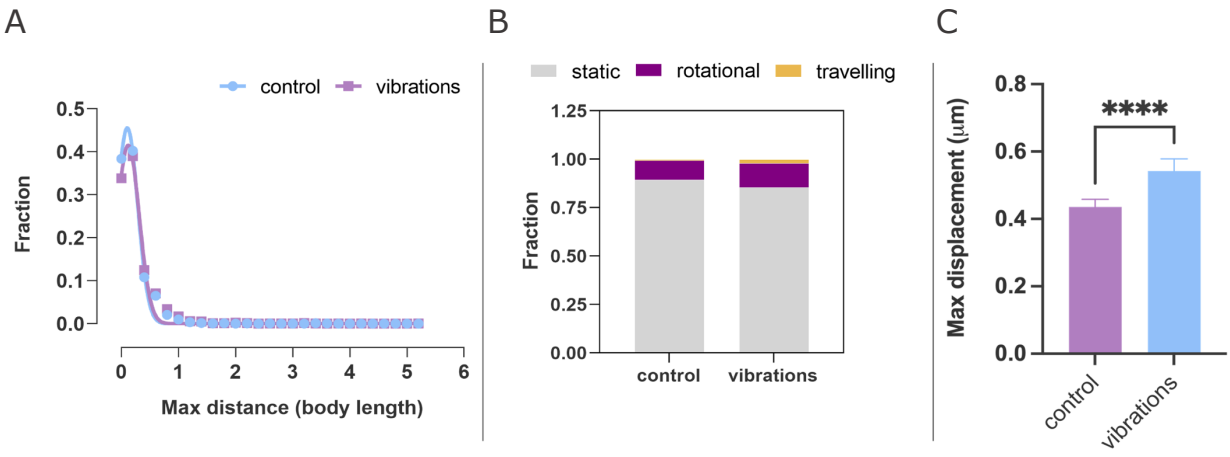

Figure 59: A) Frequency distributions of cells max displacement for both vibrated samples and controls. B) Classification of cells motion from the distributions in a. C) Average max displacement of control and vibrated populations. Data represents the mean with 95% C.I. (n > 1600 for both conditions, solid lines in a are gaussian interpolations, R^2 > 0.98 for both).

only 4 % and ~100 nm respectively. Because of this, it is unlikely that such difference in motility would be responsible for the 1/3 reduction in surface coverage caused by vibrational stimulation. Explaining this behaviour are two non-mutually exclusive reasons: first, from these data I do not have any information about the rate at which the above fractions of stationary, rotating and travelling cells evolved with time. In fact, when these results are compared to those from the preceding session, I saw that motility greatly

decreased during 2 hours of surface colonisation. Specifically, form cells culture overnight in minimal medium, this diminished from 65 % to only 15 % (Figure 57 B and Figure 59 B). This increase of static cells could in fact be happening differently between vibrated samples and controls. Under this light, vibrations could be altering not the final proportion of motile cells but how quickly these transition from motile to static. Second, statistical biases due to the small number motile cells, could have led to either statistically significant or non-significant results depending on the handling of a limited number or outliers.

In conclusion, while the above results proved that vibrations can affect cells motility, it is unlikely that this is responsible for the concomitant change in coverage caused by vibrations. For this reason, I excluded changings in motility as part of the causal chain connecting hampered polarisation to hindered colonisation.

4.4 Flagella's motors are necessary for vibrations to alter cells surface behaviour

In the introduction to this section I mentioned how flagella could act as a Janus connector in the causal chain between reduced cells polarisation and surface colonisation and how this can be brought about by a single feature: their motors. In fact, two of it composing proteins, *motA/B,* fulfil this role by both using cells polarisation to power flagella rotation and by affecting cells adhesion through motility and mechanotransduction [206,223]. In the preceding section we saw how motility varied little upon mechanical stimulation, suggesting that this is less likely to explain the resulting change in surface colonisation. Purpose of this section wouldbe to assess flagella's second

way to influence this process: surface sensing (Figure 60).

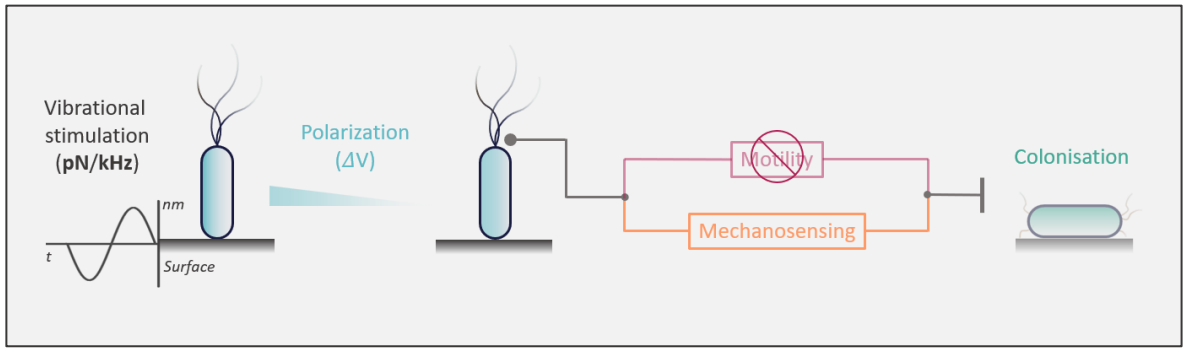

Figure 60: Schematic representation of the connection between cells polarisation and surface colonisation. Upon mechanical stimulation the former is decreased with potential consequences for both cells motility and flagella mechanosensing. Having excluded motility as a mediator between polarisation and colonisation I are now about to explore how this role could be fulfilled by flagella mechanosensing instead.

How bacteria use their flagella to sense and response to surfaces is still lively debated within the scientific community, but many accounts exist of their involvement in the process. To connect to what I discussed in the introduction of this text, this comes in the form of both mechanosensing and mechanotransduction. The former has been reported to occur in *E. coli* as it adjust flagella rotation based on external load [60]. In fact, when bacteria engage a more viscous environment or approach a surface, flagella's rotation slow down under increasing torque. As a response, more motor units co-operatively assemble to power rotation and restore swimming speed. This mechanosensitive correction of flagella rotation based on mechanical load is among the best understood and stronger evidences of this process happening in bacteria.

Following these direct observations are then a broader number of mechanotransduction pathways that have also be suggested in the past years and which

connect flagella surface induced behaviours. Despite many of these accounts lack a complete mechanistic connection between flagella and surface colonisation, their associations have been widely reported to occur in many different species. All these share the same theme of observing impaired surface colonisation and decreased c-di-GMP spikes when flagella, particularly their motors, are removed from the cells. Recent and clear examples of these have been observed in both *C. crescentus* and *P. aeruginosa* [74,79,228,233]. Within the former, removing flagella's motors decrease colonisation by limiting the on-time secretion of their holdfast, a surface adhesin that ease cells adhesion. In *P. aeruginosa* reduced pili activity was observed when surface engaging cells were deprived of flagella's motors [74]. Despite its differences in kind among species, these observations are unified by the common effect that bacterial flagella's motors (BMF) appear to have on cells upon surface landing: increased c-di-GMP signalling. As this is usually found in much higher concentration within sessile cells, its concentration spikes in response to surface contact and their reduction following BMFs removal had provided strong evidence of their involvement in surface sensing and sessile transition.

Because of the above evidence of BFM influence on surface colonisation, I tested how this process could play a role in explaining cells altered colonisation upon vibrational stimulation. Rather than assessing one of the specific pathways linking the two, I looked instead at their relation of necessity. Specifically, as I have done many times in our work, I did this by removing BFMs and observed how this affected cells response to vibrations. Once more, if this was suppressed by the mutation then BFM would have been a necessary mean through which mechanical stimulation could affect cells surface behaviour.

Therefore, to achieve the above I mutated my fluorescent MG1655 strain and removed the genes responsible for the assembly of flagella's motors: *motAB*. This was done as a cooperative effort with Alex Osgerby, another PhD. candidate in the lab that has been responsible for the design and execution of the required mutagenic steps. Briefly, these made use of Gene-doctoring to knock out the target genes [234] while all the plasmids needed by the method were prepared through Gibson-assembly (Materials and Methods). The resulting mutants were then used to assess BFM influence on cells vibrational response which I did this by comparing their vibrational change in surface coverage to that of the mother strain.

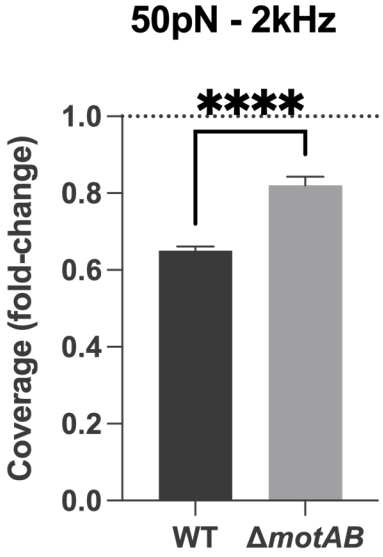

Figure 61: Fold change in surface coverage following 2 hours stimulation at 50 pN and 2 kHz of both WT (MG1655) and Δ*motAB* mutants lacking BFMs. Data are the mean and SD of the fold-change in coverage between vibrated samples and control for each condition. (n = 121 and 77 for WT and Δ*motAB* respectively. p.value **** < 0.0001).

Flagella play an important role in surface adhesion primarily because they help cells swimming to the surface. As a result, mutants that lack flagella are likely to display lower surface adhesion. To prevent this from biassing experimental results, I compared the change in surface coverage of non-vibrated to vibrated mutants. As a result, the intrinsically lower adhesion caused by the mutation would equally affect both control and vibrated samples, allowing any difference to be solely attributed to the lack of flagellar motors.

Experimentally I then achieve this by resuspending overnight M63+ cultures of the above mutants in 5 mL of fresh medium within small petri dishes. Surface adhesion was then allowed for 2 hours by incubating the samples in the dark at 30˚C while these were stimulated at 50 pN and 2 kHz. I then washed them and collected 30 to 40 pictures from the surface using fluorescence microscopy. All images gathered from three independent replicas were then grouped together and used to determined change in surface coverage between vibrated samples and controls for both the WT and mutants (Materials and Methods).

From these experiments I observed that removing BFM halved vibrational effect as this changed from a 35 % to a 18 % reduction in surface coverage (Figure 61). This shows BFMs are necessary for vibrations to alter cells colonisation, suggesting that they are part of the causal chain connecting vibrational stimulation to hampered adhesion.

However, similarly to what I observed with dead cells, removing flagella did not entirely suppressed cells response to stimulation. While this behaviour requires further investigation, I envisage two possible explanations of it. First, disruption to cells' specific interactions with the surface could still affect mutants adhesion on vibrated samples. From the dead cells results I discussed above, this process appears in fact to be one way in which vibrations affect surface adhesion. Because the mutation preserves cells' envelope, vibrational stimulation could still act on the same set of specific interactions and affect mutants' adhesion. Consequently, while removing flagella would sap the active component of cells response, vibrational disruption to cells' specific interactions can explain mutants residual decrease in coverage.

As a second explanation, flagella are not the only mechanical transducer through which mechanical stimulation could influence cells surface behaviour. Removing flagella

would therefore reduce vibrations effect on cells without entirely suppressing it.

What these other elements of signal integration could be is hard to tell at this stage, but the mechanical nature of the vibrational stimulation suggests the involvement of mechanosensitive channels. Further experimental work is needed to elucidate complementary signalling pathways to flagellar dependent one.

4.5 Conclusion

The last finding from the above section begs one question regarding which mechanism would weave together my observations? I would like to put forward one such mechanism that by integrating cells surface response and my findings could explain how vibrations affect colonisation (Figure 62).

When *E. coli* cells approach a surface the increased torque on flagella reduces their rotation which also decreases the number of H^+ ions consumed to fuel this process. Consequently, as more of them accumulate on cells membrane, its potential rises inducing cells hyperpolarisation [235]. I observed this happening as surface colonising cells had bimodally distributed membrane polarisations which suggest different extents of torque induced hyperpolarisation. As less H^+ ions flow across the membrane, this process is also associated to cells cytoplasm alkalinisation which rise its pH. Recent findings support this observation showing that alkaline spikes occur in *E. coli* during surface colonisation [82].

The polarisation dynamics I monitored appear then as a voltaic representation of these subjacent alkaline spikes. Such cytoplasm alkalinisation had finally been proved to promote surface adhesion and sessile transition by rising c-di-GMP intracellular concentrations [82]. Within this framework, I propose that vibrations influence cell adhesion

by limiting flagellar torque-induced hyperpolarisation thereby reducing c-di-GMP signalling and so impeding both cell sessile transition and surface adhesion.

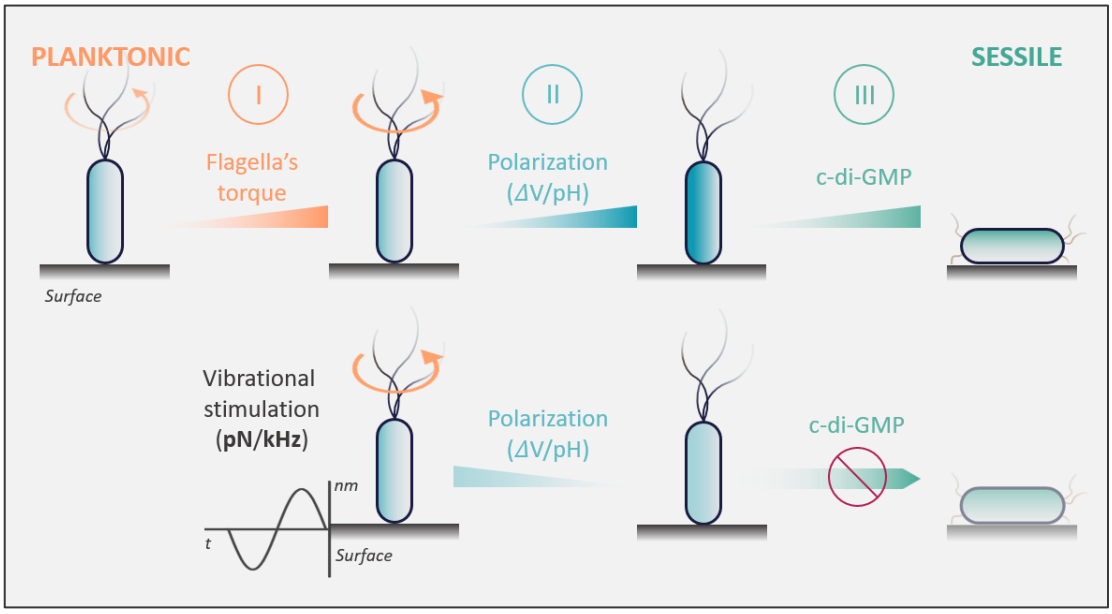

Figure 62: Schematic representation of cells tickling through which vibro-mechanical stimulation can influence surface colonisation and planktonic to sessile transition. Upon approaching a surface, cells experience increased flagella torque which slow their rotation (I). As less protons are consumed to power their functioning, cells cytoplasm become more negative causing both cells to hyperpolarise and their pH to increase (II). This ultimately stimulate diguanylate cyclase activity rising intracellular c-di-GMP concentrations favouring both cells sessile transition and surface colonisation. Vibrations interfere with the above process hindering cells hyperpolarisation in response to increasing flagella's torque. As such, cytoplasm alkalinisation is reduced, limiting c-di-GMP intracellular concentration and with it both cells sessile transition and surface colonisation.

While this hypothesis merges my results with recent developments on *E. coli* surface response, further work is needed to consolidate the above model.

First, the connection between changings in membrane potential and c-di-GMP

synthesis, while sensible, demands further experimental evidence. Successfully capturing reduced intracellular expression of c-di-GMP on vibrated samples would provide such much-needed proofs.

Second, how do vibrational cues dissipate cells' membrane potential? In this sense, I envision two scenarios centred on vibrationally induced ion fluxes and reduced flagellar torque generation. In the first hypothesis, mechanical forces acting on cells' membrane could cause mechanosensitive or ion channels to open, allowing cation fluxes to counter flagellar induced hyperpolarisation. As previously stated, flagella rotating speed reduces near the surface, consuming fewer protons that then accumulate outside cells' inner membrane. The ensuing hyperpolarisation could be countered by offsetting protons electrochemical gradient via the transmembrane migration of positively and negatively charged species. The most abundant of these such as Na^+, K^+, Mg^{2+}, Cl^- and glutamate could move according to their own electrochemical gradients through mechanosensitive or ion channels, the opening of which can be triggered by the piconewton forces or pascal pressures exerted on cells' membrane.

Alternatively, mechanical stimulation can hinder surface hyperpolarisation by affecting the very same torque increase experienced near surfaces by flagella. Stimulating forces acting on their filaments or membrane embedded motors could then reduce the torque generated on surface contact, thereby decreasing the strengthening of protons electrochemical gradients and resulting membrane hyperpolarisation. The above mechanism are not mutually exclusive and they can jointly explain how mechanical stimulation limit cells hyperpolarisation during surface adhesion.

Finally, if ions fluxes are to occur during cells' mechanical stimulation, it would be interesting to understand their nature and specificity. Are cations or anions fluxes

involved? Would there be any specific sensitivity to monovalent (Na^+ and K^+) or divalent (Ca^{2+} and Mg^{2+}) cation fluxes?

In summary, bacteria stimulation with piconewton intensity inhibits surface colonisation by hindering membrane hyperpolarisation. Such tickling sensation, while fitting nicely into the establishing frame of *E. coli* surface sensing, deepens our understanding of this phenomenon and set cells' mechanobiology as a new way to control it.

5. CONCLUSION & PERSPECTIVE

With the above it ends not only this chapter but also my experimental effort and journey, which started with both a narrow and broad question. On the narrow side I wondered *if mechanical stimulation could influence bacteria surface colonisation,* while on the broad side the scope of my work was oriented toward understanding *if bacteria mechanobiology is a viable path to control their behaviour*. Looking back to the preceding chapters the answer to both the above is *yes*.

Starting with my narrower investigation, this was firmly proved by observing that nanometric vibrations with piconewton intensities decrease cells' ability to colonise surfaces. This effect appears to be mostly dependent on stimulating frequency rather than intensity, as lower frequencies of 0.5 and 1 kHz diminished cells response compared to 2 kHz where all tested intensities equally reduced surface colonisation. Aside from purely engineering parameters such as frequency and magnitude, the observed effect is also strongly dependent on surface sedimentation. Specifically, the resulting clusters and sediments can damp vibrational transmission, reducing their influence on cells behaviour. Accounting for this effect and stimulating cells under limited sedimentation, vibrations can reduce surface colonisation by up to 36 %.

While these results proved the clear influence that mechanical stimulation has on cells surface behaviour, stimulation is the core feature that supports my claim. In fact, different mechanical forces can be applied to cells but this does not automatically qualify them as effective stimulants. To act as such, forces need to play around cells physiology, more specifically they need to influence their sensing pathways. Not only I reasoned about

what the right scales for bacteria mechanical stimuli could be, but different evidence in my work supports that I successfully identified them. First, I excluded cells damage as an explanation to my findings since this was negligible following mechanical stimulation. Second, non-living equivalents such as abiotic beads and dead cells both failed in responding to stimulation, suggesting that the effect is not based on a passive physical ground, but it requires instead an active physiological component. Rather than disrupting physical interactions between cells and surfaces, vibrational stimulation alters their behaviour by acting as a genuine stimulant.

From this the question then centred around the effect of this stimulation, which part of cells physiology it touched and most importantly, how was this influenced? On this regard I first noticed that vibrational effect on cells was independent from protein synthesis as when this was suppressed their response didn't change, suggesting that it has a posttranscriptional nature. In fact, cells' response was induced by their altered polarisation dynamics. Specifically, vibrations appear to hinder surface colonisation by limiting cells' ability to hyperpolarise.

Flagella mechanosensitivity and transduction rather than motility provides the link between altered polarisation and surface behaviour. In fact, as I found comparable cells motilities between vibrated samples and controls, the lack of bacteria flagella's motors completely suppressed their response to vibrations.

The success of my narrow task in establishing the influence that vibrational stimulation has on surface colonisation can be ultimately formalised into a mechanistic pathway. For this one, mechanical stimulation acts similarly to a tickling sensation that prevents flagella's dependent hyperpolarisation, ultimately hampering sessile transition and surface colonisation. Such simple and previously unreported phenomenon in

bacteria, other than being an interesting observation by itself, can serve the scientific endeavour in few ways.

On one side it provides a sensible strategy to deal with bacterial biofilms by either influencing their formation or controlling their development. Mechanical stimulation and its inhibitory effect on sessile transition can delay or outright prevent biofilm growth. This can be achieved either employing vibrations by themselves or as a complement to existing strategies. Moreover, given the strong influence that mechanical clues have on biofilm development, mechanical vibrations can affect this process by applying cues of both controlled intensity and frequency. On the other side, the above mechanism and observations can benefit current mechanosensing and mechanobiological efforts by confirming several experimental observations and bringing them together into a unified picture.

This new knowledge supports and expands our understanding of the role of surface displacement in biofilm formation. Vibrations with static surface wave patterns are used in kinetic techniques to contain biofilm development. These have demonstrated that biofilms form selectively at points of zero surface displacement (vibrational nodes) but not at maximum displacement (antinodes) [183,184]. While this is commonly explained by the insurgence of hydrodynamic fluxes and cells' transport to the surface, the same locations might subject cells to respectively minimal and maximal acceleration forces. As a result, mechanical stimulation, by reducing cells' surface adhesion, can contribute to explain the suppression of biofilm formation at wave antinodes. Also, in those instances where homogeneous surface vibrations have also been used [180,181], I believe that mechanical forces acting on surface vibrated cells explains the reduced biofilm development by hindered surface adhesion and sessile transition.

Mindful of such tickling sensitivity, biofilms control strategies can be enhanced by shifting our attention from the surface to the cell. On this sense, I can foresee the merging of surface physico-chemical modification to cells mechanical stimulation, leading to rounder strategies capable to exploit both surface properties and cells sensing. Seeing the low cost and ample flexibility of vibrational approaches, such a future is at close experimental reach. Finally, while I focussed on surface adhesion, it is intriguing to think that mechanical stimuli could also control other force dependent behaviours such as virulence. Upon surface contact, several mechanotransductive pathways supersede its activation in both *P. aeruginosa* and pathogenic *E. coli* [53,72,75] which make it a prime target to exogenous mechano-control.

Coming now to the broader perspective of my work, I intended this to act as a proof of concept by showing that our ability to control cells behaviour can be extended from chemical and optical to also mechanical cues. As this has already successfully be done within eukaryotes, my results are the first supporting evidence that this can also be possible with bacteria. Moreover, my findings are reassuring in nowadays abilities to overcome technical limitation that prevented bacteria mechanobiology from being exploited in the past. Specifically, as bacteria can be up to 40 times smaller than eukaryotes, it had been difficult to apply and monitor the effect that mechanical cues have on them. However, I believe that today advances in cells imaging and mechanical engineering make the above possible allowing bacteria mechanobiology to join chemical, optical and electrical toolkit available for scientists to influence cells behaviour.

Moving in this direction and capitalising on cells mechanical response could open entirely new ways to control them. Taking inspiration from my own work, mechanically induced changings in cells polarisation can be used to specifically activate transformed

genetic elements. This mechanically induced genetic transcription (or *mechano-genetics*) could innovate fields such as synthetic biology and bioengineering. In fact, this would give experimenters a new tool to activate genetic circuitry on a completely different physical channels with potentially no interference with existing chemical and optical cues.

I hope that this work could be beneficial in expanding the current understanding of bacteria surface colonisation, highlighting how this can be influenced using mechanical stimulation and underlying the importance that cells polarisation has on this process. On a wider scale, I also hope that my findings could vouch for the possibilities that awaits when cells mechanobiology is exploited to control their behaviour. The field is young, fast expanding and fertile to interdisciplinary approaches serving a prime opportunity to harness and learn from tickling bacteria.

6. Materials and Methods

1. PDMS synthesis:

This was performed by Dr. Nasim Mahmoodi using Slygard 184 elastomer kit in a 10:1 base to crosslinker ratio following manufacturer instructions. Briefly, the two components (vinyl-terminated base and curing agent) are mixed at the desired ratio. To remove any air bubbles formed while mixing, mixtures were degassed through 5 pumping cycles in a low vacuum chamber. These were then moulded onto foil wrapped silicon wafers at a volume allowing the obtention of 2 mm thick uniform films which were then cured for 45 minutes on a hotplate at 100˚C. The resulting PDMS films were finally post-cured in a conventional oven at 165˚C over a period of 48 hours.

2. Surface samples preparation:

Samples were assembled from 35 x 10 mm triple vented polystyrene sterile dishes (Sarstedt) to which 34 x 1 mm polished iron disks were fixed at their outer bottom surface using epoxy-glue (Loctite). In the case of polystyrene, surfaces were readily available by the dishes inner bottom surface themselves while for PDMS, sample dishes were plasma treated (2 minutes, air plasma) and submerged for 20 minutes with 3 mL of a 5% (weight/volume) APTES solution in water ((3-Aminopropyl)triethoxysilane, Sigma-Aldrich). 6 x 6 x 2 mm (L x W x H) PDMS patches were then plasma treated (1 min, air plasma) and bonded to the polystyrene dishes bottom. After binding, samples were rinsed with 20 mL of distilled water and blown dry with argon gas. Surface samples were finally sterilised for 20 minutes using short UV radiation (280 nm) before been sealed with parafilm and let to recover surface hydrophobicity over a minimum period of 24 hours.

3. Media preparations:

LB broth (Sigma-Aldrich) was prepared in deionised water, autoclave before employment and stored at room temperature for up to two months. M63+, a minimal and low osmolarity medium, was prepared as a variation of standard M63. This is using succinate as extra carbon source and has reduced glucose content (0.2%, weight/volume). 5X stocks were prepared with the following additions: $(NH_4)_2SO_4$ (15mM, Sigma-Aldrich), KH_2PO_4 (100mM, Sigma-Aldrich), sodium succinate (17mM, ThermoFisher) and $FeSO_4$ (1.8µM, Sigma-Aldrich). The mixture was then neutralised to pH 7 with KOH 5M (Sigma-Aldrich). Before employment, the medium was diluted to 1X in deionised water and supplemented with $MgSO_4$ (1mM, ThermoFisher) and D-glucose (10mM, 0.2%, ThermoFisher). Stock solutions were stored at -4˚C for a maximum of six months before employment.

4. Bacterial strains and growing conditions:

I employed the following *E.coli* K-12 sub-strains throughout our experiments: SCC1, MG1655

and PHL644. SCC1, is a MG1655 mutant constitutively expressing Gfpmut3* while PHL644 is an MC4100 strain carrying a mutation at the *ompR* operon causing curli overexpression [236]. For each strain a single colony from an LB agar plate was collected with a sterile inoculation loop, inoculated within a 120 mL flask containing 10 mL of M63+ minimal medium and incubated overnight (16 - 20 hours) at 30 ℃ and 150 rpm. LB growth was achieved instead by inoculating 5 mL of medium with a single colony within 25 mL culturing tubes. Cultures were then incubated at 37˚C overnight. LB agar plates with colonies were stored at -4 ℃ and employed when less than a week old. All strains came from separate 50% glycerol stocks stored at -80 ℃ and refreshed monthly.

5. Curli expression monitored though flowcytometry:

Curli expression was monitored overtime using E.coli MC4100 harbouring pJTL-TET plasmids causing fused CsgA-Gfp expression. Cultures were setup in 200 mL M63+ at 30˚C, aliquots were taken every hour and passed on the flow-cytometer (BD Accurri C6 Plus) to monitor variation in cells fluorescence.

6. Bacteria colonisation of polystyrene samples:

Overnight *E.coli* SCC1 cultures in M63+ were centrifuged at 3200 g and resuspended in 5 mL of fresh medium at the desired suspension density (OD_{600}) within polystyrene petri dishes (35 mm in diameter). Surface colonisation was then allowed by incubating the samples at 30˚C in the dark for variable times depending on experimental needs (mostly between 10 to 240 minutes). Samples surfaces were then washed to remove unattached cells and surface coverage determined from fluorescence pictures as explained in the following sections.

7. Washing methodologies:

Air-loose methodologies allowed samples to get exposed to the air. These have been tested as two different techniques: (i) *Dipping:* samples dishes containing cellular suspensions were dipped three times in and out of boxes containing 400 mL of PBS buffer; ii) *Pipetting:* sample dishes containing cellular suspensions were first emptied and then then their surfaces washed with 50 mL of PBS buffer using a serological pipette.

Air-tight methodologies avoided instead samples surfaces from being directly exposed to the air during washing. Sample dishes containing cellular suspensions were submerged in 400 mL PBS within plastic boxes and held in position at their bottom using magnets attached on the back of said boxes. These were then shaken for 1 minutes and 30 seconds using a longitudinal shaker (150 strokes per minute). This process was repeated twice with fresh buffer.

After any of the above methodologies, to prevent spillages, 5 mL of excess buffer were removed from the dish using a pipette.

8. Fluorescent microscopy:

Cluster monitoring in suspension and cells stranding: to compare *E.coli* MG1655 clusters formation in either overnight cultures or 0.1 OD_{600} resuspensions in M63+, 10 µL from both were respectively stained with 5 µL of a 200 µM Syto9 solution in PBS (ThermoFisher). 10 µL of the stained suspension were then transferred on a glass slide, covered with a 24 x 24 mm coverslip and imaged using a 100 x oil objectives (Zeiss Axiolab E-re). A minimum of 15 images were recorded per sample for three experimental replicates. When interested in cells stranding on the surface, I loaded cells on a glass slide as for the above procedure. Then I imaged the edges of the thin liquid film between this one and the supported coverslip. A total of 15 to 20 pictures were collected for each of the three replicates. Video records of the retracting films were recorded for 20 seconds at 30fps, using a Moticam 1080.

Surface coverage quantification: 30 to 40 pictures from polystyrene samples were taken at random locations on the surface using a 40 x dipping objective (Zeiss Axiolab E-re).

9. Bacteria vibrational stimulation

Overnight *E.coli* SCC1 cultures in M63+ were centrifuged at 3200g and resuspended in 5mL of fresh medium at 0.4 OD_{600} within polystyrene petri dishes. These were then placed on our vibrational device, incubated in the dark at 30°C and stimulated for 2 hours at variable combinations of pN intensities and kHz frequencies (Table 1). Samples were then washed (*Air-tight*) and 30 to 40 pictures gathered from the surface using fluorescence microscopy. These were then digitally processed and analysed to derive cells surface coverage on both vibrated samples and non-vibrated controls. The resulting change in coverage between these was then expressed as percentages by normalising the results from the vibrated samples by the mean coverage of their associated control. All tested conditions and experiments were performed in triplets.

10. Vibrational stimulation under variable cells concentrations:

Overnight *E.coli* SCC1 cultures in M63+ were centrifuged at 3200 g and resuspended in 5 mL of fresh medium at variable OD_{600} (0.1, 0.2, 0.4, 0.8 and 1.2) within polystyrene petri dishes. These were then placed on our vibrational device, incubated in the dark at 30°C and stimulated for 2 hours at 30 pN and 2 kHz. Samples were then washed (Air-tight), imaged (8) and surface coverage quantified (27).

11. Over time stimulation with sedimentation:

Overnight *E.coli* SCC1 cultures in M63+ were centrifuged at 3200 g and resuspended in 5 mL of fresh medium at 0.4 OD_{600} within polystyrene petri dishes. These were then placed on our vibrational device, incubated in the dark at 30°C and stimulated at 30 pN intensity and 2 kHz frequency for either 60, 120 or 240 minutes. Samples were then washed (Air-tight), imaged (8) and surface coverage quantified (27).

12. Surface sedimentation fractions:

Overnight *E.coli* SCC1 cultures in M63+ were centrifuged at 3200 g and resuspended in 5 mL of fresh medium within polystyrene samples dishes at variable OD_{600} of 0.2, 0.4 and 0.8. For each condition samples were incubated at 30°C in the dark for variable times (1, 10, 30, 60, 120 and 240 minutes) at the end of which 10 to 15 pictures of the surface were gathered and analysed to infer the fraction of sediments covering the surface (27). The average values coming from three independent replicates were then plotted for every time point of each condition and interpolated using sigmoidal curves.

13. Over time bacteria stimulation without surface sedimentation

Overnight *E.coli* SCC1 cultures in M63+ were centrifuged at 3200 g and resuspended in 5 mL of fresh medium within polystyrene samples dishes at OD_{600} of 0.2 or 0.4 when stimulation length was respectively above and below 1 hour. Samples were then loaded on or vibrational device, incubated at 30°C in the dark and stimulated at 30pN and 2kHz for progressively longer times of 10, 30, 60 and 120 minutes. Samples were then washed (Air-tight), imaged (8) and surface coverage quantified (27).

14. Improved surface adhesion over time

Overnight *E.coli* SCC1 cultures in M63+ were centrifuged at 3200 g and resuspended in 5 mL of fresh medium within polystyrene samples dishes at different OD_{600} depending on surface colonisation times and reported in the table below.

Colonisation time (minutes)	Cell concentration (OD_{600})
120	0.2
60	0.25
30	0.28
15	0.33

Surface colonisation was then allowed by incubating the samples at 30°C in the dark for longer times (from 15 to 120 minutes). Samples were then washed (Air-tight), imaged (8) and surface coverage quantified (27).

15. Effect of colonisation time on vibrational stimulation

Overnight *E.coli* SCC1 cultures in M63+ were centrifuged at 3200 g and resuspended in 5 mL of fresh medium within polystyrene samples dishes at variables OD_{600} depending on surface colonisation length and according to the table in 14. Cells in samples were incubated at 30°C in the dark and let to colonise the surfaces for progressively longer times of 15, 30, 60 and 120 minutes. After

this, samples were diluted 1 in 25 by replacing 4 mL of suspension with the same amount of fresh medium twice using a serological pipette. Samples were then loaded onto the vibrational device, incubated once again at 30°C in the dark and vibrations were applied for 2 hours at 30pN and 2kHz. Samples were finally washed (Air-tight), imaged (8) and surface coverage quantified (27).

16. Vibrational damage on cells envelope

Overnight *E.coli* SCC1 cultures in M63+ were centrifuged at 3200 g and resuspended in 5 mL of fresh medium within polystyrene samples at 0.2 OD_{600}. Samples were then incubated at 30°C in the dark and vibrations were applied for 2 hours at 30pN and 2kHz. After 1 hour and 40 minutes cells were stained within the samples for the remaining 20 minutes with a mixture of Syto9 (3.5μM w.c.) and Propidium Iodide (18μM w.c., ThermoFisher LIVE/DEAD Bac-light kit). This was done by replacing 1 mL of suspension with the same volume of a preprepared staining mixture. To prepare this one, both dyes were diluted in the ration of 1 μL of stock per mL of sample. After staining and vibrations were completed, samples were washed (Air-tight) and 30 pictures gathered from the surface on both the red and green channel using fluorescence microscopy. These were finally analysed to derive the ratio of damaged cells according to 27.

17. Vibrational response of polystyrene functionalised beads and dead cells

(1) Abiotic particles: Fluorescent carboxy and ammine functionalised beads (L4655 and L2778, Sigma-Aldrich) were used directly from stock to prepare 5 mL PBS suspensions within polystyrene petri dishes (35 mm) at 0.6 OD_{600}. Samples were then incubated at 30°C in the dark and vibrations applied for 2 hours at 30 pN and 2kHz. Surfaces were then washed (Air-tight), imaged (8) and surface coverage quantified (27). All experiments were performed as triplets.

(2) Dead cells: Overnight *E.coli* SCC1 cultures in M63+ were centrifuged at 3200 g and resuspended in 15 mL of fresh medium within polystyrene samples at 0.4 OD_{600}. Cells were then treated with 50 μg/mL of kanamycin (~100 μM) and incubated at 30°C overnight. From this suspension, 5 mL were transferred into polystyrene petri dishes (35 mm), incubated at 30°C in the dark and vibrations applied for 2 hours (30pN, 2kHz). After this, samples were washed (Air-tight), imaged (8) and surface coverage quantified (27). Experiments were performed in triplets.

18. Cells depolarisation using CCCP

Overnight *E.coli* MG1655 cultures in M63+ were centrifuged at 3200 g and resuspended in 5 mL of fresh medium within polystyrene samples at 0.05 OD_{600}. To these, I added different volumes of CCCP (carbonyl cyanide 3-chlorophenilhydrazone, Fisher Scientific) to achieve concentrations of 0, 2, 5 and 20 μM. Samples were then incubated in the dark at 30°C for 2 hours and during the remaining

20 minutes they were stained with $DiOC_2(3)$ (3,3'-Diethyloxacarbocyanine Iodide, Thermo Fisher). This was done by replacing 3 mL of suspension with the same amount of a staining mixture in M63+ which contained the required amount of dye (150 μM w.c.) and EDTA (11 mM, Thermo Fisher). Samples were then diluted 1 in 25 by twice replacing 4 mL of stained suspension with the same volume of fresh M63+ and were finally imaged using fluorescence microscopy. For every condition, 5 to 15 pictures of the surface were gathered on both the red and green channel which were then used to determine the ratio of red to green cells (27). Results were averaged across three replicates, plotted and interpolated with an exponential decay function.

19. Vibrational effect on antibiotic treated cells

Overnight *E.coli* SCC1 cultures in M63+ were centrifuged at 3200 g and resuspended in 5 mL of fresh medium within polystyrene samples at 0.2 OD_{600}. These were then treated with both inhibitory and sub-inhibitory concentrations of kanamycin (10 and 100 μM, Thermo Fisher), chloramphenicol (6 and 60 μM Thermo Fisher) and CCCP (5 and 20 μM, Fisher Scientific). For each condition, samples were loaded on the vibrational device, incubated in the dark at 30°C and stimulated for 2 hours at 50 pN and 2 kHz. Following this, sample were washed (Air-tight), imaged (8) and surface coverage quantified (27). The resulting values were then normalised by the mean change in coverage of untreated cells and these results coming from three independent replicates were plotted.

20. $DiOC_2(3)$ staining optimisation

Overnight *E.coli* MG1655 cultures in M63+ were centrifuged at 3200 g and resuspended in 5 mL of fresh medium within polystyrene samples at 0.05 OD_{600}. These were then incubated for 2 hours and during the remaining 20 minutes cells were stained using different combinations of dye and EDTA according to the table below.

$DiOC_2(3)$ (μM)	EDTA (mM)
150	2
150	11
30	2
30	11

These were supplied by replacing 4 mL of suspension with the same amount of a staining mixture in M63+ containing the required amount of dye and EDTA. Finally, samples were diluted 1 in 25 by replacing 4 mL of stained suspension with the same volume of fresh M63+ before being imaged using fluorescence microscopy to gather 15 to 20 pictures on both the red and green channels. These were used to qualitatively judge stain effectiveness.

21. Changings in cells polarisation following vibrational stimulation and magnesium treatment

(1) Vibrational stimulation: Overnight *E.coli* MG1655 cultures in M63+ were centrifuged at 3200 g and resuspended in 5 mL of fresh medium within polystyrene dishes (35 mm) at 0.05 OD_{600}. These were then incubated in the dark at 30°C and vibrationally stimulated for 2 hours at 50 pN and 2 kHz. During the remaining 20 minutes, cells were stained using 150 μM $DiOC_2(3)$ and 11 mM EDTA. To do this, 4 mL of samples suspension were replaced with the same volume of a staining mixture containing dye and EDTA amounts required for the above working concentrations. After staining, samples were diluted 1 in 25 by replacing twice 4 mL of stained suspension with the same amount of fresh M63+. Cells on surfaces were then imaged using fluorescence microscopy to gather 20 pictures as pairs on both the green and red channels. These pictures were the analysed (27-4b) to derive both the fractions and distributions of polarised cells on the surface for both vibrated samples and their controls. All the relevant experiments were performed in triplets.

(2) Magnesium treatment: Overnight *E.coli* MG1655 cultures in M63+ were centrifuged at 3200 g and resuspended in 5 mL of fresh M63+ within polystyrene dishes (35 mm) at 0.05 OD_{600}. Magnesium concentration was then adjusted by adding either 1 mM (controls) or 10 mM (samples) $MgSO_4$. These were subsequently incubated in the dark at 30° C for 2 hours. During the remaining 20 minutes cells were stained with $DiOC_2(3)$ (150 μM) and EDTA (11 mM) by replacing 4 mL of suspension with the same volume of a staining mixture in M63+ containing the required amounts of dye and EDTA for the above working concentrations. To ensure no change in Mg^{2+} concentration during staining, the above mixtures also contained either 1 mM (controls) or 10 mM (samples) $MgSO_4$. Following this, controls and samples were diluted 1 in 25 with fresh M63+ at respectively 1 mM or 10 mM magnesium content by replacing twice 4 mL of stained mixture with the same amount of fresh medium. Samples were then imaged using fluorescence microscopy to gather 20 pictures of cells on the surface on both the red and green channels. To determine both polarisation ratios and changings in fluorescence intensity, samples were finally analysed according to 27-4b.

22. Changing in cells colonisation following magnesium and CCCP treatment

To determine the effect that cells depolarisation and inhibited hyperpolarisation have on surface colonisation, overnight *E.coli* SCC1 cultures in M63+ were centrifuged at 3200 g and resuspended in 5 mL of fresh medium within polystyrene dishes (35 mm) at 0.2 OD_{600}. Samples were supplemented with either 10 mM $MgSO_4$ or 5 μM CCCP and then incubated in the dark at 30° C. Control and CCCP samples were supplied with standard magnesium content (1 mM). Finally, surfaces

were washed (Air-tight), imaged (8) and surface coverage quantified (27-1).

23. Cells and beads motility on polystyrene surfaces

I compared surface motilities of abiotic beads and cells using tracking algorithms. To do this, when cells were used, I grew them in either M63+ or LB. For growth in minimal medium *E.coli* SCC1 was cultured overnight at 30° C while for growth in rich medium cells were first grown overnight at 37° C then reinoculated as 1% (v/v) in fresh medium for 3 more hours at 37° C. From the resulting cultures, cells were then centrifuged at 3200 g and resuspended in motility buffer (0.2% glucose in PBS) at 0.1 OD_{600}. When beads were used, similar suspensions in the same medium were prepared from direct dilution of particles from stock (polystyrene carboxy functionalised beads fluorescents 1 µm in diameter, L4655 Sigma-Aldrich). The resulting suspension were then images using fluorescence microscopy and three to four videos (20 seconds, 30fps, Moticam 1080) were recorded for each condition at random locations on the surface. The above experiments were performed in triplets and the resulting videos analysed using the FIJI plugin TrackMate to derive cells and beads trajectory length and max displacement.

24. Vibrations effect on cells motility

To determine the effect of mechanical stimulation on cells surface motility, overnight *E.coli* SCC1 cultures in M63+ were centrifuged at 3200cg and resuspended in 5 mL of fresh medium within polystyrene dishes (35 mm) at 0.02 OD_{600}. Samples were then incubated in the dark at 30°C and vibrations applied for 2 hours at 30 pN and 2 kHz. They were then diluted by replacing 4 mL of suspension with motility buffer (0.2% glucose in PBS) and imaged using fluorescence microscopy. Between three to four videos (20 seconds, 30fps, Moticam 1080) were recorded at random locations on the surface for both vibrated samples and controls. The above experiments were performed in triplets and the resulting 9 to 12 videos per conditions analysed using FIJI's plugin TrackMate to derive cells trajectory lengths and max displacements.

25. *motA/B* knockout mutation in *E.coli* SCC1

The method used for recombineering is based on 'Gene doctoring: a method for recombineering in laboratory and pathogenic *Escherichia coli* strains' [234]. First I design a pDOC-C recombineering donor plasmid (RDP) which contained the desired recombineering substrate (in our case an Kan resistance cassette flanked by homologous regions to motAB in the genome). Then the recipient host strain SCC1 was co-transformed via electroporation with the RDP and the recombineering plasmid pACBSR (already available in the lab). Selection happened by inoculating a single transformed colony in 1 mL LB + amp + kan + cam + 0.5% (w/v) glucose. Glucose is suggested as to prevent leaky expression of λ-Red and I-SceI genes from pACBSR via catabolite repression. Cells were cultured at 37°C, 200 rpm for 2 hours and then centrifuge at 10,000 rpm for 5 minutes. After

having discarded the supernatant, cells were resuspend then culture in 1 mL LB + 0.5% (w/v) L-arabinose. These were re-cultured at 37˚C, 200 rpm until turbid (~ 4 - 5 hours), then diluted (1 x 10^{-6}), plated onto LBA + kan + 5% (w/v) sucrose and incubate plates at 30˚C overnight. On the resulting colonies I checked loss of residual RDP by patching onto LBA + amp and pACBSR loss by patching onto LBA + cam. Finally, colony PCR was performed and the purified product sent for sequencing.

26. *motA/B* mutants response to vibrations

To investigate the involvement of bacteria flagella motors (BFM) on vibrational response, I monitored the response of mutants that lack both motor proteins MotA and B. Overnight *E.coli* SCC1 ΔmotAB cultures in M63+ were centrifuged at 3200 g and resuspended in 5mL of fresh medium within polystyrene dishes (35 mm) at 0.2 OD_{600}. Samples were then incubated for 2 hours in the dark at 30°C while cells were stimulated at 50 pN and 2 kHz. Surfaces were then washed (Air-tight), imaged (8) and surface coverage quantified (27-1). All the relevant experiments were performed in triplets.

27. Image processing and analysis:

All image processing steps were performed using FIJI as either sequencies of manual or automated steps using task specific scripts.

(1) Surface coverage quantification: fluorescence images were processed and analysed using ImageJ and the process automated through custom scripts (see below). These determined the number and fraction of area covered by cells in each picture. These values were then averaged among all the pictures coming from three replicates of a specific condition and statistically compared.

(2) Surface sedimentation: to determine sedimentation fraction, for each picture a script was manually run. This one first determined the total surface area covered by cells. Then, it performed the same operation but analysing only objects whose surface are in the pictures was the size of our cells (4 $\mu m^2 \pm 0.9$). This value was subtracted from the total allowing one to determine the area covered by sediments. This was finally divided by the total to derive the sedimentation ratio in each picture.

(3) Membrane damage: images from both red and green channels were analysed and the total number of cells in them determined using the same script as for surface coverage determination. For every pair of green and red picture of a visited location on the surface, the number of red to green cells was computed. For each condition, the resulting values among all pictures from three independent replicates were statistically compared and plotted as bar plots.

(4) Membrane polarisation:

(a) *Ratio-metric*: Pairs of red and green images from specific locations on the surface

were independently analysed with custom scripts. These determined the number of red to green cells for each pair of which their grand mean was computed by averaging the result from all the pairs belonging to three independent replicates.

(b) *Fluorometric:* Pictures on the red channels were analysed to identify cells and determine their fluorescence as pixel intensity in the images. To do this custom FIJI scripts were used. These automatically segmented the images to isolate single cells from the background. Then, these regions of interest (ROI) were used to determine their average pixel intensity. Finally, for a give condition, these values were plotted as histograms and normalised by the total number of cells. This value was determined instead from the analysis of paired pictures in the green channels. Always using custom script their number was determined in pictures and used to normalise red fluorescence frequency distributions. These were then interpolated using Sum of Gaussian functions and the fraction of hyperpolarised cells was determined as the area under the curve passed 2 standard deviations of the left-most peak of the control distribution.

28. Data analysis and statistical comparison:

Where statistical comparison between samples was required, I used both parametric and non-parametric tests depending on data normality and homoscedasticity. When both were met, I used either t-tests or ANOVA, when only the latter was met Welch's correction to the preceding techniques were used instead. Finally, when samples were neither normally distributed nor homoscedastic, non-parametric equivalents such as Mann Withney U-test and Kruskal-Wallis were used. All statistical analysis and data handling were performed using GraphPad Prism, Microsoft Excel and R respectively.

29. Custom FIJI scripts:

Surface coverage quantification for SCC1: The following script was employed to determined surface coverage, cells number or their average surface area depending on the parameter defined at line 60.

```
//The current script take files from up to 2 sub-nested folders
//The processing steps are oriented toward maximising contour extrapolation of features for further segmentations


#@String(label = "specify a file extension") extension
//#@File(label = "specify a folder containing images", style = "directory") mainDir
// Turn on batch processing
setBatchMode(true);

// Get the names of all files in given directory
mainDir = getDirectory("Choose a main directory ");
mainList = getFileList(mainDir);

for (k=0; k<mainList.length; k++) {  // for loop to parse through names in main folder
     if(endsWith(mainList[k], "/")){   // if the name is a subfolder...
          subDir = mainDir + mainList[k];
          subList = getFileList(subDir);
          subDirName = File.getName(subDir);

          //ANALYSED SUB-SUBFOLDERS i
           for (i = 0; i < subList.length; i++) {
                if(endsWith(subList[i], "/")){   // if the name is a subfolder...
                     subsubDir = subDir + subList[i];
                     fileNames = getFileList(subsubDir);
                     subsubDirName = File.getName(subsubDir);
                     //PICTURES j in i
                     for (j = 0; j < fileNames.length; j++) {
                          // Only open if it's a .tif file open and process it
                          if (endsWith(fileNames[j], extension) == true) {

                          // Open the Image
                          open(subsubDir+fileNames[j]); //need to specify directory path for files
                          /////////////// Recorded commands go here !! ////////////////////


                              //run REMOVE BACKGROUND and filter Median
                          //correct for uneven illumination_100-120 work well
                          //run("Pseudo flat field correction", "blurring=120 hide");
                          //remove now even background
                          run("Subtract Background...", "rolling=20");
                          //sharpen pixel contrast
                          //run("Sharpen"); // run before Gaussian homogenization
                          //Gaussian homogenaisation
                          run("Gaussian Blur...", "sigma=2");
                          //second subctraction to further accentuate shapes
                          //run("Subtract Background...", "rolling=20");
                          //enhance feature contrast on polished image limiting the number of saturation to a minimum
                          //this could cause issues in extrapolating features from close bright objects
                          //run("Enhance Contrast...", "saturated=0.1");
                          //final homogenaisation after enhancement
                          //run("Mean...", "radius=2");

                          run("8-bit");
                          run("Auto Threshold", "method=Otsu white");
                          setOption("BlackBackground", true);
                          //remove extra edge pixels
                          run("Open");
                          //apply watershed algorithm for segmentation
                          run("Watershed");
                          run("Analyze Particles...", "size=0-Infinity display clear include summarize add in_situ");
                          //saveAs("Results", "mainDir/Summary"+subDir+".csv");
                          //run("Close All");
                                 /////////////// End of recorded commands ////////////////////

                          }
                     }
                 //save .csv for every i sub-subfolder
                 saveAs("Results", mainDir+subsubDirName+"_"+subDirName+".csv");
                }
          }
     }
}

```

Surface coverage quantification for MG1655 stained with $DiOC_2(3)$: The following script perform the same work as the one above only with adjusted parameters to better work with stained cells.

```
//The current script take files from up to 2 sub-nested folders
//The processing steps are oriented toward maximising contour extrapolation of features for further segmentations


#@String(label = "specify a file extension") extension
//#@File(label = "specify a folder containing images", style = "directory") mainDir
// Turn on batch processing
setBatchMode(true);

// Get the names of all files in given directory
mainDir = getDirectory("Choose a main directory ");
mainList = getFileList(mainDir);

for (k=0; k<mainList.length; k++) {  // for loop to parse through names in main folder
     if(endsWith(mainList[k], "/")){   // if the name is a subfolder...
          subDir = mainDir + mainList[k];
          subList = getFileList(subDir);
          subDirName = File.getName(subDir);

          //ANALYSED SUB-SUBFOLDERS i
           for (i = 0; i < subList.length; i++) {
                if(endsWith(subList[i], "/")){   // if the name is a subfolder...
                     subsubDir = subDir + subList[i];
                     fileNames = getFileList(subsubDir);
                     subsubDirName = File.getName(subsubDir);
                     //PICTURES j in i
                     for (j = 0; j < fileNames.length; j++) {
                          // Only open if it's a .tif file open and process it
                          if (endsWith(fileNames[j], extension) == true) {

                          // Open the Image
                          open(subsubDir+fileNames[j]); //need to specify directory path for files
                          /////////////// Recorded commands go here !! ////////////////////
                          //remove even background
                          run("Subtract Background...", "rolling=20");
                          run("Mean...", "radius=2");
                          run("8-bit");
                          run("Auto Threshold", "method=Otsu white");
                          setOption("BlackBackground", true);
                          //remove extra edge pixels
                          run("Open");
                          //apply watershed algorithm for segmentation
                          run("Watershed");
                          run("Analyze Particles...", "size=0-Infinity display clear include summarize add in_situ");
                          //run("Close All");
                          /////////////// End of recorded commands ////////////////////

                          }
                     }
                     //save .csv for every i sub-subfolder
                     saveAs("Results", mainDir+subsubDirName+"_"+subDirName+".csv");
                    }
               }
          }
}
```

Fluorometric determination: The following script was employed to determine the fluorescence (pixel intensity) and number of cells in both green and red pictures.

```
/* WHAT IT DOES AND HOW TO USE IT?
 * The following script allow the quantification of individual cells fluorescence
 * via ROI looping
 *
 * It require an input folder containing a sample and control folder having each
 * a red and gree subfolder. These latter need to be named this way for the script to work
 * No .bmp.mwi picture have to be in the channel folder for the script to run
 *
 * the script will then loop trhough the samples folder, then the channel folders
 * processing the pictures in them. A master folder containing the samples folder need then to
 * be provided to the script for it to work
 *
 * Every image will be duplicated and a mask will be created to obtains ROI that,
 * looping through them, will allow to quintify cell fluorescence in the original
 * image.
*/

/*////////////////////////
 * SETTING UP DIRECTORIES-------------------------------------------------------------
 *////////////////////////

//get input dir, parent dir and make output dir
inputDirPath = getDirectory("Select input directory");
inputDirFiles = getFileList(inputDirPath);
inputDirName = File.getName(inputDirPath);
setBatchMode(true);

/*////////////////////////
 * LOOP THROUGH DIRECTORIES-----------------------------------------------------------------------
 *////////////////////////

// loop SAMPLE folder (control/sample)_____________________________________
for (i = 0; i < inputDirFiles.length; i++) {
    if (endsWith(inputDirFiles[i], "/")) {
        sampleFolderPath = inputDirPath + inputDirFiles[i];
        sampleFolderFiles = getFileList(sampleFolderPath);
        sampleFolderName = File.getName(sampleFolderPath);

        //loop through CHANNEL folders (red/green)_____________________________
        for (j = 0; j < sampleFolderFiles.length; j++) {
            if (endsWith(sampleFolderFiles[j], "green/")) {
                channelFolderPath = sampleFolderPath + sampleFolderFiles[j];
                channelFolderFiles = getFileList(channelFolderPath);
                channelFolderName = File.getName(channelFolderPath);
                run("Clear Results"); //clear results table for next channel

                //loop throught the IMAGES in the channel folder_______________
                for (k = 0; k < channelFolderFiles.length; k++) {

```

```
                    ////////////////////////
                    //IMAGE PROCESSING green----------------------------------------------------------------
                    ////////////////////////
                    imagePath = channelFolderPath + channelFolderFiles[k];
                    imageName = channelFolderFiles[k];
                    greenChannel = imageName + " (green)";
                    open(imagePath);
                    roiManager("reset");

                    run("Set Scale...", "distance=1832 known=100 unit=um");
                    run("Split Channels");
                    selectWindow(greenChannel);

                    run("Subtract Background...", "rolling=20");
                    run("Mean...", "radius=2");

                    run("8-bit");
                    setAutoThreshold("Otsu dark");
                    setOption("BlackBackground", true);
                    run("Create Mask");
                    run("Open");
                    run("Watershed");
                    run("Set Measurements...", "mean redirect=None decimal=2");
                    run("Analyze Particles...", "size=0.4-2.4 include add"); //analysing a mask does not add to results

                    selectWindow(greenChannel);
                    roiManager("deselect");
                    roiManager("Measure");
                    roiManager("reset");

                    run("Close All"); // close all the pictures
                    run("Collect Garbage"); // free the RAM
                }
                saveAs("Results", inputDirPath + sampleFolderName + "_meanFluo_" + channelFolderName + ".csv"); //save channel specific results
                run("Clear Results"); //clear results table for next channel
            }
            if (endsWith(sampleFolderFiles[j], "red/")) {
                channelFolderPath = sampleFolderPath + sampleFolderFiles[j];
                channelFolderFiles = getFileList(channelFolderPath);
                channelFolderName = File.getName(channelFolderPath);
                run("Clear Results"); //clear results table for next channel

                //loop throught the IMAGES in the channel folder_____________
                for (k = 0; k < channelFolderFiles.length; k++) {

                    ////////////////////////
                    //IMAGE PROCESSING red------------------------------------------------------------------
                    ////////////////////////
                    imagePath = channelFolderPath + channelFolderFiles[k];
                    imageName = channelFolderFiles[k];
                    redChannel = imageName + " (red)";
                    open(imagePath);
                    roiManager("reset");

                    run("Set Scale...", "distance=1832 known=100 unit=um");
                    run("Split Channels");
                    selectWindow(redChannel);

                    run("Subtract Background...", "rolling=20");
                    run("Mean...", "radius=2");

                    run("8-bit");
                    setAutoThreshold("Otsu dark");
                    setOption("BlackBackground", true);
                    run("Create Mask");
                    run("Open");
                    run("Watershed");
                    run("Set Measurements...", "mean redirect=None decimal=1");
                    run("Analyze Particles...", "size=0.4-2.4 include add"); //analysing a mask does not add to results

                    selectWindow(redChannel);
                    roiManager("deselect");
                    roiManager("Measure");
                    roiManager("reset");

                    run("Close All"); // close all the pictures
                    run("Collect Garbage"); // free the RAM
                }
                saveAs("Results", inputDirPath + sampleFolderName + "_meanFluo_" + channelFolderName + ".csv"); //save channel specific results
                run("Clear Results"); //clear results table for next channel
            }
        }
    }
}
```

Ratio-metric determination of red and green cells in paired images: The following script determine the number of red and green cells in paired pictures from the surface.

```
/*////////////////////////
 * SETTING UP DIRECTORIES--------------------------------------------------------------
 *////////////////////////

//get input dir, parent dir and make output dir
inputDirPath = getDirectory("Select input directory");
inputDirFiles = getFileList(inputDirPath);
inputDirName = File.getName(inputDirPath);
setBatchMode(true);

/*//////////////////////////
 * LOOP THROUGH DIRECTORIES-----------------------------------------------------------------------------
 *//////////////////////////

// loop SAMPLE folder (control/sample)_____________________________________
for (i = 0; i < inputDirFiles.length; i++) {
    if (endsWith(inputDirFiles[i], "/")) {
        sampleFolderPath = inputDirPath + inputDirFiles[i];
        sampleFolderFiles = getFileList(sampleFolderPath);
        sampleFolderName = File.getName(sampleFolderPath);

        //loop through CHANNEL folders (red/green)_____________________________
        for (j = 0; j < sampleFolderFiles.length; j++) {
            if (endsWith(sampleFolderFiles[j], "green/")) {
                channelFolderPath = sampleFolderPath + sampleFolderFiles[j];
                channelFolderFiles = getFileList(channelFolderPath);
                channelFolderName = File.getName(channelFolderPath);
                run("Clear Results"); //clear results table for next channel

                //loop throught the IMAGES in the channel folder_______________
                for (k = 0; k < channelFolderFiles.length; k++) {

                    ////////////////////////
                    //IMAGE PROCESSING green-------------------------------------------------------------
                    ////////////////////////
                    imagePath = channelFolderPath + channelFolderFiles[k];
                    imageName = channelFolderFiles[k];
                    greenChannel = imageName + " (green)";
                    open(imagePath);
                    //roiManager("reset");

                    ////////////////////////
                    //IMAGE PROCESSING green-------------------------------------------------------------
                    ////////////////////////
                    imagePath = channelFolderPath + channelFolderFiles[k];
                    imageName = channelFolderFiles[k];
                    greenChannel = imageName + " (green)";
                    open(imagePath);
                    //roiManager("reset");

                    //run("Set Scale...", "distance=1832 known=100 unit=um");
                    run("Split Channels");
                    selectWindow(greenChannel);
                    run("Subtract Background...", "rolling=20");
                    run("Mean...", "radius=2");
                    run("8-bit");
                    setAutoThreshold("Otsu dark");
                    setOption("BlackBackground", true);
                    run("Create Mask");
                    run("Open");
                    run("Watershed");

                    run("Analyze Particles...", "size=0-Infinity display clear include summarize add in_situ");

                    run("Close All"); // close all the pictures
                    run("Collect Garbage"); // free the RAM
                }
                saveAs("Results", inputDirPath + sampleFolderName + "_%coverage_" + channelFolderName + ".csv"); //save channel specific results
                run("Clear Results"); //clear results table for next channel
            }
            if (endsWith(sampleFolderFiles[j], "red/")) {
                channelFolderPath = sampleFolderPath + sampleFolderFiles[j];
                channelFolderFiles = getFileList(channelFolderPath);
                channelFolderName = File.getName(channelFolderPath);
                run("Clear Results"); //clear results table for next channel

                //loop throught the IMAGES in the channel folder_____________
                for (k = 0; k < channelFolderFiles.length; k++) {

                    ////////////////////////
                    //IMAGE PROCESSING red---------------------------------------------------------------
                    ////////////////////////
                    imagePath = channelFolderPath + channelFolderFiles[k];
                    imageName = channelFolderFiles[k];
                    redChannel = imageName + " (red)";
                    open(imagePath);
                    roiManager("reset");
```

```
                    //run("Set Scale...", "distance=1832 known=100 unit=um");
                    run("Split Channels");
                    selectWindow(redChannel);
                    run("Subtract Background...", "rolling=20");
                    run("Mean...", "radius=2");
                    run("8-bit");
                    setAutoThreshold("Otsu dark");
                    setOption("BlackBackground", true);
                    run("Create Mask");
                    run("Open");
                    run("Watershed");

                    run("Analyze Particles...", "size=0-Infinity display clear include summarize add in_situ");

                    run("Close All"); // close all the pictures
                    run("Collect Garbage"); // free the RAM
                }
                saveAs("Results", inputDirPath + sampleFolderName + "_%coverage_" + channelFolderName + ".csv"); //save channel specific results
                run("Clear Results"); //clear results table for next channel
            }
        }
    }
}

```

Surface sedimentation: The following script determine the fraction of cells sediments formed on the surface. These are manually performed and the place holder names can vary according to the pictures opened.

```
selectWindow("ImageName");
run("Subtract Background...", "rolling=100");
run("Median...", "radius=2");
run("Duplicate...", " ");
selectWindow("ImageName");
run("8-bit");
run("Auto Threshold", "method=Default white");
run("Analyze Particles...", " size=100-1000 circularity=0.00-infinity display clear include summarize add");
roiManager("Invert");
roiManager("Fill");
selectWindow("Duplicate of ImageName");
run("Auto Threshold");
run("8-bit");
run("Auto Threshold", "method=Default white");
run("Analyze Particles...", "  circularity=0.00-infinity display clear include summarize add");
imageCalculator("Subtract create", "ImageName.bmp","Duplicate of Image Name.bmp");
selectWindow("Result of Subtraction.bmp");
roiManager("Invert");
run("Analyze Particles...", "  circularity=0.00-infinity display clear include summarize add");

```

Bibliography

1. Patricia Curd and Daniel Graham. *The Oxford Handbook of Presocratic Philosophy*. Oxford University Press; 2008. doi:10.1093/oxfordhb/9780195146875.001.0001

2. Thompson DW. *On Growth and Form*. (Bonner JT, ed.). Cambridge University Press; 1992. doi:10.1017/CBO9781107325852

3. Katta S, Krieg M, Goodman MB. Feeling Force: Physical and Physiological Principles Enabling Sensory Mechanotransduction. *Annual Review of Cell and Developmental Biology*. 2015;31(1):347-371. doi:10.1146/annurev-cellbio-100913-013426

4. Jansen KA, Donato DM, Balcioglu HE, Schmidt T, Danen EHJ, Koenderink GH. A guide to mechanobiology: Where biology and physics meet. *Biochimica et Biophysica Acta (BBA) - Molecular Cell Research*. 2015;1853(11, Part B):3043-3052. doi:10.1016/j.bbamcr.2015.05.007

5. Iskratsch T, Wolfenson H, Sheetz MP. Appreciating force and shape — the rise of mechanotransduction in cell biology. *Nature Reviews Molecular Cell Biology*. 2014;15(12):825-833. doi:10.1038/nrm3903

6. Dufrêne YF, Persat A. Mechanomicrobiology: how bacteria sense and respond to forces. *Nature Reviews Microbiology*. Published online January 20, 2020. doi:10.1038/s41579-019-0314-2

7. Wolfenson H, Yang B, Sheetz MP. Steps in Mechanotransduction Pathways that Control Cell Morphology. *Annual Review of Physiology*. 2019;81(1):585-605. doi:10.1146/annurev-physiol-021317-121245

8. Hoffman BD, Grashoff C, Schwartz MA. Dynamic molecular processes mediate cellular mechanotransduction. *Nature*. 2011;475(7356):316-323. doi:10.1038/nature10316

9. Feng Q, Kornmann B. Mechanical forces on cellular organelles. *Journal of Cell Science*. 2018;131(21):jcs218479. doi:10.1242/jcs.218479

10. Kirby TJ, Lammerding J. Emerging views of the nucleus as a cellular mechanosensor. *Nature Cell Biology*. 2018;20(4):373-381. doi:10.1038/s41556-018-0038-y

11. Miroshnikova YA, Wickström SA. Mechanical Forces in Nuclear Organization. *Cold Spring Harb Perspect Biol*. 2022;14(1):a039685. doi:10.1101/cshperspect.a039685

12. Mammoto A, Mammoto T, Ingber DE. Mechanosensitive mechanisms in transcriptional regulation. *Journal of Cell Science*. Published online January 1, 2012:jcs.093005. doi:10.1242/jcs.093005

13. Tajik A, Zhang Y, Wei F, et al. Transcription

upregulation via force-induced direct stretching of chromatin. *Nature Mater*. 2016;15(12):1287-1296. doi:10.1038/nmat4729

14. Abu Shah E, Keren K. Mechanical forces and feedbacks in cell motility. *Current Opinion in Cell Biology*. 2013;25(5):550-557. doi:10.1016/j.ceb.2013.06.009

15. Vining KH, Mooney DJ. Mechanical forces direct stem cell behaviour in development and regeneration. *Nat Rev Mol Cell Biol*. 2017;18(12):728-742. doi:10.1038/nrm.2017.108

16. Hallou A, Brunet T. On growth and force: mechanical forces in development. *Development*. 2020;147(4):dev187302. doi:10.1242/dev.187302

17. Kumar A, Placone JK, Engler AJ. Understanding the extracellular forces that determine cell fate and maintenance. *Development*. 2017;144(23):4261-4270. doi:10.1242/dev.158469

18. Li J, Wang Z, Chu Q, Jiang K, Li J, Tang N. The Strength of Mechanical Forces Determines the Differentiation of Alveolar Epithelial Cells. *Developmental Cell*. 2018;44(3):297-312.e5. doi:10.1016/j.devcel.2018.01.008

19. Hodgkinson T, Kelly DC, Curtin CM, O'Brien FJ. Mechanosignalling in cartilage: an emerging target for the treatment of osteoarthritis. *Nat Rev Rheumatol*. 2022;18(2):67-84. doi:10.1038/s41584-021-00724-w

20. Zhen G, Guo Q, Li Y, et al. Mechanical stress determines the configuration of TGFβ activation in articular cartilage. *Nat Commun*. 2021;12(1):1706. doi:10.1038/s41467-021-21948-0

21. Wang L, You X, Zhang L, Zhang C, Zou W. Mechanical regulation of bone remodeling. *Bone Res*. 2022;10(1):1-15. doi:10.1038/s41413-022-00190-4

22. Lemke SB, Schnorrer F. Mechanical forces during muscle development. *Mechanisms of Development*. 2017;144:92-101. doi:10.1016/j.mod.2016.11.003

23. Forceful synapses reveal mechanical interactions in the brain. *Nature*. Published online November 24, 2021:d41586-021-03516-0. doi:10.1038/d41586-021-03516-0

24. Tyler WJ. The mechanobiology of brain function. *Nat Rev Neurosci*. 2012;13(12):867-878. doi:10.1038/nrn3383

25. Huse M. Mechanical forces in the immune system. *Nat Rev Immunol*. 2017;17(11):679-690. doi:10.1038/nri.2017.74

26. Fritzsche M. What Is the Right Mechanical Readout for Understanding the Mechanobiology of the Immune Response? *Frontiers in Cell and Developmental Biology*. 2021;9. Accessed April 30, 2022. https://www.frontiersin.org/article/10.3389/fcell.2021.612539

27. Yue B. Biology of the Extracellular Matrix: An

Overview. *Journal of Glaucoma*. 2014;23:S20. doi:10.1097/IJG.0000000000000108

28. Fletcher DA, Mullins RD. Cell mechanics and the cytoskeleton. *Nature*. 2010;463(7280):485-492. doi:10.1038/nature08908

29. Koch AL, Higgins ML, Doyle RJY 1982. The Role of Surface Stress in the Morphology of Microbes. *Microbiology*. 1982;128(5):927-945. doi:10.1099/00221287-128-5-927

30. Sukharev SI, Blount P, Martinac B, Blattner FR, Kung C. A large-conductance mechanosensitive channel in E. coli encoded by mscL alone. *Nature*. 1994;368(6468):265-268. doi:10.1038/368265a0

31. Milo R, Phillips R. *Cell Biology by the Numbers*. Garland Science, Taylor & Francis Group; 2016.

32. Auer GK, Weibel DB. Bacterial Cell Mechanics. *Biochemistry*. 2017;56(29):3710-3724. doi:10.1021/acs.biochem.7b00346

33. Harper CE, Hernandez CJ. Cell biomechanics and mechanobiology in bacteria: Challenges and opportunities. *APL Bioengineering*. 2020;4(2):021501. doi:10.1063/1.5135585

34. Shi H, Bratton BP, Gitai Z, Huang KC. How to Build a Bacterial Cell: MreB as the Foreman of E. coli Construction. *Cell*. 2018;172(6):1294-1305. doi:10.1016/j.cell.2018.02.050

35. Silber N, Matos de Opitz CL, Mayer C, Sass P. Cell division protein FtsZ: from structure and mechanism to antibiotic target. *Future Microbiology*. 2020;15(9):801-831. doi:10.2217/fmb-2019-0348

36. Persat A. Bacterial mechanotransduction. *Current Opinion in Microbiology*. 2017;36:1-6. doi:10.1016/j.mib.2016.12.002

37. Persat A, Nadell CD, Kim MK, et al. The Mechanical World of Bacteria. *Cell*. 2015;161(5):988-997. doi:10.1016/j.cell.2015.05.005

38. Booth IR. Bacterial mechanosensitive channels: progress towards an understanding of their roles in cell physiology. *Curr Opin Microbiol*. 2014;18(100):16-22. doi:10.1016/j.mib.2014.01.005

39. Peyronnet R, Tran D, Girault T, Frachisse JM. Mechanosensitive channels: feeling tension in a world under pressure. *Frontiers in Plant Science*. 2014;5. doi:10.3389/fpls.2014.00558

40. Bremer E, Krämer R. Responses of Microorganisms to Osmotic Stress. *Annual Review of Microbiology*. 2019;73(1):313-334. doi:10.1146/annurev-micro-020518-115504

41. Cox CD, Bavi N, Martinac B. Bacterial Mechanosensors. *Annual Review of Physiology*. 2018;80(1):71-93. doi:10.1146/annurev-physiol-021317-121351

42. Chure G, Lee HJ, Rasmussen A, Phillips R. Connecting the Dots between Mechanosensitive Channel Abundance, Osmotic Shock, and Survival at Single-Cell Resolution. *Journal of Bacteriology*. 2018;200(23):e00460-18. doi:10.1128/JB.00460-18

43. Booth IR, Blount P. The MscS and MscL Families of Mechanosensitive Channels Act as Microbial Emergency Release Valves. *Journal of Bacteriology*. 2012;194(18):4802-4809. doi:10.1128/JB.00576-12

44. Haswell ES, Phillips R, Rees DC. Mechanosensitive Channels: What Can They Do and How Do They Do It? *Structure*. 2011;19(10):1356-1369. doi:10.1016/j.str.2011.09.005

45. Kung C, Martinac B, Sukharev S. Mechanosensitive Channels in Microbes. *Annual Review of Microbiology*. 2010;64(1):313-329. doi:10.1146/annurev.micro.112408.134106

46. Betanzos M, Chiang CS, Guy HR, Sukharev S. A large iris-like expansion of a mechanosensitive channel protein induced by membrane tension. *Nat Struct Mol Biol*. 2002;9(9):704-710. doi:10.1038/nsb828

47. Booth IR, Miller S, Müller A, Lehtovirta-Morley L. The evolution of bacterial mechanosensitive channels. *Cell Calcium*. 2015;57(3):140-150. doi:10.1016/j.ceca.2014.12.011

48. Rojas E, Theriot JA, Huang KC. Response of Escherichia coli growth rate to osmotic shock. *Proceedings of the National Academy of Sciences*. 2014;111(21):7807-7812. doi:10.1073/pnas.1402591111

49. Mathelié-Guinlet M, Viela F, Alsteens D, Dufrêne YF. Stress-Induced Catch-Bonds to Enhance Bacterial Adhesion. *Trends in Microbiology*. 2021;29(4):286-288. doi:10.1016/j.tim.2020.11.009

50. Sauer MM, Jakob RP, Eras J, et al. Catch-bond mechanism of the bacterial adhesin FimH. *Nat Commun*. 2016;7(1):10738. doi:10.1038/ncomms10738

51. Müller CM, Åberg A, Straseviçiene J, Emődy L, Uhlin BE, Balsalobre C. Type 1 Fimbriae, a Colonization Factor of Uropathogenic Escherichia coli, Are Controlled by the Metabolic Sensor CRP-cAMP. *PLOS Pathogens*. 2009;5(2):e1000303. doi:10.1371/journal.ppat.1000303

52. Le Trong I, Aprikian P, Kidd BA, et al. Structural Basis for Mechanical Force Regulation of the Adhesin FimH via Finger Trap-like β Sheet Twisting. *Cell*. 2010;141(4):645-655. doi:10.1016/j.cell.2010.03.038

53. Stærk K, Khandige S, Kolmos HJ, Møller-Jensen J, Andersen TE. Uropathogenic *Escherichia coli* Express Type 1 Fimbriae Only in Surface Adherent Populations Under Physiological Growth Conditions. *J Infect Dis*. 2016;213(3):386-394. doi:10.1093/infdis/jiv422

54. Gordon VD, Wang L. Bacterial mechanosensing: the force will be with you, always. *Journal of Cell Science*. 2019;132(7):jcs227694. doi:10.1242/jcs.227694

55. Subramanian S, Kearns DB. Functional Regulators of Bacterial Flagella. *Annual Review of*

Microbiology. 2019;73(1):225-246. doi:10.1146/annurev-micro-020518-115725

56. Lele PP, Hosu BG, Berg HC. Dynamics of mechanosensing in the bacterial flagellar motor. *Proceedings of the National Academy of Sciences*. 2013;110(29):11839-11844. doi:10.1073/pnas.1305885110

57. Tipping MJ, Delalez NJ, Lim R, Berry RM, Armitage JP. Load-Dependent Assembly of the Bacterial Flagellar Motor. Bassler B, ed. *mBio*. 2013;4(4). doi:10.1128/mBio.00551-13

58. Nord AL, Gachon E, Perez-Carrasco R, et al. Catch bond drives stator mechanosensitivity in the bacterial flagellar motor. *Proceedings of the National Academy of Sciences*. 2017;114(49):12952-12957. doi:10.1073/pnas.1716002114

59. Nirody JA, Nord AL, Berry RM. Load-dependent adaptation near zero load in the bacterial flagellar motor. *Journal of The Royal Society Interface*. 2019;16(159):20190300. doi:10.1098/rsif.2019.0300

60. Wadhwa N, Phillips R, Berg HC. Torque-dependent remodeling of the bacterial flagellar motor. *Proceedings of the National Academy of Sciences*. Published online May 29, 2019:201904577. doi:10.1073/pnas.1904577116

61. Ito KI, Nakamura S, Toyabe S. Cooperative stator assembly of bacterial flagellar motor mediated by rotation. *Nat Commun*. 2021;12(1):3218. doi:10.1038/s41467-021-23516-y

62. Doyle TB, Hawkins AC, McCarter LL. The Complex Flagellar Torque Generator of Pseudomonas aeruginosa. *J Bacteriol*. 2004;186(19):6341-6350. doi:10.1128/JB.186.19.6341-6350.2004

63. Toutain CM, Zegans ME, O'Toole GA. Evidence for Two Flagellar Stators and Their Role in the Motility of Pseudomonas aeruginosa. *Journal of Bacteriology*. 2005;187(2):771-777. doi:10.1128/JB.187.2.771-777.2005

64. Berne C, Ducret A, Hardy GG, Brun YV. Adhesins Involved in Attachment to Abiotic Surfaces by Gram-Negative Bacteria. *Microbiology Spectrum*. 2015;3(4). doi:10.1128/microbiolspec.MB-0018-2015

65. Mattick JS. Type IV Pili and Twitching Motility. *Annual Review of Microbiology*. 2002;56(1):289-314. doi:10.1146/annurev.micro.56.012302.160938

66. Talà L, Fineberg A, Kukura P, Persat A. Pseudomonas aeruginosa orchestrates twitching motility by sequential control of type IV pili movements. *Nature Microbiology*. 2019;4(5):774-780. doi:10.1038/s41564-019-0378-9

67. Wong GCL, Antani JD, Lele PP, et al. Roadmap on emerging concepts in the physical biology of bacterial biofilms: from surface sensing to community formation. *Phys Biol*. 2021;18(5):051501. doi:10.1088/1478-

3975/abdc0e

68. Grobas I, Polin M, Asally M. Swarming bacteria undergo localized dynamic phase transition to form stress-induced biofilms. *eLife*. 10:e62632. doi:10.7554/eLife.62632

69. Mordue J, O'Boyle N, Gadegaard N, Roe AJ. The force awakens: The dark side of mechanosensing in bacterial pathogens. *Cellular Signalling*. 2021;78:109867. doi:10.1016/j.cellsig.2020.109867

70. Jenal U, Reinders A, Lori C. Cyclic di-GMP: second messenger extraordinaire. *Nature Reviews Microbiology*. 2017;15(5):271-284. doi:10.1038/nrmicro.2016.190

71. Rodesney CA, Roman B, Dhamani N, et al. Mechanosensing of shear by Pseudomonas aeruginosa leads to increased levels of the cyclic-di-GMP signal initiating biofilm development. *Proceedings of the National Academy of Sciences*. 2017;114(23):5906-5911. doi:10.1073/pnas.1703255114

72. Persat A, Inclan YF, Engel JN, Stone HA, Gitai Z. Type IV pili mechanochemically regulate virulence factors in <i>Pseudomonas aeruginosa<i>. *Proceedings of the National Academy of Sciences*. 2015;112(24):7563-7568. doi:10.1073/pnas.1502025112

73. Almblad H, Rybtke M, Hendiani S, Andersen JB, Givskov M, Tolker-Nielsen T. High levels of cAMP inhibit Pseudomonas aeruginosa biofilm formation through reduction of the c-di-GMP content. *Microbiology*. 2019;165(3):324-333. doi:10.1099/mic.0.000772

74. Laventie BJ, Sangermani M, Estermann F, et al. A Surface-Induced Asymmetric Program Promotes Tissue Colonization by Pseudomonas aeruginosa. *Cell Host & Microbe*. 2019;25(1):140-152.e6. doi:10.1016/j.chom.2018.11.008

75. Siryaporn A, Kuchma SL, O'Toole GA, Gitai Z. Surface attachment induces *Pseudomonas aeruginosa* virulence. *Proceedings of the National Academy of Sciences*. 2014;111(47):16860-16865. doi:10.1073/pnas.1415712111

76. Ellison CK, Kan J, Dillard RS, et al. Obstruction of pilus retraction stimulates bacterial surface sensing. Published online 2017:5.

77. Del Medico L, Cerletti D, Schächle P, Christen M, Christen B. The type IV pilin PilA couples surface attachment and cell-cycle initiation in *Caulobacter crescentus*. *Proceedings of the National Academy of Sciences*. Published online April 15, 2020:201920143. doi:10.1073/pnas.1920143117

78. Sangermani M, Hug I, Sauter N, Pfohl T, Jenal U. Tad Pili Play a Dynamic Role in Caulobacter crescentus Surface Colonization. 2019;10(3):18.

79. Hug I, Deshpande S, Sprecher KS, Pfohl T, Jenal U. Second messenger–mediated tactile response by a bacterial rotary motor. *Science*. 2017;358(6362):531-534. doi:10.1126/science.aan5353

80. Kralj JM, Hochbaum DR, Douglass AD, Cohen AE. Electrical Spiking in *Escherichia coli* Probed with a Fluorescent Voltage-Indicating Protein. *Science*. 2011;333(6040):345-348. doi:10.1126/science.1204763

81. Bruni GN, Weekley RA, Dodd BJT, Kralj JM. Voltage-gated calcium flux mediates *Escherichia coli* mechanosensation. *Proceedings of the National Academy of Sciences*. 2017;114(35):9445-9450. doi:10.1073/pnas.1703084114

82. Vrabioiu AM, Berg HC. Signaling events that occur when cells of *Escherichia coli* encounter a glass surface. *Proc Natl Acad Sci USA*. 2022;119(6):e2116830119. doi:10.1073/pnas.2116830119

83. Robertson SN, Campsie P, Childs PG, et al. Control of cell behaviour through nanovibrational stimulation: nanokicking. *Philosophical Transactions of the Royal Society A: Mathematical, Physical and Engineering Sciences*. 2018;376(2120):20170290. doi:10.1098/rsta.2017.0290

84. Tsimbouri PM, Childs PG, Pemberton GD, et al. Stimulation of 3D osteogenesis by mesenchymal stem cells using a nanovibrational bioreactor. *Nature Biomedical Engineering*. 2017;1(9):758-770. doi:10.1038/s41551-017-0127-4

85. Childs PG, Boyle CA, Pemberton GD, et al. Use of nanoscale mechanical stimulation for control and manipulation of cell behaviour. *Acta Biomaterialia*. 2016;34:159-168. doi:10.1016/j.actbio.2015.11.045

86. Pemberton GD, Childs P, Reid S, et al. Nanoscale stimulation of osteoblastogenesis from mesenchymal stem cells: nanotopography and nanokicking. *Nanomedicine*. 2015;10(4):547-560. doi:10.2217/nnm.14.134

87. Nikukar H, Childs PG, Curtis ASG, et al. Production of Nanoscale Vibration for Stimulation of Human Mesenchymal Stem Cells. *Journal of Biomedical Nanotechnology*. 2016;12(7):1478-1488. doi:10.1166/jbn.2016.2264

88. Nikukar H, Reid S, Tsimbouri PM, Riehle MO, Curtis ASG, Dalby MJ. Osteogenesis of Mesenchymal Stem Cells by Nanoscale Mechanotransduction. *ACS Nano*. 2013;7(3):2758-2767. doi:10.1021/nn400202j

89. Flemming HC, Wingender J, Szewzyk U, Steinberg P, Rice SA, Kjelleberg S. Biofilms: an emergent form of bacterial life. *Nature Reviews Microbiology*. 2016;14(9):563-575. doi:10.1038/nrmicro.2016.94

90. Flemming HC, Wingender J. The biofilm matrix. *Nature Reviews Microbiology*. 2010;8(9):623-633. doi:10.1038/nrmicro2415

91. Tolker-Nielsen T. Biofilm Development. *Microbiology Spectrum*. 2015;3(2). doi:10.1128/microbiolspec.MB-0001-2014

92. Rumbaugh KP, Sauer K. Biofilm dispersion. *Nature Reviews Microbiology*. Published online

June 12, 2020. doi:10.1038/s41579-020-0385-0

93. Futo M, Opašić L, Koska S, et al. Embryo-Like Features in Developing *Bacillus subtilis* Biofilms. Perna N, ed. *Molecular Biology and Evolution*. 2021;38(1):31-47. doi:10.1093/molbev/msaa217

94. Flemming HC, Wuertz S. Bacteria and archaea on Earth and their abundance in biofilms. *Nature Reviews Microbiology*. 2019;17(4):247-260. doi:10.1038/s41579-019-0158-9

95. Battin TJ, Besemer K, Bengtsson MM, Romani AM, Packmann AI. The ecology and biogeochemistry of stream biofilms. *Nature Reviews Microbiology*. 2016;14(4):251-263. doi:10.1038/nrmicro.2016.15

96. Nadell CD, Drescher K, Foster KR. Spatial structure, cooperation and competition in biofilms. *Nature Reviews Microbiology*. 2016;14(9):589-600. doi:10.1038/nrmicro.2016.84

97. Penesyan A, Paulsen IT, Kjelleberg S, Gillings MR. Three faces of biofilms: a microbial lifestyle, a nascent multicellular organism, and an incubator for diversity. *npj Biofilms Microbiomes*. 2021;7(1):1-9. doi:10.1038/s41522-021-00251-2

98. Remis JP, Costerton JW, Auer M. Biofilms: structures that may facilitate cell–cell interactions. *ISME J*. 2010;4(9):1085-1087. doi:10.1038/ismej.2010.105

99. Stewart PS, Franklin MJ. Physiological heterogeneity in biofilms. *Nature Reviews Microbiology*. 2008;6(3):199-210. doi:10.1038/nrmicro1838

100. West SA, Cooper GA. Division of labour in microorganisms: an evolutionary perspective. *Nature Reviews Microbiology*. 2016;14(11):716-723. doi:10.1038/nrmicro.2016.111

101. van Gestel J, Vlamakis H, Kolter R. Division of Labor in Biofilms: the Ecology of Cell Differentiation. *Microbiology Spectrum*. 2015;3(2). doi:10.1128/microbiolspec.MB-0002-2014

102. Molin S, Tolker-Nielsen T. Gene transfer occurs with enhanced efficiency in biofilms and induces enhanced stabilisation of the biofilm structure. *Current Opinion in Biotechnology*. 2003;14(3):255-261. doi:10.1016/S0958-1669(03)00036-3

103. Drescher K, Nadell CD, Stone HA, Wingreen NS, Bassler BL. Solutions to the Public Goods Dilemma in Bacterial Biofilms. *Current Biology*. 2014;24(1):50-55. doi:10.1016/j.cub.2013.10.030

104. Liu J, Prindle A, Humphries J, et al. Metabolic co-dependence gives rise to collective oscillations within biofilms. *Nature*. 2015;523(7562):550-554. doi:10.1038/nature14660

105. Lyons NA, Kolter R. On the evolution of bacterial multicellularity. *Current Opinion in Microbiology*. 2015;24:21-28. doi:10.1016/j.mib.2014.12.007

106. Simpson DR. Biofilm processes in biologically

active carbon water purification. *Water Research*. 2008;42(12):2839-2848. doi:10.1016/j.watres.2008.02.025

107. Heveran CM, Williams SL, Qiu J, et al. Biomineralization and Successive Regeneration of Engineered Living Building Materials. *Matter*. Published online January 2020. doi:10.1016/j.matt.2019.11.016

108. Huang J, Liu S, Zhang C, et al. Programmable and printable Bacillus subtilis biofilms as engineered living materials. *Nat Chem Biol*. 2019;15(1):34-41. doi:10.1038/s41589-018-0169-2

109. Roell GW, Zha J, Carr RR, Koffas MA, Fong SS, Tang YJ. Engineering microbial consortia by division of labor. *Microb Cell Fact*. 2019;18(1):35. doi:10.1186/s12934-019-1083-3

110. Tsoi R, Wu F, Zhang C, Bewick S, Karig D, You L. Metabolic division of labor in microbial systems. *Proc Natl Acad Sci USA*. 2018;115(10):2526-2531. doi:10.1073/pnas.1716888115

111. Cavaliere M, Feng S, Soyer OS, Jiménez JI. Cooperation in microbial communities and their biotechnological applications. *Environmental Microbiology*. 2017;19(8):2949-2963. doi:10.1111/1462-2920.13767

112. Lindemann SR, Bernstein HC, Song HS, et al. Engineering microbial consortia for controllable outputs. *ISME J*. 2016;10(9):2077-2084. doi:10.1038/ismej.2016.26

113. Jiang Y, Dong W, Xin F, Jiang M. Designing Synthetic Microbial Consortia for Biofuel Production. *Trends in Biotechnology*. 2020;38(8):828-831. doi:10.1016/j.tibtech.2020.02.002

114. Che S, Men Y. Synthetic microbial consortia for biosynthesis and biodegradation: promises and challenges. *Journal of Industrial Microbiology and Biotechnology*. 2019;46(9-10):1343-1358. doi:10.1007/s10295-019-02211-4

115. Wang F, Zhao J, Li Q, et al. One-pot biocatalytic route from cycloalkanes to α,ω-dicarboxylic acids by designed Escherichia coli consortia. *Nat Commun*. 2020;11(1):5035. doi:10.1038/s41467-020-18833-7

116. Maes S, Vackier T, Nguyen Huu S, et al. Occurrence and characterisation of biofilms in drinking water systems of broiler houses. *BMC Microbiology*. 2019;19(1). doi:10.1186/s12866-019-1451-5

117. Chan S, Pullerits K, Keucken A, Persson KM, Paul CJ, Rådström P. Bacterial release from pipe biofilm in a full-scale drinking water distribution system. *npj Biofilms and Microbiomes*. 2019;5(1). doi:10.1038/s41522-019-0082-9

118. Drescher K, Shen Y, Bassler BL, Stone HA. Biofilm streamers cause catastrophic disruption of flow with consequences for environmental and medical systems. *Proceedings of the National Academy of Sciences*. 2013;110(11):4345-4350.

doi:10.1073/pnas.1300321110

119. Wingender J, Flemming HC. Biofilms in drinking water and their role as reservoir for pathogens. *International Journal of Hygiene and Environmental Health*. 2011;214(6):417-423. doi:10.1016/j.ijheh.2011.05.009

120. Callow JA, Callow ME. Trends in the development of environmentally friendly fouling-resistant marine coatings. *Nature Communications*. 2011;2(1). doi:10.1038/ncomms1251

121. Banerjee I, Pangule RC, Kane RS. Antifouling Coatings: Recent Developments in the Design of Surfaces That Prevent Fouling by Proteins, Bacteria, and Marine Organisms. *Advanced Materials*. 2011;23(6):690-718. doi:10.1002/adma.201001215

122. Shirakawa MA, Zilles R, Mocelin A, et al. Microbial colonization affects the efficiency of photovoltaic panels in a tropical environment. *Journal of Environmental Management*. 2015;157:160-167. doi:10.1016/j.jenvman.2015.03.050

123. Coughlan LM, Cotter PD, Hill C, Alvarez-Ordóñez A. New Weapons to Fight Old Enemies: Novel Strategies for the (Bio)control of Bacterial Biofilms in the Food Industry. *Frontiers in Microbiology*. 2016;7. doi:10.3389/fmicb.2016.01641

124. Zhao X, Zhao F, Wang J, Zhong N. Biofilm formation and control strategies of foodborne pathogens: food safety perspectives. *RSC Advances*. 2017;7(58):36670-36683. doi:10.1039/C7RA02497E

125. Galié S, García-Gutiérrez C, Miguélez EM, Villar CJ, Lombó F. Biofilms in the Food Industry: Health Aspects and Control Methods. *Front Microbiol*. 2018;9. doi:10.3389/fmicb.2018.00898

126. Passman FJ. Microbial contamination and its control in fuels and fuel systems since 1980 – a review. *International Biodeterioration & Biodegradation*. 2013;81:88-104. doi:10.1016/j.ibiod.2012.08.002

127. McNamara CJ, Perry TD, Leard R, Bearce K, Dante J, Mitchell R. Corrosion of aluminum alloy 2024 by microorganisms isolated from aircraft fuel tanks. *Biofouling*. 2005;21(5-6):257-265. doi:10.1080/08927010500389921

128. Zea L, Nisar Z, Rubin P, et al. Design of a spaceflight biofilm experiment. *Acta Astronautica*. 2018;148:294-300. doi:10.1016/j.actaastro.2018.04.039

129. Kim W, Tengra FK, Young Z, et al. Spaceflight Promotes Biofilm Formation by Pseudomonas aeruginosa. *PLOS ONE*. 2013;8(4):e62437. doi:10.1371/journal.pone.0062437

130. Gus JD, Romanb M, Esselmanc T, Mitchell R. The role of microbial biofilms in deterioration of space station candidate materials'. Published online 1997:9.

131. Stacy A, McNally L, Darch SE, Brown SP,

Whiteley M. The biogeography of polymicrobial infection. *Nature Reviews Microbiology*. 2016;14(2):93-105. doi:10.1038/nrmicro.2015.8

132. Arciola CR, Campoccia D, Montanaro L. Implant infections: adhesion, biofilm formation and immune evasion. *Nature Reviews Microbiology*. 2018;16(7):397-409. doi:10.1038/s41579-018-0019-y

133. Blair JMA, Webber MA, Baylay AJ, Ogbolu DO, Piddock LJV. Molecular mechanisms of antibiotic resistance. *Nature Reviews Microbiology*. 2015;13(1):42-51. doi:10.1038/nrmicro3380

134. Stewart PS. Antimicrobial Tolerance in Biofilms. *Microbiology Spectrum*. 2015;3(3). doi:10.1128/microbiolspec.MB-0010-2014

135. Hall CW, Mah TF. Molecular mechanisms of biofilm-based antibiotic resistance and tolerance in pathogenic bacteria. *FEMS Microbiology Reviews*. 2017;41(3):276-301. doi:10.1093/femsre/fux010

136. Estrela S, Brown SP. Community interactions and spatial structure shape selection on antibiotic resistant lineages. Alizon S, ed. *PLOS Computational Biology*. 2018;14(6):e1006179. doi:10.1371/journal.pcbi.1006179

137. Geredew Kifelew L, Mitchell JG, Speck P. Mini-review: efficacy of lytic bacteriophages on multispecies biofilms. *Biofouling*. Published online May 30, 2019:1-10. doi:10.1080/08927014.2019.1613525

138. Dieltjens L, Appermans K, Lissens M, et al. Inhibiting bacterial cooperation is an evolutionarily robust anti-biofilm strategy. *Nature Communications*. 2020;11(1). doi:10.1038/s41467-019-13660-x

139. Jones CJ, Utada A, Davis KR, et al. C-di-GMP Regulates Motile to Sessile Transition by Modulating MshA Pili Biogenesis and Near-Surface Motility Behavior in Vibrio cholerae. *PLOS Pathogens*. 2015;11(10):e1005068. doi:10.1371/journal.ppat.1005068

140. Laventie BJ, Jenal U. Surface Sensing and Adaptation in Bacteria. *Annual Review of Microbiology*. 2020;74(1):735-760. doi:10.1146/annurev-micro-012120-063427

141. Kimkes TEP, Heinemann M. How bacteria recognise and respond to surface contact. *FEMS Microbiology Reviews*. Published online November 26, 2019. doi:10.1093/femsre/fuz029

142. Pratt LA, Kolter R. Genetic analysis of Escherichia coli biofilm formation: roles of flagella, motility, chemotaxis and type I pili. *Molecular Microbiology*. 1998;30(2):285-293. doi:10.1046/j.1365-2958.1998.01061.x

143. Berne C, Ellison CK, Ducret A, Brun YV. Bacterial adhesion at the single-cell level. *Nature Reviews Microbiology*. 2018;16(10):616-627. doi:10.1038/s41579-018-0057-5

144. Tuson HH, Weibel DB. Bacteria-surface

interactions. *Soft Matter*. 2013;9(17):4368. doi:10.1039/c3sm27705d

145. Lee CK, de Anda J, Baker AE, et al. Multigenerational memory and adaptive adhesion in early bacterial biofilm communities. *Proceedings of the National Academy of Sciences*. 2018;115(17):4471-4476. doi:10.1073/pnas.1720071115

146. Alsharif G, Ahmad S, Islam MS, Shah R, Busby SJ, Krachler AM. Host attachment and fluid shear are integrated into a mechanical signal regulating virulence in *Escherichia coli* O157:H7. *Proceedings of the National Academy of Sciences*. 2015;112(17):5503-5508. doi:10.1073/pnas.1422986112

147. Verstraeten N, Braeken K, Debkumari B, et al. Living on a surface: swarming and biofilm formation. *Trends in Microbiology*. 2008;16(10):496-506. doi:10.1016/j.tim.2008.07.004

148. Palmer J, Flint S, Brooks J. Bacterial cell attachment, the beginning of a biofilm. *Journal of Industrial Microbiology and Biotechnology*. 2007;34(9):577-588. doi:10.1007/s10295-007-0234-4

149. Carniello V, Peterson BW, van der Mei HC, Busscher HJ. Physico-chemistry from initial bacterial adhesion to surface-programmed biofilm growth. *Advances in Colloid and Interface Science*. 2018;261:1-14. doi:10.1016/j.cis.2018.10.005

150. Rigo S, Cai C, Gunkel-Grabole G, et al. Nanoscience-Based Strategies to Engineer Antimicrobial Surfaces. *Advanced Science*. 2018;5(5):1700892. doi:10.1002/advs.201700892

151. Buhl KB, Agergaard AH, Lillethorup M, Nikolajsen JP, Pedersen SU, Daasbjerg K. Polymer Brush Coating and Adhesion Technology at Scale. *Polymers (Basel)*. 2020;12(7):1475. doi:10.3390/polym12071475

152. Mahanta U, Khandelwal M, Deshpande AS. Antimicrobial surfaces: a review of synthetic approaches, applicability and outlook. *J Mater Sci*. 2021;56(32):17915-17941. doi:10.1007/s10853-021-06404-0

153. Beaussart A, Retourney C, Quilès F, et al. Supported lysozyme for improved antimicrobial surface protection. *Journal of Colloid and Interface Science*. 2021;582:764-772. doi:10.1016/j.jcis.2020.08.107

154. Di Somma A, Moretta A, Canè C, Cirillo A, Duilio A. Antimicrobial and Antibiofilm Peptides. *Biomolecules*. 2020;10(4):652. doi:10.3390/biom10040652

155. Liu S, Cao S, Guo J, et al. Graphene oxide–silver nanocomposites modulate biofilm formation and extracellular polymeric substance (EPS) production. *Nanoscale*. 2018;10(41):19603-19611. doi:10.1039/C8NR04064H

156. Applerot G, Lellouche J, Perkas N, Nitzan Y,

Gedanken A, Banin E. ZnO nanoparticle-coated surfaces inhibit bacterial biofilm formation and increase antibiotic susceptibility. *RSC Advances*. 2012;2(6):2314. doi:10.1039/c2ra00602b

157. Qayyum S, Khan AU. Nanoparticles vs. biofilms: a battle against another paradigm of antibiotic resistance. *MedChemComm*. 2016;7(8):1479-1498. doi:10.1039/C6MD00124F

158. Stolzer L, Ahmed I, Rodriguez-Emmenegger C, et al. Light-induced modification of silver nanoparticles with functional polymers. *Chem Commun*. 2014;50(34):4430-4433. doi:10.1039/C4CC00960F

159. Tallet L, Gribova V, Ploux L, Vrana NE, Lavalle P. New Smart Antimicrobial Hydrogels, Nanomaterials, and Coatings: Earlier Action, More Specific, Better Dosing? *Advanced Healthcare Materials*. 2021;10(1):2001199. doi:10.1002/adhm.202001199

160. Li X, Wu B, Chen H, et al. Recent developments in smart antibacterial surfaces to inhibit biofilm formation and bacterial infections. *Journal of Materials Chemistry B*. 2018;6(26):4274-4292. doi:10.1039/C8TB01245H

161. Wei T, Tang Z, Yu Q, Chen H. Smart Antibacterial Surfaces with Switchable Bacteria-Killing and Bacteria-Releasing Capabilities. *ACS Appl Mater Interfaces*. 2017;9(43):37511-37523. doi:10.1021/acsami.7b13565

162. Yu Q, Li X, Zhang Y, Yuan L, Zhao T, Chen H. The synergistic effects of stimuli-responsive polymers with nano- structured surfaces: wettability and protein adsorption. *RSC Adv*. 2011;1(2):262-269. doi:10.1039/C1RA00201E

163. Kayes MI, Galante AJ, Stella NA, Haghanifar S, Shanks RMQ, Leu PW. Stable lotus leaf-inspired hierarchical, fluorinated polypropylene surfaces for reduced bacterial adhesion. *Reactive and Functional Polymers*. 2018;128:40-46. doi:10.1016/j.reactfunctpolym.2018.04.013

164. Dundar Arisoy F, Kolewe KW, Homyak B, Kurtz IS, Schiffman JD, Watkins JJ. Bioinspired Photocatalytic Shark-Skin Surfaces with Antibacterial and Antifouling Activity via Nanoimprint Lithography. *ACS Appl Mater Interfaces*. 2018;10(23):20055-20063. doi:10.1021/acsami.8b05066

165. Quirk T. Insect wings shred bacteria to pieces. *Nature*. Published online March 4, 2013. doi:10.1038/nature.2013.12533

166. Jaggessar A, Shahali H, Mathew A, Yarlagadda PKDV. Bio-mimicking nano and micro-structured surface fabrication for antibacterial properties in medical implants. *Journal of Nanobiotechnology*. 2017;15(1). doi:10.1186/s12951-017-0306-1

167. Marguier A, Poulin N, Soraru C, et al. Bacterial Colonization of Low-Wettable Surfaces is Driven by Culture Conditions and Topography. *Advanced Materials Interfaces*. 2020;7(20):2000179. doi:10.1002/admi.202000179

168. Wen G, Guo Z, Liu W. Biomimetic polymeric superhydrophobic surfaces and nanostructures: from fabrication to applications. *Nanoscale*. 2017;9(10):3338-3366. doi:10.1039/C7NR00096K

169. Linklater DP, Juodkazis S, Ivanova EP. Nanofabrication of mechano-bactericidal surfaces. *Nanoscale*. 2017;9(43):16564-16585. doi:10.1039/C7NR05881K

170. Velic A, Hasan J, Li Z, Yarlagadda PKDV. Mechanics of Bacterial Interaction and Death on Nanopatterned Surfaces. *Biophysical Journal*. 2021;120(2):217-231. doi:10.1016/j.bpj.2020.12.003

171. Pogodin S, Hasan J, Baulin VA, et al. Biophysical Model of Bacterial Cell Interactions with Nanopatterned Cicada Wing Surfaces. *Biophys J*. 2013;104(4):835-840. doi:10.1016/j.bpj.2012.12.046

172. Linklater DP, Baulin VA, Juodkazis S, Crawford RJ, Stoodley P, Ivanova EP. Mechano-bactericidal actions of nanostructured surfaces. *Nat Rev Microbiol*. 2021;19(1):8-22. doi:10.1038/s41579-020-0414-z

173. Andersson DI, Hughes D. Microbiological effects of sublethal levels of antibiotics. *Nature Reviews Microbiology*. 2014;12(7):465-478. doi:10.1038/nrmicro3270

174. Levy SB, Marshall B. Antibacterial resistance worldwide: causes, challenges and responses. *Nature Medicine*. 2004;10(12s):S122-S129. doi:10.1038/nm1145

175. Hasan J, Webb HK, Truong VK, et al. Selective bactericidal activity of nanopatterned superhydrophobic cicada Psaltoda claripennis wing surfaces. *Appl Microbiol Biotechnol*. 2013;97(20):9257-9262. doi:10.1007/s00253-012-4628-5

176. Elbourne A, Crawford RJ, Ivanova EP. Nano-structured antimicrobial surfaces: From nature to synthetic analogues. *Journal of Colloid and Interface Science*. 2017;508:603-616. doi:10.1016/j.jcis.2017.07.021

177. Yu Q, Cho J, Shivapooja P, Ista LK, López GP. Nanopatterned Smart Polymer Surfaces for Controlled Attachment, Killing, and Release of Bacteria. *ACS Appl Mater Interfaces*. 2013;5(19):9295-9304. doi:10.1021/am4022279

178. Gristina AG, Naylor PT, Myrvik Q. The Race for the Surface: Microbes, Tissue Cells, and Biomaterials. In: Switalski L, Höök M, Beachey E, eds. *Molecular Mechanisms of Microbial Adhesion*. Springer; 1989:177-211. doi:10.1007/978-1-4612-3590-3_15

179. Pham VTH, Truong VK, Orlowska A, et al. "Race for the Surface": Eukaryotic Cells Can Win. *ACS Appl Mater Interfaces*. 2016;8(34):22025-22031. doi:10.1021/acsami.6b06415

180. Robertson SN, Childs PG, Akinbobola A, et al. Reduction of Pseudomonas aeruginosa biofilm formation through the application of nanoscale

vibration. *Journal of Bioscience and Bioengineering*. Published online October 2019. doi:10.1016/j.jbiosc.2019.09.003

181. Paces WR, Holmes HR, Vlaisavljevich E, et al. Application of Sub-Micrometer Vibrations to Mitigate Bacterial Adhesion. *J Funct Biomater*. 2014;5(1):15-26. doi:10.3390/jfb5010015

182. Carvalho EO, Fernandes MM, Padrao J, et al. Tailoring Bacteria Response by Piezoelectric Stimulation. *ACS Applied Materials & Interfaces*. Published online July 16, 2019. doi:10.1021/acsami.9b05013

183. Murphy MF, Edwards T, Hobbs G, Shepherd J, Bezombes F. Acoustic vibration can enhance bacterial biofilm formation. *Journal of Bioscience and Bioengineering*. 2016;122(6):765-770. doi:10.1016/j.jbiosc.2016.05.010

184. Hong SH, Gorce JB, Punzmann H, Francois N, Shats M, Xia H. Surface waves control bacterial attachment and formation of biofilms in thin layers. *Science Advances*. 2020;6(22):eaaz9386. doi:10.1126/sciadv.aaz9386

185. Ko H, Park HH, Byeon H, et al. Undulatory topographical waves for flow-induced foulant sweeping. *Sci Adv*. 2019;5(11). doi:10.1126/sciadv.aax8935

186. Tsuzuki T, Baassiri K, Mahmoudi Z, et al. Hydrophobic Recovery of PDMS Surfaces in Contact with Hydrophilic Entities: Relevance to Biomedical Devices. *Materials (Basel)*. 2022;15(6):2313. doi:10.3390/ma15062313

187. Miao H, Ratnasingam S, Pu CS, Desai MM, Sze CC. Dual fluorescence system for flow cytometric analysis of Escherichia coli transcriptional response in multi-species context. *J Microbiol Methods*. 2009;76(2):109-119. doi:10.1016/j.mimet.2008.09.015

188. Bhoite S, van Gerven N, Chapman MR, Remaut H. Curli Biogenesis: Bacterial Amyloid Assembly by the Type VIII Secretion Pathway. *EcoSal Plus*. 2019;8(2). doi:10.1128/ecosalplus.ESP-0037-2018

189. Hufnagel DA, Depas WH, Chapman MR. The Biology of the Escherichia coli Extracellular Matrix. *Microbiology Spectrum*. 2015;3(3). doi:10.1128/microbiolspec.MB-0014-2014

190. Perni S, Preedy EC, Landini P, Prokopovich P. Influence of csgD and ompR on Nanomechanics, Adhesion Forces, and Curli Properties of *E. coli*. *Langmuir*. 2016;32(31):7965-7974. doi:10.1021/acs.langmuir.6b02342

191. Ogasawara H, Yamamoto K, Ishihama A. Role of the Biofilm Master Regulator CsgD in Cross-Regulation between Biofilm Formation and Flagellar Synthesis. *Journal of Bacteriology*. 2011;193(10):2587-2597. doi:10.1128/JB.01468-10

192. Ogasawara H, Yamada K, Kori A, Yamamoto K, Ishihama A. Regulation of the Escherichia coli csgD promoter: interplay between five transcription factors. *Microbiology*.

2010;156(8):2470-2483. doi:10.1099/mic.0.039131-0

193. Martins BM, Locke JC. Microbial individuality: how single-cell heterogeneity enables population level strategies. *Current Opinion in Microbiology*. 2015;24:104-112. doi:10.1016/j.mib.2015.01.003

194. Curtis ASG, Reid S, Martin I, et al. Cell Interactions at the Nanoscale: Piezoelectric Stimulation. *IEEE Transactions on NanoBioscience*. 2013;12(3):247-254. doi:10.1109/TNB.2013.2257837

195. Alam F, Kumar S, Varadarajan KM. Quantification of Adhesion Force of Bacteria on the Surface of Biomaterials: Techniques and Assays. *ACS Biomaterials Science & Engineering*. 2019;5(5):2093-2110. doi:10.1021/acsbiomaterials.9b00213

196. Craig L, Forest KT, Maier B. Type IV pili: dynamics, biophysics and functional consequences. *Nature Reviews Microbiology*. 2019;17(7):429-440. doi:10.1038/s41579-019-0195-4

197. Maier B, Potter L, So M, Seifert HS, Sheetz MP. Single pilus motor forces exceed 100 pN. *Proceedings of the National Academy of Sciences*. 2002;99(25):16012-16017. doi:10.1073/pnas.242523299

198. Magariyama, Y., Sugiyama, S., Muramoto, K. et al. Very fast flagella rotation. *Nature*. 1994;371(752).

199. Costa OYA, Raaijmakers JM, Kuramae EE. Microbial Extracellular Polymeric Substances: Ecological Function and Impact on Soil Aggregation. *Frontiers in Microbiology*. 2018;9. Accessed May 1, 2022. https://www.frontiersin.org/article/10.3389/fmicb.2018.01636

200. Straub H, Bigger CM, Valentin J, et al. Bacterial Adhesion on Soft Materials: Passive Physicochemical Interactions or Active Bacterial Mechanosensing? *Advanced Healthcare Materials*. Published online February 18, 2019:1801323-. doi:10.1002/adhm.201801323

201. Oh JK, Yegin Y, Yang F, et al. The influence of surface chemistry on the kinetics and thermodynamics of bacterial adhesion. *Sci Rep*. 2018;8(1):17247. doi:10.1038/s41598-018-35343-1

202. Lane N, Martin WF. The Origin of Membrane Bioenergetics. *Cell*. 2012;151(7):1406-1416. doi:10.1016/j.cell.2012.11.050

203. Galera-Laporta L, Comerci CJ, Garcia-Ojalvo J, Süel GM. IonoBiology: The functional dynamics of the intracellular metallome, with lessons from bacteria. *Cell Systems*. 2021;12(6):497-508. doi:10.1016/j.cels.2021.04.011

204. Bot CT, Prodan C. Quantifying the membrane potential during E. coli growth stages. *Biophysical Chemistry*. 2010;146(2-3):133-137. doi:10.1016/j.bpc.2009.11.005

205. Philip Nelson. *Biological Physics: Energy,*

Information, Life.; 2021.

206. Biquet-Bisquert A, Labesse G, Pedaci F, Nord AL. The Dynamic Ion Motive Force Powering the Bacterial Flagellar Motor. *Front Microbiol*. 2021;12. doi:10.3389/fmicb.2021.659464

207. Stautz J, Hellmich Y, Fuss MF, et al. Molecular Mechanisms for Bacterial Potassium Homeostasis. *Journal of Molecular Biology*. 2021;433(16):166968. doi:10.1016/j.jmb.2021.166968

208. Beagle SD, Lockless SW. Unappreciated Roles for K+ Channels in Bacterial Physiology. *Trends in Microbiology*. 2021;29(10):942-950. doi:10.1016/j.tim.2020.11.005

209. Damper PD, Epstein W. Role of the membrane potential in bacterial resistance to aminoglycoside antibiotics. *Antimicrob Agents Chemother*. 1981;20(6):803-808. doi:10.1128/AAC.20.6.803

210. Liu J, Martinez-Corral R, Prindle A, et al. Coupling between distant biofilms and emergence of nutrient time-sharing. *Science*. 2017;356(6338):638-642. doi:10.1126/science.aah4204

211. Humphries J, Xiong L, Liu J, et al. Species-Independent Attraction to Biofilms through Electrical Signaling. *Cell*. 2017;168(1-2):200-209.e12. doi:10.1016/j.cell.2016.12.014

212. Strahl H, Hamoen LW. Membrane potential is important for bacterial cell division. *Proceedings of the National Academy of Sciences*. 2010;107(27):12281-12286. doi:10.1073/pnas.1005485107

213. Sirec T, Benarroch JM, Buffard P, Garcia-Ojalvo J, Asally M. Electrical Polarization Enables Integrative Quality Control during Bacterial Differentiation into Spores. *iScience*. 2019;16:378-389. doi:10.1016/j.isci.2019.05.044

214. Mancini L, Terradot G, Tian T, et al. A General Workflow for Characterization of Nernstian Dyes and Their Effects on Bacterial Physiology. *Biophysical Journal*. 2020;118(1):4-14. doi:10.1016/j.bpj.2019.10.030

215. Hudson MA, Siegele DA, Lockless SW. Use of a Fluorescence-Based Assay To Measure *Escherichia coli* Membrane Potential Changes in High Throughput. *Antimicrob Agents Chemother*. 2020;64(9):e00910-20, /aac/64/9/AAC.00910-20.atom. doi:10.1128/AAC.00910-20

216. May KL, Grabowicz M. The bacterial outer membrane is an evolving antibiotic barrier. *PNAS*. 2018;115(36):8852-8854. doi:10.1073/pnas.1812779115

217. Muheim C, Götzke H, Eriksson AU, et al. Increasing the permeability of Escherichia coli using MAC13243. *Sci Rep*. 2017;7(1):17629. doi:10.1038/s41598-017-17772-6

218. Finnegan S, Percival SL. EDTA: An Antimicrobial and Antibiofilm Agent for Use in Wound Care. *Adv Wound Care (New Rochelle)*. 2015;4(7):415-421. doi:10.1089/wound.2014.0577

219. Kirchhoff C, Cypionka H. Boosted Membrane Potential as Bioenergetic Response to Anoxia in Dinoroseobacter shibae. *Front Microbiol*. 2017;8. doi:10.3389/fmicb.2017.00695

220. Lee D yeon D, Galera-Laporta L, Bialecka-Fornal M, et al. Magnesium Flux Modulates Ribosomes to Increase Bacterial Survival. *Cell*. 2019;177(2):352-360.e13. doi:10.1016/j.cell.2019.01.042

221. Bruni GN, Kralj JM. Membrane voltage dysregulation driven by metabolic dysfunction underlies bactericidal activity of aminoglycosides. *eLife*. 2020;9:e58706. doi:10.7554/eLife.58706

222. Laganenka L, López ME, Colin R, Sourjik V. Flagellum-Mediated Mechanosensing and RflP Control Motility State of Pathogenic *Escherichia coli*. Groisman EA, ed. *mBio*. 2020;11(2). doi:10.1128/mBio.02269-19

223. Krasnopeeva E, Barboza-Perez UE, Rosko J, Pilizota T, Lo CJ. Bacterial flagellar motor as a multimodal biosensor. *Methods*. 2021;193:5-15. doi:10.1016/j.ymeth.2020.06.012

224. Suchanek VM, Esteban-López M, Colin R, Besharova O, Fritz K, Sourjik V. Chemotaxis and cyclic-di-GMP signalling control surface attachment of Escherichia coli. *Molecular Microbiology*. 2020;113(4):728-739. doi:10.1111/mmi.14438

225. Besharova O, Suchanek VM, Hartmann R, Drescher K, Sourjik V. Diversification of Gene Expression during Formation of Static Submerged Biofilms by Escherichia coli. *Front Microbiol*. 2016;7. doi:10.3389/fmicb.2016.01568

226. Dudin O, Geiselmann J, Ogasawara H, Ishihama A, Lacour S. Repression of Flagellar Genes in Exponential Phase by CsgD and CpxR, Two Crucial Modulators of Escherichia coli Biofilm Formation. *J Bacteriol*. 2014;196(3):707-715. doi:10.1128/JB.00938-13

227. Kearns DB. Flagellar Stators Activate a Diguanylate Cyclase To Inhibit Flagellar Stators. *J Bacteriol*. 2019;201(18). doi:10.1128/JB.00186-19

228. Berne C, Ellison CK, Agarwal R, et al. Feedback regulation of Caulobacter crescentus holdfast synthesis by flagellum assembly via the holdfast inhibitor HfiA. *Molecular Microbiology*. 2018;110(2):219-238. doi:10.1111/mmi.14099

229. Sim M, Koirala S, Picton D, et al. Growth rate control of flagellar assembly in Escherichia coli strain RP437. *Sci Rep*. 2017;7(1):41189. doi:10.1038/srep41189

230. Berg HC. *Random Walks in Biology*. Princeton University Press; 1993.

231. Ershov D, Phan MS, Pylvänäinen JW, et al. *Bringing TrackMate into the Era of Machine-Learning and Deep-Learning*. Bioinformatics; 2021. doi:10.1101/2021.09.03.458852

232. Song F, Brasch ME, Wang H, Henderson JH, Sauer K, Ren D. How Bacteria Respond to

Material Stiffness during Attachment: A Role of *Escherichia coli* Flagellar Motility. *ACS Applied Materials & Interfaces*. 2017;9(27):22176-22184. doi:10.1021/acsami.7b04757

233. Schniederberend M, Williams JF, Shine E, et al. Modulation of flagellar rotation in surface-attached bacteria: A pathway for rapid surface-sensing after flagellar attachment. Rao C, ed. *PLOS Pathogens*. 2019;15(11):e1008149. doi:10.1371/journal.ppat.1008149

234. Lee DJ, Bingle LE, Heurlier K, et al. Gene doctoring: a method for recombineering in laboratory and pathogenic Escherichia coli strains. *BMC Microbiology*. 2009;9(1):252. doi:10.1186/1471-2180-9-252

235. Van Dellen KL, Houot L, Watnick PI. Genetic Analysis of Vibrio cholerae Monolayer Formation Reveals a Key Role for $\Delta\Psi$ in the Transition to Permanent Attachment. *Journal of Bacteriology*. 2008;190(24):8185-8196. doi:10.1128/JB.00948-08

236. Vidal O, Longin R, Prigent-Combaret C, Dorel C, Hooreman M, Lejeune P. Isolation of an Escherichia coli K-12 Mutant Strain Able To Form Biofilms on Inert Surfaces: Involvement of a New ompR Allele That Increases Curli Expression. *Journal of Bacteriology*. 1998;180(9):2442-2449.